

UC Riverside

UC Riverside Electronic Theses and Dissertations

Title

Regulation of Heterotrimeric G Alpha Subunits in the Filamentous Fungus, Neurospora crassa

Permalink

<https://escholarship.org/uc/item/9qj605qd>

Author

Wright, Sara Josephine

Publication Date

2010

Peer reviewed|Thesis/dissertation

UNIVERSITY OF CALIFORNIA
RIVERSIDE

Regulation of Heterotrimeric G Alpha Subunits
in the Filamentous Fungus, *Neurospora crassa*

A Dissertation submitted in partial satisfaction
of the requirements for the degree of

Doctor of Philosophy

in

Biochemistry and Molecular Biology

by

Sara Josephine Wright

August 2010

Dissertation Committee:
Dr. Katherine A. Borkovich, Chairperson
Dr. Kathryn A. Defea
Dr. David A. Johnson

Copyright by
Sara Josephine Wright
2010

The Dissertation of Sara Josephine Wright is approved:

Chairperson

University of California, Riverside

ACKNOWLEDGEMENTS

I am deeply grateful to my advisor, Dr. Katherine Borkovich, for her guidance and support. Kathy's pure enthusiasm for science, expansive knowledge, and innovative thinking has inspired me to always think outside the box and to always look forward. I would also like to acknowledge dissertation committee members, Dr. David Johnson and Dr. Kathryn Defea, whose advice and patience helped make my dissertation possible.

I am thankful to the members of the Borkovich lab, especially Dr. Svetlana Krystofova, Dr. Hyojeong Kim, and Dr. Gyungsoon Park for their advice and guidance during various times in my dissertation research. I would also like to thank Regina Inchausti, an extremely talented undergraduate student who assisted with the construction and expression of the proteins described in Chapter 4.

I am also thankful to those who have lent endless support during my Ph.D. studies. I would like to thank the former student affairs office for the Biochemistry and Molecular Biology program, Janet Fast, who helped me through some really tough times and was my surrogate mother at UCR. I would also like to thank my mentor at Cal Poly Pomona, Dr. Barbara Burke, who encouraged me to pursue graduate school and continues to support and encourage me.

DEDICATION

This dissertation is dedicated to my entire family and close friends. Though at times they did not understand why I worked so much, why I couldn't attend some family functions, or what I was even doing, they supported me unconditionally.

To my parents, Gary and Alison Augustine, thank you for your constant understanding and patience through this long process, and for being a solid ground for me when things were uncertain. To my dad, Pete Martinez, thank you for always being there when I needed you most. To my sister Lisa, thank you for your friendship and for always providing a shoulder to cry on, a laugh to participate in the delirium, and a heart full of love. To my sister Ashlee, thank you for always being the rational voice for me and always lending an ear and reassuring me when I feel down.

Finally, this dissertation is dedicated to my wonderful husband Richard and daughter Lily. This process has been a journey for us, and has brought us closer together as a family and has made us stronger. To my daughter Lily, you have brought so much joy and meaning to my life and you make me want to be the best I can be.

ABSTRACT OF THE DISSERTATION

Regulation of Heterotrimeric G Alpha Subunits
in the Filamentous Fungus, *Neurospora crassa*

by

Sara Josephine Wright

Doctor of Philosophy, Graduate Program in Biochemistry and Molecular Biology
University of California, Riverside, August 2010
Dr. Katherine Borkovich, Chairperson

Heterotrimeric G protein signaling pathways are crucial for eukaryotic cells to regulate environmental sensing, growth and development. G protein signaling involves a membrane spanning receptor called a G protein-coupled receptor (GPCR) that can be activated by an extracellular signal. GPCR's are bound intracellularly by a trimer of proteins: the G α subunit, which binds and hydrolyzes GTP, and a tightly associated G $\beta\gamma$ dimer. Upon receptor activation, a conformational change causes the G α subunit to exchange GDP for GTP and become dissociated from the GPCR and G $\beta\gamma$. The GPCR is thus considered a guanine-nucleotide exchange factor (GEF) for the G α subunit. The G α subunit has intrinsic GTPase activity which converts GTP to GDP, causing G α to re-associate with the receptor and G $\beta\gamma$.

This dissertation focuses on the regulation of G protein signaling in the filamentous fungus *Neurospora crassa*. *N. crassa* has three G α proteins (GNA-1, GNA-

2, GNA-3), one G β (GNB-1), one G γ (GNG-1), and 10 predicted GPCR's. The G α subunit GNA-1 in *Neurospora crassa* has been shown to be vital for proper cell growth and differentiation, and a variety of functions have been identified for GNA-1. Using a yeast two-hybrid screen, I identified interesting potential partners of GNA-1 including two metabolic enzymes, two proteins involved in protein synthesis, an actin nucleating protein, and proteins involved in vitamin synthesis, lipid, and two fungal specific proteins with unknown function.

The majority of this dissertation focuses on a homolog of a non-GPCR GEF, RIC8, which has been shown to be important in mechanisms for G α regulation in animals. RIC8 is present in filamentous fungi, but is absent from the genomes of *Saccharomyces cerevisiae* and sequenced protists, including *Dictyostelium discoideum*. Deletion of *ric8* leads to defects in polar growth and asexual and sexual development in *Neurospora*, and constitutively activated alleles of *gna-1* and *gna-3* rescue many defects of $\Delta ric8$ mutants. RIC8 interacts *in vitro* with GNA-1 and GNA-3 and preliminary results show that RIC8 has GEF activity toward GNA-1. This data shows both a functional and physical interaction between RIC8, GNA-1 and GNA-3. Hyphae from *Neurospora* $\Delta ric8$ mutants have small cell compartments that contain nuclei that are smaller and morphologically abnormal compared to wild-type, which also suggest a role in polar cell growth. Taken together, our results support a role for RIC8 and G proteins in regulation of polar growth in *Neurospora*.

Table of Contents

Chapter 1. Introduction

Introduction to Fungi	1
<i>Neurospora crassa</i> : History and Importance of a Model Organism	3
Life-cycle of <i>N. crassa</i>	4
Introduction to Heterotrimeric G protein signaling	6
Heterotrimeric G protein signaling in fungi	10
Regulators of G protein signaling - RGS proteins.	14
Non-GPCR guanine nucleotide exchange factors - RIC8 and Arr4p.	17
Specific aims and major conclusions	19

Chapter 2. Identification of novel GNA-1 binding partners

Abstract	22
Introduction	23
Materials and Methods	25
Results	42
Discussion	46

Chapter 3. Characterization of RIC8 in *Neurospora crassa*

Abstract	53
Introduction	54
Materials and Methods	56

Results	72
Discussion	80
Chapter 4. Expression and purification of RIC8 and Gα subunits and their use in	
GTP binding assays	
Abstract	94
Introduction	95
Materials and Methods	96
Results	109
Discussion	114
Chapter 5. Conclusions	126
References	130
Appendix 1.	
Expression of the <i>N. crassa</i> adenylyl cyclase protein, CR-1, from <i>E. coli</i>	143
Appendix 2.	
Construction of RGS gene deletion mutants in <i>N. crassa</i>	149
References for Appendices	153
Vita	154

List of Figures

Chapter 1. Introduction

Figure 1.2: Heterotrimeric G protein signaling pathway. 21

Chapter 2. Identification of novel GNA-1 binding partners

Figure 2.1: Schematic for the yeast two-hybrid assay and cDNA library screening . . . 48

Figure 2.2: RNA, mRNA, and cDNA used for library construction 49

Figure 2.3: GAPDH enzyme activity is reduced in the *gna-1*^{Q204L} strain. 50

Figure 2.4: mRNA transcript and protein levels of GAPDH (*ccg-7*) in WT, Δ *gna-1*, and *gna-1** strains. 51

Chapter 3. Characterization of RIC8 in *Neurospora crassa*

Figure 3.1: *ric8* gene structure, mutant verification, and protein molecular weight. . . . 83

Figure 3.2: RIC8 homologs. 84

Figure 3.3: RIC8 homologues in other fungi. 85

Figure 3.4: Epistatic and physical relationships between *ric8* and G α genes 86

Figure 3.5: Epistatic relationships between Δ *ric8* and G α genes 87

Figure 3.6: RIC8 interacts with GNA-1 and GNA-3 in the yeast two-hybrid assay . . . 88

Figure 3.7: Relationship to the cAMP pathway 89

Figure 3.8: Hyphal morphology in Δ G α and Δ *ric8* strains 90

Figure 3.9: RIC8 localization and nuclear morphology of Δ *ric8* mutants 91

Chapter 4: Expression and purification of RIC8 and G α subunits and their use in GTP binding assays

Figure 4.1: Purification of MBP tagged G α and RIC8 proteins from *E. coli* 116

Figure 4.2: Purification of poly-histidine tagged G α and RIC8 proteins from *E. coli*. .117

Figure 4.3: GTP binding of MBP-G α subunits and GEF activity of MBP-RIC8118

Figure 4.4: GTP binding of 6H-G α subunits and GEF activity of MBP-RIC8119

Figure 4.5: GTP binding of 6H-G α subunits and GEF activity of HIS-RIC8121

Figure 4.6: Removal of MBP tag from RIC8, GNA-1, and GNA-3 122

Figure 4.7: Additional purification steps for 6H tagged G α proteins 123

Figure 4.8: Immuno-precipitation of RIC8-V5 from *Neurospora crassa*124

Appendix 1. Expression of the *N. crassa* adenylyl cyclase protein, CR-1, from *E. coli*

Figure A1.1: Schematic of the deletion of introns in the *cr-1* gene 146

Figure A1.2: Expression of CR-1-6H in *E. coli* 147

Appendix 2. Construction of RGS gene deletion mutants in *N. crassa*

Figure A2.1: Δ *rgs* mutants: southern verifications and basic phenotypes 151

List of Tables

Chapter 2. Identification of novel GNA-1 binding partners

Table 2.1. Potential GNA-1 interacting proteins from the cDNA library screen 52

Chapter 3. Characterization of RIC8 in *Neurospora crassa*

Table 3.1. *N. crassa* strains used in this study 92

Table 3.2. Oligonucleotides used in this study 93

Chapter 4. Expression and purification of RIC8 and G α subunits and their use in GTP binding assays

Table 4.1. Oligonucleotides used in this study 125

Appendix 1. Expression of the *N. crassa* adenylyl cyclase protein, CR-1, from *E. coli*

Table A1.1. Oligonucleotides used in this study 146

Appendix 2. Construction of RGS gene deletion mutants in *N. crassa*

Table A2.1. *N. crassa* Δ *rgs* mutants, and RGS homologs in *N. crassa*, *A. nidulans*, and *S. cerevisiae* 152

Chapter 1: Introduction

Introduction to Fungi

The fungi consist of a large and diverse group of organisms that are found in almost every ecological niche in the world (Alexopoulos et al., 1996). Worldwide, there are an estimated 1.5 million species of fungi, many of which have not been characterized (Hawksworth, 2001). The kingdom Fungi contains five major phyla: Ascomycota, Basidiomycota, Glomeromycota, Chytridiomycota and Zygomycota (Alexopoulos et al., 1996; James et al., 2006). The Glomeromycota, Chytridiomycota, and Zygomycota account for a small percentage of all fungal species, though their phylogenetic classification is highly debatable and has been traditionally intertwined (Hibbett et al., 2007; Stajich et al., 2009). Fungi in these three phyla play very important roles in the ecosystem. For example, members of the Glomeromycota associate with about 90% of all plant roots to create a symbiotic relationship important for plant biodiversity and resistance to pathogens (Schwarzott et al., 2001; Smith and Read, 2008). Another example are anaerobic chytrids in the ruminant stomachs of animals, which are responsible for the breakdown of cellulose (Moore and Frazer, 2002).

A majority of all fungi are members of the phyla Basidiomycota or Ascomycota. Basidiomycetes account for nearly one-third of all fungi and are home to the mushroom family, which includes the edible button mushroom (*Agaricus bisporus*) and Shiitake mushroom (*Lentinula edodes*), and model organisms *Coprinus cinereus* and *Schizophyllum commune* (Kues and Liu, 2000). Some basidiomycetes are devastating

pathogens of plants and humans. *Ustilago maydis*, the cause of corn smut disease, induces tumor formation on corn plants and destroys crops (Banuett, 1995). *Cryptococcus neoformans*, an opportunistic human pathogen, causes meningoencephalitis in immunocompromised individuals (Hull and Heitman, 2002).

Approximately two-thirds all known fungi are Ascomycetes (Moore and Frazer, 2002; Stajich et al., 2009) and include a wide variety of species which range from unicellular to filamentous, and pathogenic to beneficial. Wood-decaying fungi decompose cellulose and lignin from dead trees into nutrients, which are recycled back into the environment (Alexopoulos et al., 1996), and the well-known yeast *Saccharomyces cerevisiae* is used in the production of fermented food such as bread and beer, and also serves as a model organism for eukaryotes (Legras et al., 2007). Ascomycete fungi are also important in the biotech industry, where they are used to mass-produce antibiotics, enzymes, and organic molecules (Bennett, 1998).

Ascomycetes account for a majority of all plant and human fungal pathogens. *Candida albicans*, a normal inhabitant of the human body, can cause infection when the immune system is weakened (Odds et al., 2004). *Fusarium graminearum*, the cause of head blight disease in wheat crops (De Wolf et al., 2003), and *Magnaporthe grisea*, the cause of rice blast disease (Dean et al., 2005) are considered some of the most devastating destroyers of agricultural crops. Perhaps the most versatile ascomycete for the study of genetics, biochemistry, and relationships to fungal pathogens and animals is the filamentous fungus *Neurospora crassa*. This organism is a model for filamentous fungi and eukaryotes in general, and is the organism of study in this dissertation.

***Neurospora crassa* - History and importance of a model organism**

Neurospora was first discovered as a contaminant of French bakeries in the 1800's and is commonly known as the red bread mold (Davis, 2000). This fungus was thought to be asexual until 1927 when the lab of Bernard O. Dodge discovered sexual fruiting bodies in cultures, and found that the sexual spores, termed ascospores, could only be activated by incubation at 60°C for 30-60 min. (Shear and Dodge, 1927). The ability to cultivate the sexual progeny from genetic crosses was a huge discovery that led to the use of *Neurospora* as a model genetic organism. Work by George W. Beadle and Edward L. Tatum, which included random mutagenesis and genetic crosses using *Neurospora*, led to the monumental 'one gene, one enzyme' theory (Beadle and Tatum, 1941). The other important outcome of this work was the discovery that *Neurospora* could be used to easily isolate genes involved in biochemical and metabolic processes in eukaryotes. Most experimental studies henceforth concentrated on the self-sterile (heterothallic) species *Neurospora crassa*.

N. crassa is an ideal organism for laboratory studies. Not only is there a large amount of biochemical and genetic information available for this model organism, there are also many molecular biological and bioinformatics tools available. We have the ability to create targeted and random DNA insertions, deletions, and replacements in the genome; and a wide variety of protocols for standard molecular biology techniques have been adapted for use with filamentous fungi. The complete genome sequence of *N. crassa* was released in 2003 and is available at the Broad Institute at MIT website (<http://www.broadinstitute.org/annotation/genome/neurospora>). The *Neurospora crassa*

database is a wonderful tool that includes the annotation of genes and additional information that continues to be updated by the *Neurospora* community (Galagan et al.). In addition, the community annotated more than 1000 of the genes in a review article shortly after the genome sequence release, and this information was available to the public for immediate use (Borkovich et al., 2004). Shortly after the genome sequence was completed, work on the *Neurospora* genome project began, with the goal of creating gene-deletion mutants for all 10,000-plus genes in *N. crassa*. This a multi-institution project which also includes mass phenotypic, microarray, and protein interaction studies. The knowledge gained from the genome sequence and the genome project will surely catapult *N. crassa* into being one of the premiere model organisms in science.

Life-cycle of *N. crassa*

N. crassa is a filamentous, polarized growth fungus with more than 28 tissue types (Bistis et al., 2003). The life-cycle is categorized by two major stages: vegetative growth and asexual or sexual sporulation. Vegetative growth begins with the germination of an asexual or sexual spore to form a germ tube, which continues to grow to form a complex hyphal network, termed the mycelium (Davis, 2000). The vegetative hyphae are tip-growing and regularly form branches which extend radially away from the point of inoculation and also undergo cell fusion, both of which contribute to the unique hyphal network. The hyphae are also multinucleate, with incomplete cross-walls, termed septa, which serve to strengthen the hyphal cell walls and allow the flow of cytoplasmic

contents, including organelles, proteins, and nutrients, through the hyphal network (Borkovich et al., 2004; Davis, 2000).

Sporulation in *N. crassa* involves formation of two major spore types, asexual and sexual. The asexual sporulation pathways are macroconidiation and microconidiation (Springer, 1993). As the hyphal network grows and nutrients and moisture are depleted, specialized hyphae, termed aerial hyphae, branch from vegetative hyphae and extend perpendicular to the mycelium. The aerial hyphae form structures called conidiophores, which result from a series of apical budding and constrictions to form a string of asexual spores with a bright orange pigmentation, termed macroconidia (Springer, 1993).

Macroconidia, are multinucleate, hydrophobic spores which are easily dispersed by air and function to allow the distribution and survival of a strain. A more minor pathway of asexual sporulation is the formation of microconidia. Microconidia are uninucleate spores which originate from within the hyphal compartment and emerge by rupturing the cell wall (Springer, 1993).

Sexual sporulation involves the mating of two strains of opposite mating type, which are determined by alternative forms of the mating type locus, *matA* and *mata* (Kronstad and Staben, 1997). Mating begins with the formation of specialized female structures termed protoperithecia, which form under nitrogen limiting conditions (Davis, 2000; Springer, 1993). The protoperithecia extend specialized hyphae (trichogyne) in search of a male cell (conidium or hyphal fragment). Opposite mating type trichogynes and male cells sense each other through chemotropism by emitting and responding to pheromones. A trichogyne grows toward the male and undergoes cell fusion, and the

nucleus from the male then travels through the trichogyne and into the protoperithecium. Inside the protoperithecium, the male and female nuclei undergo multiple rounds of mitosis, and opposite mating type nuclei pair and undergo fusion. These diploid nuclei then undergo meiosis and one more round of mitosis to create eight nuclei, each contained in a melanized spore called an ascospore. During this process, the protoperithecium grows larger and becomes melanized, eventually becoming a mature, fertilized female structure termed the perithecium (Davis, 2000). The perithecium forms a pore at the tip (beak) called an ostiole, and when the pressure inside the perithecium is high, the ostiole will violently shoot the ascospores in the direction of blue light. These ascospores are very resilient, with the ability to survive for long periods of time in suboptimal conditions. The germination of an ascospore requires heat activation, which is why *N. crassa* is often the only life form seen growing shortly after a wildfire (Pandit and Maheshwari, 1996).

Introduction to Heterotrimeric G protein signaling

In order to respond to changes in their environment, it is important for eukaryotic organisms to be able to sense the environment outside the cell and relay this information inside the cell, where changes in protein modification, gene expression, and metabolite profile can occur. This ability is essential not only for the survival and fitness of single cells, but also for the cooperative dynamics of the network of cells residing in multicellular organisms. One of the major signaling pathways in eukaryotic cells, heterotrimeric G protein signaling, is the focus of this dissertation. Heterotrimeric G

protein signaling begins with a seven-helical, membrane-spanning protein called a G protein-coupled receptor (GPCR). GPCRs sense the presence of external stimuli and relay information inside the cell, where changes in protein interactions and gene expression occur in response to environmental conditions. In humans, GPCRs sense a wide variety of chemicals, proteins and other stimuli, including ions, hormones, neurotransmitters, lipids, nucleotides, and light. (Fredriksson et al., 2003; McCudden et al., 2005; Neves et al., 2002; Rosenbaum et al., 2009). GPCRs are the target of more than 50% of all drugs on the market today, and the sequencing of the human genome has uncovered an estimated 800 GPCR genes, many of which were previously uncharacterized (Fredriksson et al., 2003; Venter et al., 2001). The five classes of GPCRs characterized in mammals consists of the rhodopsin, glutamate, adhesion, frizzled/taste2, and secretin families (Fredriksson et al., 2003). The largest and most researched GPCR family is the rhodopsin-related family. In fact, the dark-adapted bovine rhodopsin protein was the first GPCR for which a high resolution crystal structure was solved (Palczewski et al., 2000). There are an estimated 701 members of this family, with approximately 460 of these being putative olfactory receptors (Fredriksson et al., 2003; Zozulya et al., 2001). Thus, GPCR signaling is very appealing for research not only in the pharmaceutical industries, but also in the food and cosmetic industries (Krohn et al., 2008).

GPCRs interact intracellularly with a trimer of proteins called heterotrimeric G proteins, which can be activated to affect a number of downstream signaling targets. The heterotrimer consists of $G\alpha$, which can bind and hydrolyze GTP, and a tightly associated

G $\beta\gamma$ dimer. In the absence of signal, the heterotrimer is associated with the receptor and the G α subunit is bound to GDP. Upon ligand binding and/or receptor activation, a conformational change in the receptor causes the G α subunit to bind GTP, which causes disruption of the heterotrimeric complex, allowing G α -GTP and G $\beta\gamma$ to dissociate from the receptor and regulate downstream signaling pathways (Hamm, 1998; McCudden et al., 2005; Neves et al., 2002). Thus, the GPCR acts as a guanine nucleotide exchange factor (GEF) for the G α protein. Free G α -GTP or G $\beta\gamma$ can affect a number of targets including adenylyl cyclases, phosphodiesterases, phospholipases, and ion channels (Neves et al., 2002; Simon et al., 1991). Eventually the G α subunit will cleave a phosphate group from the GTP molecule, converting it to GDP. This causes the G α subunit to form a heterotrimer with G $\beta\gamma$ and return to the receptor for another round of activation. Apart from GPCR activation and the intrinsic GTPase activity of the G α subunit, there are additional proteins which can regulate the GTP or GDP binding status of the G α protein, which are described later in this chapter.

There are 16 G α genes in mammals, which are categorized into four super families: G α_i , G α_s , G α_q and G α_{12} (McCudden et al., 2005; Oldham and Hamm, 2008; Simon et al., 1991). The G α_i family proteins are inhibitors of the enzyme adenylyl cyclase, while the G α_s family proteins activate adenylyl cyclase. Mammalian adenylyl cyclase is a membrane spanning protein which converts ATP to cAMP. The major downstream target of cAMP is Protein Kinase A (PKA), which is a tetramer containing two catalytic subunits (PKA-C) and two regulatory subunits (PKA-R). cAMP binds the

PKA-R subunits, which subsequently dissociate from the PKA-C subunits. The free PKA-C is the active form of PKA which can phosphorylate a variety of downstream targets (Cooper, 2003). The $G\alpha_q$ family of proteins activate phospholipase C, which converts the membrane bound phospholipid PIP_2 into PIP_3 and diacylglyceride (Venter et al.); and the $G\alpha_{12/13}$ family of proteins activate Rho GTPases (McCudden et al., 2005).

There are five $G\beta$ and twelve $G\gamma$ subunits encoded in the human genome, which have the potential to form 1440 thermostable $G\beta\gamma$ dimers, although a small amount of combinations are incompatible (Clapham and Neer, 1997; McCudden et al., 2005). $G\beta$ subunits consist of a seven-bladed propeller structure made of anti-parallel β repeats (WD repeats), and an N-terminal 20 amino α -helix. $G\gamma$ subunits consists of two α -helices; the N-terminal α helix forms a coiled-coil with the N-terminal $G\beta$ helix, and the C-terminal helix contacts the seven-bladed propeller structure. $G\gamma$ subunits are prenylated, which is important for membrane localization of the $G\beta\gamma$ dimer. For the formation of the heterotrimer, the $G\alpha$ subunit binds to the $G\beta$ subunit at the C-terminal side of the seven-bladed propeller structure (Clapham and Neer, 1997; McCudden et al., 2005). It was initially thought that the sole function of the $G\beta\gamma$ dimer was to act as a guanine-nucleotide dissociation inhibitor (GDI) for the GPCR-bound $G\alpha$ subunit, preventing exchange of GDP for GTP. However, many downstream targets for the free $G\beta\gamma$ subunit have been discovered, including Na^{2+} , K^+ and Ca^{2+} channels; phospholipase A, phospholipase C, serine/threonine and tyrosine kinases, small GTPases, and various adenylyl cyclase isoforms (Jones et al., 2004).

Heterotrimeric G protein signaling in fungi

In fungi, GPCRs sense changes in nutrients, light, pH, osmolarity, and the presence of pheromones (Bolker, 1998; Li et al., 2007b). The initial sequencing and annotation of *N. crassa*, which was the first of the filamentous fungi, revealed five classes of GPCRs: pheromone receptors, cAMP receptor-like proteins, carbon sensors, putative nitrogen sensors, and microbial opsins; these groups have been used as a convention for all filamentous fungi (Borkovich et al., 2004; Galagan et al., 2003; Li et al., 2007b). Three additional GPCR classes were predicted after the release of the *M. grisea* genome: the PTH11-related receptors, which are homologs of *M. grisea* PTH11, a GPCR required for pathogenicity; the mPR-related receptors, which are similar to the human mPR steroid receptor; and proteins homologous to the rat growth hormone releasing factor-related proteins (Kulkarni et al., 2005). Additionally, a homolog of Arabidopsis AtRGS-1, which contains an RGS box and a seven-transmembrane helical region, has been identified in *A. nidulans* (GprK) and some other fungi (Chen et al., 2003; Lafon et al., 2006; Li et al., 2007b). RGS proteins accelerate the GTPase activity of G α subunits and will be described in greater detail later in this Chapter. The seven-transmembrane region of AtRGS-1 is very different from any GPCR in animals, and a functional GPCR protein has yet to be described in plants. Given this and the observation that the Arabidopsis G α subunit AtGpa1p has very slow GTPase activity and very fast exchange rate of GDP for GTP, a mechanism has been theorized where by plant G α subunits are by default in the GTP-bound state and are ‘activated’ by RGS proteins

(Temple and Jones, 2007). Therefore, it is interesting that fungi contain an AtRGS-1 homolog, as there is no homolog in animals.

There are three main classes of G α subunits in filamentous fungi, classified as group I, II, or III (Bolker, 1998; Kays and Borkovich, 2004b; Li et al., 2007b). The group I G α 's are highly conserved among most filamentous fungi. The first group I G α identified in filamentous fungi was *N. crassa* GNA-1, which is 55% identical to mammalian G α_i (Turner and Borkovich 1993). GNA-1 was discovered using combinations of degenerate primers with homology to conserved regions of G α proteins from various organisms (Turner and Borkovich, 1993). GNA-1 contains a consensus sequence for myristoylation (MGXXS) at the N-terminus (Buss et al., 1987) and a site for ADP-ribosylation by pertussis toxin (CXXX) at the C-terminus (West et al., 1985), which is conserved in G α_i proteins.

Group I proteins have been implicated in a wide variety of functions in filamentous fungi. In *N. crassa*, GNA-1 is involved in growth rate, aerial hyphae formation, conidiation, osmotic stress, heat stress, female fertility, and has also been shown to positively regulate adenylyl cyclase activity (Ivey et al., 1996; Yang and Borkovich, 1999). Defects in $\Delta gna-1$ also resulted in small, infertile protoperithecia in less abundance than wild-type (Yang and Borkovich, 1999). In *Aspergillus nidulans*, FadA plays a role in growth, asexual and sexual sporulation, and ST toxin production (Hicks et al., 1997; Yu et al., 1996). Genetically FadA was shown to be upstream of PKA, which suggests that FadA negatively regulates sporulation and toxin production through a conserved cAMP signaling pathway (Shimizu and Keller, 2001). In the grey

mold fungus *Botrytis cinerea*, the group I G α BCG-1 is important for colony morphology, protease secretion, and pathogenicity (Gronover et al., 2001). In other fungi, group I G α proteins have been found to play a role in growth, virulence, asexual sporulation, and mating (Bolker, 1998). This suggests a role for group I G α proteins in multiple downstream signaling pathways.

The group II G α proteins were characterized based on their homology to GNA-2, the group II G α in *N. crassa*, which was isolated the same way as GNA-1 (Kays and Borkovich, 2004b; Turner and Borkovich, 1993). GNA-2 is 49% identical to GNA-1, yet lacks the consensus sequences for N-terminal myristoylation and the C-terminal ADP-ribosylation site. G α proteins belonging to group II are unique to the filamentous fungi. The function of group II G α proteins is less obvious than group I in most organisms. So far, the only phenotype found for a single gene deletion mutant of *gna-2* is a decrease in hyphal mass when grown on medium containing glycerol as a carbon source (Li and Borkovich, 2006). In addition, introduction of a GTPase-deficient allele of *gna-2* (*gna-2*^{Q205L}) caused a slight increase in germination rate and aerial hyphae height (Baasiri et al., 1997). However, the strongest phenotype for Δ *gna-2* is noted when this gene is deleted in a background lacking *gna-1* or *gna-3* (a Group III G α); such studies revealed an intensification of the single mutant phenotypes (Baasiri et al., 1997; Kays and Borkovich, 2004a-b). This suggests a compensatory and/or highly specialized role for GNA-2 in *N. crassa*. In *M. grisea*, deletion of *magC* gene caused a reduction in conidia formation, but had no effect on vegetative growth or virulence (Liu and Dean 1997). In *B. cinerea*, *bcg-2* deletion mutants show slight reduction in pathogenicity, but are still

able to infect plants (Gronover et al 2001). All other group II G α studies have either not been studied or no substantial function has been reported.

The group III G α proteins were tentatively named the G α_s analogous group due to the fact that some group III proteins were shown to activate adenylyl cyclase (Bolker 1998). However, *N. crassa* GNA-3 has no similarity to G α_s proteins and actually has some homology to human G α_{i2} (49%), although no consensus sequences for myristoylation or ADP-ribosylation by pertussis toxin are present on the protein. Therefore, like Group II G α proteins, Group III G α proteins are unique to fungi. The *gna-3* gene was discovered using PCR with degenerate G α primers in a *N. crassa* mutant lacking both *gna-1* and *gna-2* (Kays et al., 2000a). The gene deletion mutant of *gna-3* has short aerial hyphae, premature, dense conidiation in plate cultures, and inappropriate conidiation in submerged cultures. Furthermore, GNA-3 may be involved in the stability of adenylyl cyclase protein levels (Kays and Borkovich 2000, Ivey et al 2002). This is similar to *A. nidulans* GanB, which negatively regulates asexual sporulation (Chang et al 2004) and is necessary for production of cAMP (Chang et al., 2004; Lafon et al., 2006). In *B. cinerea*, BCG3 is upstream of cAMP production and is required for germination and virulence ((Doehlemann et al., 2005). Group III G alphas are generally involved in conidiation, germination, and pathogenicity, through cAMP-mediated pathways.

In contrast to animals, most fungi contain only one G β and one G γ subunit (Li et al., 2007b). In the yeast pheromone response pathway, the G $\beta\gamma$ dimer (Ste4p/Ste18p) activates the Ste11p MAPK cascade, which causes the transcription of mating type specific genes; and binds to Far1p, which inhibits the cell cycle (Bardwell 2005). Until

recently it was thought that the $G\alpha$ subunit, Gpa1p, played a minor role in the pheromone pathway as a negative regulator of the $G\beta\gamma$ dimer. However, it has recently been reported that Gpa1p localizes to the endosome to facilitate the production of PIP3, which is thought to recruit Bem1p, an activator of the MAPK cascade (Slessareva et al., 2006). It has also been discovered that Gpa1p can bind to Kar3p, a kinesin-like motor protein that is involved in pheromone-induced nuclear migration in yeast (Zaichick et al., 2009). In filamentous fungi, however, the $G\alpha$ subunit acts downstream of GPCR signaling and a $G\beta\gamma$ -specific effector has yet to be identified. Gene deletion mutation of the *N. crassa* $G\beta$ (*gnb-1*) and $G\gamma$ (*gng-1*) genes have shared phenotypes, including female sterility, reduced hyphal mass, and abundant production of conidia (Krystofova and Borkovich, 2005; Yang et al., 2002). The identical phenotypes of the Δ *gnb-1* and Δ *gng-1* mutants can be attributed to the low levels of GNG-1 protein in the Δ *gnb-1* mutant, and vice versa. Most of the defects of the Δ *gnb-1* and Δ *gng-1* mutants can be explained by the low levels of $G\alpha$ proteins, a phenomenon that is also observed in the fungal plant pathogen *Cryphonectria parasitica* (Kasahara et al., 2000). This suggests a role for the $G\beta\gamma$ dimer in $G\alpha$ protein stability in filamentous fungi.

Regulators of G protein signaling- RGS proteins

There are several classes of proteins which regulate heterotrimeric G protein signaling (Siderovski and Willard, 2005). One such group, RGS proteins, are GTPase activating proteins (GAPs) which negatively regulate $G\alpha$ proteins by binding to the

transition state during GTP hydrolysis and accelerating their GTPase activity. RGS proteins contain a highly conserved, approximately 130 amino acid RGS box, and are found in a wide variety of organisms including animals, plants, and fungi (Ross and Wilkie, 2000). RGS proteins also contain a number of other functional domains, such as those for G β binding, membrane targeting, Ras binding, and GoLoco domains (McCudden et al., 2005). There are over 30 RGS proteins in mammals (Jean-Baptiste et al., 2006) and only one RGS protein in plants (Chen et al., 2003). The most well studied RGS protein is Sst2p from *S. cerevisiae* which serves as a model for RGS function in mammals. Sst2p has been shown to negatively regulate the G α protein Gpa1p in the mating pathway. There are three additional RGS proteins in *S. cerevisiae*: Rgs2p, which regulates the G α protein Gpa2p in the sugar sensing pathway, Rax1p, which is important for cell polarity, and Mdm1p, which is important for proper inheritance of mitochondria and nuclei during cell division (Hill et al., 2006).

There are five conserved RGS proteins in most filamentous fungi which have been identified and/or characterized most extensively in *Aspergillus nidulans* (Han et al., 2004; Lafon et al., 2006; Lee and Adams, 1994; Yu et al., 1996). The first *A. nidulans* RGS characterized was FlbA, which is most similar to *S. cerevisiae* Sst2p and contains an RGS domain and DEP (Dishevelled/EGL-10/Pleckstrin) domain for membrane targeting (Han et al., 2004; Lee and Adams, 1994). A *flbA* null mutant strain has undifferentiated aerial hyphae which lack conidiophores, and exhibits autolysis after a few days of growth. A GTPase-deficient allele of the G α gene *fadA* causes a similar phenotype as loss of *flbA*, and deletion of *fadA* in the *flbA* mutant background suppresses the *flbA*

phenotype (Yu et al., 1996). This suggests that the RGS protein FlbA regulates FadA during asexual sporulation. The second RGS characterized, RgsA, is most similar to *S. cerevisiae* Rgs2p, and contains a conserved RGS domain (Han et al., 2004). Deletion of *rgsA* causes decreased colony growth, increased aerial hyphae formation, and increased pigment formation. This phenotype is suppressed by deletion of the $G\alpha$ gene *ganB*, suggesting that RgsA negatively regulates GanB signaling. The three other RGS proteins in filamentous fungi have been identified, but not well characterized (Han et al., 2004; Lafon et al., 2006). *A. nidulans* RgsB is most similar to *S. cerevisiae* Rax1p and contains an RGS domain and three transmembrane regions; and RgsC is most similar to *S. cerevisiae* Mdm1p and mammalian Rgs-Px1, which has been shown to be a GAP for $G\alpha_s$ and a sorting nexin (SNX) protein in vesicular trafficking (Zheng et al., 2001). The last RGS protein found in fungi is the previously mentioned homolog of *Arabidopsis* AtRGS1, *A. nidulans* GprK (Lafon et al., 2006). AtRGS1 has been shown to exhibit GTPase acceleration activity toward the $G\alpha$ protein AtGPA1P and is involved in sugar sensing (Grigston et al., 2008; Johnston et al., 2007). A function for *A. nidulans* GprK and homologs in filamentous fungi have yet to be reported.

A few RGS proteins have been studied in other filamentous fungi. For example, *C. neoformans*, RGS protein Crg1 was found to have GAP activity toward Gpa2 and Gpa3 (GNA-1 and GNA-2 homologs), which are important in the pheromone response pathway and virulence (Li et al., 2007a; Wang et al., 2004). RGS protein Crg-2 was found to down-regulate Gpa1p (GNA-3 homolog) cAMP signaling and serve as a GAP for Gpa1p and Gpa3 (Shen et al., 2008; Xue et al., 2008). Homologs of all four *A.*

nidulans RGS proteins and the AtRGS-1 homolog have been identified in *N. crassa* and gene deletion mutants are still in the process of being characterized (Wright, Li, Schacht, and Borkovich, unpublished).

Non-GPCR guanine nucleotide exchange factors – RIC-8 and Arr4p

G α proteins are activated by the exchange of GTP for GDP. This exchange was thought to occur strictly by the GPCR, until the fairly recent discovery of two non-receptor GEFs, RIC-8 and Arr4p. RIC-8 was first discovered in a screen of *C. elegans* mutants to resistance to the drug alicarb, an inhibitor of acetylcholinesterase which causes a toxic level of acetylcholine accumulation in neurons (Miller et al., 1999). The genes identified in this screen were systematically named resistance to inhibitors of cholinesterase (RIC). Additional studies by members of this group found that RIC-8 is necessary for EGL-30 (G α_q), GOA-1 (G α_o) and GSA-1 (G α_s) signaling in the *C. elegans* nervous system, and for GOA-1 (G α_o)-mediated centrosome movement in early embryogenesis (Miller et al., 2000a; Miller and Rand, 2000b-b; Reynolds et al., 2005; Schade et al., 2005). Subsequent studies of Ric-8 in *Drosophila*, *Xenopus*, mice, and human cell culture have shown similar functions to *C. elegans* RIC-8 (Nishimura et al., 2006; Romo et al., 2008; Tonissoo et al., 2006; Wang et al., 2004). Cell division in early embryogenesis involves asymmetric positioning of the mitotic spindle by pulling forces of astral microtubules (Horvitz and Herskowitz, 1992). Data supports a mechanism where GPR1/2 (GoLoco domain) proteins localized at one end of the embryo form a membrane anchored complex with G $\alpha_{o/i}$, RIC-8, RGS7, dynein, and astral microtubules,

and that the cycling of the GDP and GTP binding of the $G\alpha$ protein causes an oscillation in microtubule pulling forces (Afshar et al., 2004; Nguyen-Ngoc et al., 2007; Tall and Gilman, 2005; Tall et al., 2003a; Woodard et al., 2010). RIC-8 homologs are found in animals and fungi, but not in plants, protists, or most yeast, including *S. cerevisiae* (Wilkie and Kinch, 2005a).

The mammalian homolog of yeast Arr4p, Asna-1, is involved in the C-terminal insertion of proteins into the ER membrane, and is early embryonic lethal when knocked out in mice (Mukhopadhyay et al., 2006; Stefanovic and Hegde, 2007). Yeast Arr4p has been recently characterized as a non-receptor guanine-nucleotide exchange factor involved in the pheromone response pathway (Lee and Dohlman 2008). Similar to RIC8 in animals, Arr4p binds to the GDP-bound form of the $G\alpha$ subunit Gpa1p and increases the exchange rate of GDP for GTP (Lee and Dohlman 2008). Arr4p is also shown to promote pheromone signaling *in vivo*, which is consistent with a role for Gpa1p independent of $G\beta\gamma$ and the GPCR in the pheromone response pathway. Though *S. cerevisiae* does not contain a RIC8 homolog, filamentous fungi contain an Arr4 homolog. In fact, the crystal structure of the Arr4p homolog from the filamentous fungus *Chaetomium thermophilum* was recently reported (Bozkurt et al., 2009).

This dissertation describes the characterization of the RIC8 protein in *N. crassa*. The only other study of a RIC8 homolog in filamentous fungi has been reported very recently in the fungal rice pathogen *Magnaporthe oryzae* (Li et al 2010). *Magnaporthe* RIC8 (MoRic8) was discovered in a screen for non-pathogenic T-DNA insertion mutants. MoRic8 was shown to bind to the $G\alpha$ subunit MagB in the yeast two-hybrid assay, and is

highly expressed in the appressorium, a specialized structure that invades plant tissue. MoRic8 was also found to be upstream of the cAMP pathway, which regulates appressorium formation. These results are discussed further in Chapter 3 and in comparison to the results I have obtained in *N. crassa*.

Specific Aims and Major Conclusions

In this dissertation, I intend to provide a contribution to the extremely complex mechanisms of G protein signaling. In *N. crassa*, the G α subunit GNA-1 is important for apical extension and hyphal mass, many aspects of the conidiation pathway, and female fertility. The multiple functions for GNA-1 suggest that it acts upstream of more than one signaling pathway. In Chapter 2, I discuss potential GNA-1 interacting proteins discovered in a screen using a yeast two-hybrid cDNA library. One of these interactors is the glycolytic enzyme GAPDH, for which I show a reduction in enzyme activity in *N. crassa* strains containing GTPase-deficient alleles of *gna-1*. I also report many interesting potential interactors for GNA-1 which are involved in protein translation, synthesis of sphingolipids, synthesis of vitamin B6, and actin filamentation; as well as two apparent fungal-specific proteins of unknown function. Further investigation into these potential interactors will surely result in novel functions for GNA-1.

The main aspect of this dissertation focuses on the characterization of a novel GEF for filamentous fungal G α subunits, RIC8. In Chapter 3, I show genetic and biochemical evidence for a role of RIC8 in the activation of GNA-1 and GNA-3. I also demonstrate a function for RIC8 in many aspects of the *N. crassa* lifestyle, including

polar cell growth, nuclear morphology, septal formation, and conidia development. In Chapter 4, I report the expression and purification of epitope-tagged versions of *N. crassa* RIC8 and G α subunits from *E. coli*. I also show that RIC8 can act as a GEF for GNA-1 and possibly GNA-3 *in vitro*.

Overall, my work demonstrates a major role for RIC8 in *N. crassa* growth and morphology, as well as G protein regulation. These results will open up doors for research of novel aspects of heterotrimeric G protein signaling in *N. crassa*.

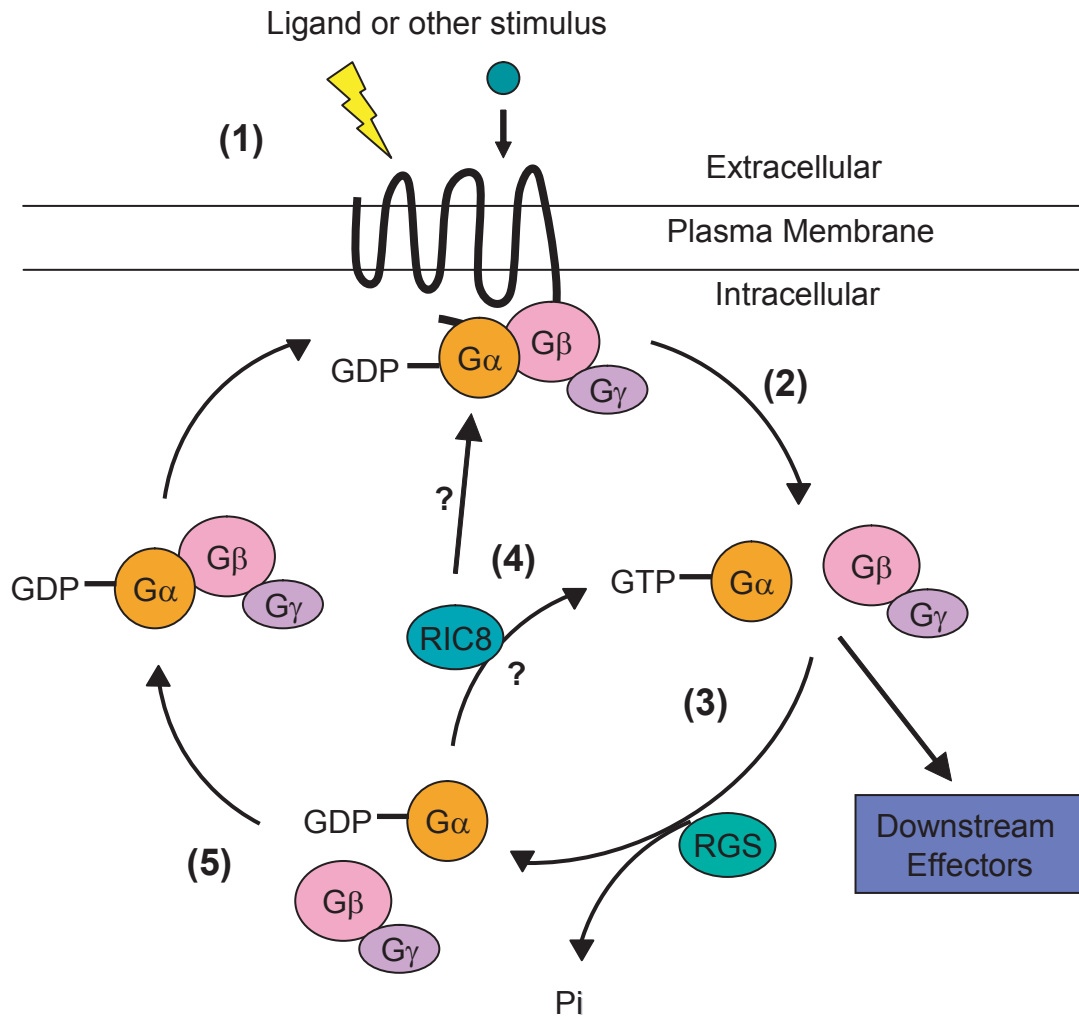


Figure 1.2: Heterotrimeric G protein signaling pathway

Heterotrimeric G protein signaling involves activation of a G protein-coupled receptor (GPCR) in response to a ligand, light, or other extracellular stimulus (1). A heterotrimer of G proteins is bound intracellular to the GPCR, with the G α subunit bound to GDP. Upon activation, a conformational change takes place in the GPCR causing the G α subunit to exchange GDP for GTP and dissociate from the G $\beta\gamma$ dimer and the GPCR (2). The free G α and G $\beta\gamma$ subunits are free to interact with downstream effectors. The intrinsic GTPase activity will cause hydrolysis of GTP to GDP and P_i (3). This GTPase activity can be accelerated by a protein called RGS. Once the G α subunit is bound to GDP, it will associate with G $\beta\gamma$ and return to the receptor (5). The GTP binding of the G α subunit can also be facilitated by a non-GPCR guanine-nucleotide exchange factor (GEF) RIC8. Though the mechanism for how this occurs is not fully understood, it is hypothesized that RIC8 activates either free G α -GDP which has been activated by one round of GPCR activation but has not yet returned to G $\beta\gamma$ and the receptor, or may be able to remove G α from the receptor as part of an unknown complex (4).

Chapter 2: Identification of novel GNA-1 binding partners

Abstract

Heterotrimeric G protein signaling pathways are important for eukaryotic cells to respond to various environmental signals. It has been previously reported that the $G\alpha_i$ homolog, GNA-1, in the filamentous fungus *Neurospora crassa*, is required for female fertility, vegetative growth and stress responses. Such a broad impact for GNA-1 suggests that there are multiple proteins with which it interacts. Results in this Chapter present novel proteins that were found to interact with GNA-1 in the yeast two-hybrid system. One of the interacting proteins, glyceraldehyde-3-phosphate dehydrogenase (GAPDH), converts glyceraldehyde-3-phosphate to 1,3 bis-phosphoglycerate during glycolysis, which is one step upstream of the first ATP-producing step. The activity of this enzyme was tested in wild-type and in strains lacking *gna-1* or containing a GTPase-deficient allele of *gna-1*, in order to determine whether the presence of the GTP-bound state of GNA-1 influences GAPDH activity. The strain containing the GTPase-deficient allele of *gna-1* exhibited more than a 1/3 reduction in GAPDH activity compared to wild type, suggesting that GNA-1 binding leads to inhibition of GAPDH activity.

Introduction

The G α subunit GNA-1 in *Neurospora crassa* has been shown to be vital for proper cell growth and differentiation. The gene deletion mutant of *gna-1* exhibits growth and developmental defects including a reduction in mass, short aerial hyphae, and smaller conidia that are delayed in formation as compared to wild-type (Ivey et al., 1996); and production of more conidia per aerial hyphae than wild-type (Yang and Borkovich, 1999). The Δ *gna-1* mutant also has defects in the sexual cycle, including production of small, infertile protoperithecia in less abundance than wild type. A strain containing a GTPase-deficient allele of *gna-1* (*gna-1*^{Q204L}) was found to have more mass, longer aerial hyphae, and less conidia per aerial hyphae and fewer and larger perithecia as compared to wild-type (Yang and Borkovich, 1999). The large number of phenotypes observed in mutants is evidence that GNA-1 affects a wide variety of cellular signaling pathways in *N. crassa*.

Adenylyl cyclase converts ATP to cAMP and is one of the downstream effectors regulated by G proteins in many systems (Neves et al., 2002). In *N. crassa*, the adenylyl cyclase protein, CR-1, has been characterized for GTP-stimulatable activity and regulation of cAMP levels (Ivey et al., 1999). In Δ *gna-1* mutants, the GTP-stimulatable activity of CR-1 is reduced in comparison to wild type, but CR-1 protein levels are unchanged, suggesting that GNA-1 regulates GTP-stimulated CR-1 activity. In addition, when anti-GNA-1 antibody is added to wild-type extracts, CR-1 activity is reduced, suggesting a direct interaction between GNA-1 and CR-1 (Ivey et al., 1999).

Since GNA-1 has been found to affect a wide variety of signaling pathways, a yeast two-hybrid cDNA library was constructed and screened to identify novel proteins that interact with GNA-1. The yeast two-hybrid assay is a technique in molecular biology that is used to study protein interactions (Fields, 1989). This technique takes advantage of the modular nature of transcription factors, as each contain a DNA binding domain which binds to a specific promoter region, and an activation or repression domain, which can either activate or repress transcription. To implement the assay, the proteins of interest are expressed in yeast as fusion proteins with either the activation domain or the DNA binding domain of the transcriptional activator Gal4. Additionally, there are engineered genes (reporters) in the yeast genome which contain specific binding sites for this transcription factor. If the two proteins of interest interact, the two modules of the transcription factor come together and can turn on expression of these 'reporter genes'. To take it a step further, a cDNA library containing a representation of all the mRNAs expressed in a cell, tissue type, or specific condition can be constructed and screened to identify novel protein interactions (Chien, 1991). I used this approach to identify novel interacting partners for GNA-1.

Materials and Methods

Strains and growth conditions

Neurospora crassa strains used in this study are wild-type (WT, FGSC #2489, *matA*), $\Delta gna-1$ ($\Delta gna-1::hph^+$, 1B2a or 1B4A, (Ivey et al., 1999) and *gna-1** ($\Delta gna-1::hph^+$, *gna-1^{Q204L}::his3⁺*, H. Kim, unpublished). All cultures were inoculated with conidia from cultures grown for 5-10 days in 125 mL flasks containing 30 mL VM agar (see below for components). Flasks were incubated at 30°C in the dark for three days and at 25°C in the light for another 2-7 days. Conidia were harvested from flasks by adding 50 mL sterile water and straining through sterile cheesecloth into a 50 mL Falcon tube (BD Biosciences, San Jose, CA). The conidia were washed two times by the addition 20-30 mL sterile water and centrifugation at 2500 RPM for 5 min. using an IEC Centra CL3 centrifuge with an IEC 243 rotor (Thermo Scientific, Waltham MA). Conidia were resuspended in 800-1200 μ L sterile water and quantified using a Bright-Line™ Hemacytometer (Pfizer, New York, NY).

All yeast strains were from the BD matchmaker library construction and screening kit (Clontech, Palo Alto, CA). *S. cerevisiae* strains Y187 (genotype *MAT α ura3-52 his3-200 ade2-101 trp1-901 leu2-3,112 gal4 $\Delta met^- gal80\Delta URA3::GAL1_{UAS}-GAL1_{TATA}-lacZ$*), and AH109 (genotype *MAT α trp1-901 leu2-3,112 ura3-52 his3-200 gal4 $\Delta gal80\Delta LYS2::GAL1_{UAS}-GAL1_{TATA}-HIS3 GAL2_{UAS}-GAL2_{TATA}-ADE2 URA3::MEL1_{UAS}-MEL1_{TATA}-lacZ$*) were used in all yeast two-hybrid assays.

Plasmids were maintained in *Escherichia coli* strain DH5 α (Hanahan, 1983). *E. coli* was transformed with purified plasmids, ligation reactions or yeast DNA by either CaCl₂ mediated transformation or electroporation. For CaCl₂ mediated (chemical competent) transformation, a 50-200 μ L aliquot of chemical competent cells (log phase cells, O.D.₆₀₀ between 0.6 and 0.8, in 10 mM MOPS pH 7.0, 10 mM RbCl, 50 mM CaCl₂, and 15% glycerol) was thawed on ice for 10-20 min. and 1-10 μ L plasmid DNA or ligation reaction was added and the solution was incubated on ice an additional 20 min. The tube was transferred to a 42°C water bath and incubated 1.5-2.5 min. To the tube, 1 mL LB medium (10 g bactotryptone, 5 g NaCl, 5 g yeast extract, and 10 g agar (if needed) in 1 L water) was added and incubated 30-60 min. at 37°C. Cells were plated on LB medium with appropriate antibiotic and incubated at 37°C for 12-18 hours. For electroporation, a mixture of 1-5 μ L DNA and 40 μ L electro-competent cells (log phase cells, O.D.₆₀₀ between 0.5 and 0.8, in 10% glycerol), was incubated on ice for 1-5 min (Dower et al., 1988). Cells were then transferred to a 2 mm cuvette and pulsed at 2500 V. SOC medium (1 mL; 2% Bactotryptone, 0.5% Yeast extract, 10 mM NaCl, 2.5 mM KCl, 10 mM MgCl₂, 10 mM, 10 mM MgSO₄, and 20 mM glucose) was added immediately and cells incubated at 37°C for 30-60 min. Cells were plated on LB plates supplemented with appropriate medium and grown as indicated above.

To obtain plasmid DNA, *E. coli* cells were inoculated in 1-5 mL LB with appropriate antibiotics, incubated 12-18 hours at 37°C and 225 RPM, and pelleted by centrifugation at 15,000 RPM for 15 sec. using a micro-centrifuge (IEC Micromax, Thermo Scientific). Plasmids were recovered by using the boiling mini-prep protocol or

the QIAprep mini-prep kit (Qiagen). For boiling mini-prep, 300 μ L STET buffer (8% sucrose, 50 mM TrisCl pH 8.0, 50 mM EDTA, and 5% Triton X-100) was added to the cell pellet and mixed by pipeting. The cells were lysed by the addition of 20 μ L of a 10 mg/mL lysozyme solution and incubated in a water bath at 95°C for 2 min. The tube was centrifuged for 5 min at 15,000 RPM and the pellet was removed carefully with a toothpick. To the supernatant, 300 μ L of ammonium acetate/isopropanol solution (5:12 mixture of 8 M ammonium acetate and 100% isopropanol) was added and mixed by inverting the tube 5-10 times. The tube was centrifuged for 5 min. at 15,000 RPM, supernatant removed, and pellet washed with 500 μ L 70% EtOH. The pellet was dried in a speed-vac concentrator (Thermo Scientific), resuspended in 25-50 μ L TE buffer (10 mM TrisCl pH 8.0, 1 mM EDTA) and stored at -20°C. The QIAprep miniprep procedure is based on alkaline lysis of bacterial cells, binding of DNA onto a silica column in the presence of high salt, and elution using a low salt buffer (Qiagen). This procedure was used when DNA free of protein, polysaccharide, or high salt was needed according to manufacturer's protocols. DNA fragments were separated by electrophoresis using a 1-2% agarose gel in TAE buffer (40 mM Tris-Cl pH 7.6, 20 mM acetic acid, and 1 mM EDTA) at 70-90 mA. Gels were soaked for 10-20 min. in a solution of Ethidium Bromide in TAE (approximately 0.5 μ g/mL) and visualized on a Biochemi System imager (UVP, Upland, CA).

Media and Solutions

Neurospora crassa strains were maintained on Vogel's minimal medium (VM;(Vogel, 1964). VM medium consists of 1.5% sucrose, 1x VM salts (from 50x VM stock), 1% agar (if needed) and water. The 50x VM stock consisted of 125 g $\text{Na}_3\text{C}_6\text{H}_5\text{O}_7 \cdot 2\text{H}_2\text{O}$, 250 g KH_2PO_4 , 100 g NH_4NO_3 , 10 g $\text{MgSO}_4 \cdot 7\text{H}_2\text{O}$, 5 g $\text{CaCl}_2 \cdot 2\text{H}_2\text{O}$ (pre-dissolved in a small amount of water), 5 mL trace element solution, 5 mL of a 50 $\mu\text{g}/\text{mL}$ solution of biotin in 50% ethanol, and 5 mL chloroform (preservative) brought up to 1 L in water (Davis and de Serres, 1970; Vogel, 1964). Trace elements were made by adding 5 g citric acid $\cdot \text{H}_2\text{O}$, 5 g $\text{ZnSO}_4 \cdot 7\text{H}_2\text{O}$, 1 g $\text{Fe}(\text{NH}_4)_2(\text{SO}_4)_2 \cdot 6\text{H}_2\text{O}$, 0.25 g $\text{CuSO}_4 \cdot 5\text{H}_2\text{O}$, 50 mg H_3BO_3 , 50 mg $\text{MnSO}_4 \cdot \text{H}_2\text{O}$, and 50 mg $\text{Na}_2\text{MoO}_4 \cdot 2\text{H}_2\text{O}$ to a total volume of 100 mL in water. Synthetic crossing medium (SCM, (Westergaard and Mitchell, 1947) was used to induce the formation of unfertilized female structures (protoperithecia). SCM media was made by adding 1 g KNO_3 , 0.7 g K_2HPO_4 , 0.5 g KH_2PO_4 , 0.1 g NaCl , 0.1 g $\text{CaCl}_2 \cdot 2\text{H}_2\text{O}$ (dissolved in water separately), 0.5 g $\text{MgSO}_4 \cdot 7\text{H}_2\text{O}$ (dissolved in water separately), 100 μL biotin stock solution, 100 μL trace element stock solution, 15 g sucrose, and 10 g agar (if needed) to a total volume of 1 L in water. YPDA yeast medium was used to culture and maintain *S. cerevisiae* without selection. YPDA was made by combining 10 g yeast extract, 20 g dextrose, 20 g peptone, 10 g agar (if needed) and 0.1 g adenine hemisulfate in 1 L water. Synthetic dextrose (Dower et al.) medium was used to culture yeast with auxotrophic selectivity. To make SD medium, 6.7 g yeast nitrogen base without amino acids and 15 g agar was added to 1 L water and pH adjusted to 5.8 with NaOH. To make SD dropout (DO) medium, 2 g of the

appropriate drop out mix (US Biological, Swampscott, MA) was added to 1 L SD medium. Dropout mix consists of all amino acids except those that are needed for selection. For example, if selection is for a yeast strain that has gained the ability to synthesize leucine, the SD medium would be made with dropout mix minus leucine, and denoted as SD/-leu. SD lacking tryptophan and leucine is denoted as SD/double dropout, or SD/DDO; SD lacking tryptophan, leucine, and histidine is denoted as SD/triple dropout, or SD/TDO; and SD lacking tryptophan, leucine, histidine and adenine is denoted as SD/quadruple dropout, or SD/QDO.

E. coli cells were grown and maintained in LB medium (10 g bactotryptone, 5 g NaCl, 5 g yeast extract, and 10 g agar (if needed) in 1 L water). Where indicated, ampicillin (amp), histidine (his), and inositol (inl) were used at 100 µg/ml; chloramphenicol (cam) at 35 µg/mL, kanamycin (kan) at 150 µg/mL and hygromycin (hyg) at 200 µg/ml. DEPC (diethyl pyrocarbonate) treated water was used for all solutions requiring RNase-free water. DEPC-H₂O was prepared as follows: add 0.2% v/v DEPC to ultra-pure water, mix well, and let stand 12-16 hours at room temperature. Autoclave for 15-20 min. to inactivate DEPC, which breaks down into ethanol and CO₂.

cDNA library construction

cDNA was generated separately from submerged liquid culture tissue (by S. Wright) and from tissue grown on SCM plates (by H. Kim), and pooled together at the yeast transformation step to create the cDNA library (see below). For submerged culture tissue, 100 mL VM liquid was inoculated with wild-type strain FGSC #2489 at 1×10^6

conidia per mL and grown at 30°C in the dark with shaking at 200 RPM for 16 hrs. Mycelia were collected by vacuum filtration on 25 µm filter paper (Whatman Inc., Piscataway, NJ), transferred to a 50 mL falcon tube and then frozen in liquid nitrogen.

Total RNA was extracted using the Purescript RNA isolation kit with some modification of the manufacturer's protocol (Gentra Systems, Minneapolis, MN). Tissue was ground to a powder in liquid nitrogen using a mortar and pestle. Approximately 25 mg ground tissue (2 scoops with a small, flat spatula) was added to 300 µL cell lysis solution and mixed gently by inverting. A volume containing 100 µL of DNA-protein precipitation solution was added; and the solution was mixed by gentle inversion and placed on ice for 10 min. The sample was then centrifuged in a microcentrifuge at 15,000 RPM for 3 min. at 4°C and the supernatant was removed and placed on ice for 10 min. This centrifugation step, which separates supernatant (RNA-enriched) from pellet (DNA and protein), was repeated once. To the supernatant, 300 µL isopropanol was added and the solution left at 25°C for 1-3 min. to precipitate RNA. The solution was then centrifuged at 15,000 RPM for 3 min. at 25°C. The supernatant was removed, and then 300 µL of 70% ethanol in DEPC-H₂O was added, followed by centrifugation at 15,000 RPM for 1 min. at 25°C. This wash step was repeated once. The pellet was air-dried for 15 min. at room temperature and then hydrated in 100 µL DEPC-H₂O with 0.5 µL RNA guard (GE Healthcare, Piscataway, NJ) for 30 min. on ice. The sample was mixed by dragging the tube against a microtube rack (to avoid shearing RNA), centrifuged at 15,000 RPM for 10 sec., and stored at -80°C. mRNA was isolated from total RNA using the Oligotex mRNA minikit (Qiagen, Inc., Valencia, CA), which

captures mRNA based on hybridization of the polyA (adenosine monophosphate) 3' end of the mRNA to a polystyrene-latex immobilized oligo containing 30 dT (deoxythreonine monophosphate).

The cDNA library was generated using the BD matchmaker library construction and screening kit (Clontech). For the reverse transcription reaction, Moloney Murine Leukemia Virus Reverse Transcriptase (MMLV RT) was used to transcribe cDNA from mRNA using primer CDSIII (Clontech). The MMLV RT also adds a few residues, primarily deoxycytosine (dC), to the 5' end of the cDNA. Also added to the RT reaction was the BD SMART III primer (Clontech), which anneals to the dC enriched 5' end of the cDNA. The mRNA was primed for the RT reaction by adding 2 μ L mRNA (0.6-1.2 μ g), 1 μ L CDS III primer, 1 μ L BD SMART III primer, and 1 μ L DEPC-H₂O to a PCR tube and incubating at 72°C for 2.5 min.; then cooled on ice for 2 min. After a 10 sec. spin, 2 μ L of 5X first strand buffer (Clontech), 1 μ L of 20 mM dithiothreitol (DTT), 1 μ L of 10 mM dNTPs, and 1 μ L of MMLV RT were added to the RNA and the RT reaction was carried out for 1 hour at 42°C. cDNA was amplified using LA Taq polymerase (Takara, Japan). Primers were used that anneal to the 5' and 3' priming sites (5' PCR primer and 3' PCR primer, Clontech). The PCR reaction mixture contained 2 μ L RT reaction, 73 μ L water, 10 μ L 10X LA Taq buffer, 10 μ L dNTP, 2 μ L 5' PCR primer, 2 μ L 3' PCR primer, and 1 μ L LA Taq polymerase. Thermocycler temperatures used were: 95°C for 30 sec. (initial denaturation), 25 cycles of: 98°C for 10 sec. and 68°C for 6 min. (denaturation and annealing/elongation step); and 68°C for 5 min. (final elongation).

Double-stranded cDNA was purified using the BD Chroma Spin TE-400 column (Clontech). Sequences added to the ends of the cDNA during the RT and PCR reactions are homologous to the ends of *Sma*I restriction enzyme-digested pGADT7rec plasmid; therefore homologous recombination in *S. cerevisiae* was used to directly create the library. cDNA created from submerged liquid culture and SCM tissue (10 μ L each, 20 μ L total) and linearized pGADT7rec (6 μ L, provided in kit) were co-transformed into yeast strain AH109 using a modified lithium-chloride mediated transformation protocol. Strain AH109 was cultured by diluting 1 mL of an overnight culture into 50 mL YPDA, and cultured until the O.D.₆₀₀ was between 0.6 and 1.0. Cells were then centrifuged for 5 min. at 2500 RPM. Cells were washed with water, pelleted again, and 1 mL of 100 mM LiCl was used to wash the cells. Cells were then centrifuged for 15 sec. and resuspended to a final concentration of 400 μ L of 100 mM LiCl per 1.0 Absorbance unit of cells.

Individual transformations were carried out using 50 μ L of LiCl-suspended cells centrifuged for 15 sec. to remove liquid. To the cell pellet, 326 μ L of transformation mix was added (250 μ L 50% polyethylene glycol 3350, 36 μ L 1M LiCl, and 50 μ L carrier DNA (salmon sperm DNA, boiled 5 min., cooled on ice). To this transformation mix, 34 μ L of DNA mix (20 μ L cDNA, 6 μ L plasmid, 8 μ L water) was added and the suspension mixed by pipeting. The samples were incubated at 30°C for 20-30 min. and then at 42°C for 30 min. After addition of 1 mL YPDA and incubation for 2-3 hours at 30°C, the transformed cells were plated on SD-leu solid medium and grown at 30°C to select for transformants. Positive colonies were pooled in approximately 100 mL YPDA with 20% added glycerol. Aliquots containing 1 mL were made and stored at -80°C.

cDNA library screening

S. cerevisiae strains containing the cDNA library ‘prey’ (AH109, mating type a) and *gna-1* cDNA ‘bait’ (Y187, mating type α) were mated with each other to create heterozygous yeast strains. The bait construct, *gna-1* in pGBKT7 (G1-GBK), was constructed in *E. coli* and transformed into Y187 by H. Kim. I used three colonies of this strain to inoculate 50 mL SD/-trp medium supplemented with 20 $\mu\text{g}/\text{mL}$ kanamycin and cultured overnight at 30°C and 200 RPM. When an O.D.₆₀₀ of 0.8 was reached, the culture was centrifuged at 600 x g for 5 min. The cell pellet was resuspended in 5 mL SD/-trp medium, resulting in a concentration of 4.3×10^9 cells/mL. A 1 mL aliquot of library cells were thawed on ice and, along with the 5 mL G1-GBK culture, and added to 45 mL 2X YPDA+kanamycin (50 $\mu\text{g}/\text{mL}$). The two strains were allowed to mate for 24 hrs. at 30°C, agitating gently at 50 RPM. A strain containing the empty bait vector (pGBKT7) was also mated with a separate library aliquot as a control. The mating reactions were plated on SD/QDO solid medium. The absence of leucine and tryptophan selects for both plasmids, and the lack of adenine and histidine selects for strains with plasmids encoding proteins that bind to GNA-1, as evidenced by the activation of both nutritional reporter genes (see Figure 2.1 for more details about the yeast two-hybrid assay). The ratio of the number of colonies on the control plates versus the G1-GBK screened plates was 1:4. Colonies were streaked onto SD/QDO plates and stored at 4°C.

Analysis of interactors

All yeast strains containing bait and prey plasmids were streaked out on SC/QDO solid medium for single colony isolation two times to ensure strain purity. Positive isolates were first analyzed using two methods to eliminate false positives and self-interacting clones. The first step was to re-constitute the interactions in yeast using purified bait and prey constructs. Each strain was grown by inoculating 1 colony in 3 mL SC/-Trp-Leu overnight at 30°C. Crude DNA was extracted from each yeast strain using a modified ‘Smash N’ Grab’ protocol (Hoffman, 1987) as follows. An aliquot containing 1.5 mL of each overnight culture was centrifuged for 15 sec. to remove medium. The cell pellet was resuspended in 200 μ L lysis buffer (2% Triton X-100, 1% SDS, 100 mM NaCl, 10 mM Tris-Cl pH 8.0, and 1 mM EDTA), 200 μ L 1:1 phenol:chloroform, and approximately 0.3 g of glass beads. The solution was agitated using a vortex mixer twice for 1 min. with 1 min. rests, then centrifuged for 10 min. at 15,000 RPM. An aliquot containing 100 μ L of the supernatant was added to a tube containing 0.3M sodium acetate (10 μ L of 3 M) and 250 μ L 100% Ethanol. The solution was mixed by gently inverting and then centrifuged at 15,000 RPM for 10 min. The pellet was washed once with 70% ethanol and then air dried. The crude yeast DNA was resuspended in 50 μ L TE buffer. Plasmids were then recovered by electroporation into electro-competent *E. coli* strain DH5 α using 1-5 μ L crude yeast DNA as described above. Cells were plated on LB+amp plates and grown overnight at 37°C to select for transformants containing library (pGADT7) vectors.

Individual colonies from each transformation were grown in 2 mL LB liquid medium overnight at 37°C, and plasmids purified using the Qiaprep miniprep kit (Qiagen). Plasmids recovered from *E. coli* were used to transform AH109 using the same lithium chloride mediated transformation as the library construction, except that 5 µL plasmid DNA was used. Each yeast strain was mated to yeast strain Y187 containing either the bait construct (*gna-1* in pGBKT7) or empty vector (pGBKT7) using a method similar to that described above, except that a 25 µL overnight culture of each mating partner was incubated in 1mL YPDA. The cells were plated on SC/DDO solid medium, incubated at 30°C for 2-5 days to ensure mating occurred, then spot-tested on SC/QDO solid medium to test for positive interactions. Strains mated with empty vector that grew on SC/QDO were designated as containing self-activating clones. Strains mated with *gna-1* in pGBKT7 that did not grow on SC/QDO were excluded as false positives.

Inserts in plasmids from strains that were not false positives or self-activating were sequenced (UCR Core Instrumentation Facility, Riverside, CA) using the T7 universal primer, which initiates at the 5' end of the cDNA. The sequences were analyzed first by a BLAST search (Altschul et al., 1997) to the *N. crassa* genomic database, (http://www.broad.mit.edu/annotation/fungi/neurospora_crassa_7/index.html, (Galagan et al., 2003) which assigns each gene a NCU# (Broad Institute, Cambridge, MA). Positive sequences were verified using the BLAST 2 sequences program for aligning nucleotide sequences (NCBI, Bethesda, MD). Protein sequences for all verified nucleotide sequences were used in BLAST searches against the NCBI database (NCBI, Bethesda, MD).

Glyceraldehyde-3-phosphate dehydrogenase (GAPDH) enzyme assays

Liquid VM medium (200-1000 mL) was inoculated with 1×10^6 conidia per mL and incubated at 30°C with shaking at 200 RPM for 16 hrs. Mycelia were collected using gravity filtration by filtering through cheesecloth. Mycelia were homogenized in extraction buffer using a 50 mL bead beater chamber (Biospec Products, Bartlesville, OK) filled with approximately 15-20 mL glass beads. The extraction buffer contained either 150 mM Tris-HCl pH 8.5 (Exp. #1 and #3, see figure 2.4) or 100 mM KH_2PO_4 pH 7.6 (Exp. #2), and 0.5 mM PMSF. The extracts were centrifuged in a Beckman J2-21 refrigerated centrifuge using rotor JA 25.5 at 5,000 RPM for 10 min. at 4°C to remove cell wall debris. Protein concentration was determined using the Bradford protein assay with BSA as a standard (Bio-Rad Laboratories, Hercules, CA).

GAPDH enzyme activity was assayed in wild-type (WT, FGSC #2489, *matA*), $\Delta gna-1$ ($\Delta gna-1::hph^+$, 1B2a or 1B4A; (Ivey et al., 1999), and *gna-1** ($\Delta gna-1::hph^+$, *gna-1*^{Q204L}::*his3*⁺, H. Kim, unpublished) whole cell extracts using a protocol modified from Hochberg and Sargent (Hochberg and Sargent, 1974). During glycolysis, the GAPDH-mediated reaction uses NAD^+ and P_i , producing NADH and H^+ . Since NADH absorbs at 340 nm, the rate of formation of NADH can be monitored using a spectrophotometer. Na_2HAsO_4 was used as a substitute for P_i , which creates a non-reversible product. The general reaction conditions were as follows: 300 mM Tris-HCl pH 8.5, 10 mM cysteine, 60 mM Na_2HAsO_4 , 60 mM NaF, and 1 mM NAD^+ . Experiment #3 did not contain NaF. In all reactions, approximately 0.5 mg of protein (50-100 μL) was used and the total reaction volume was 1 mL. Extracts were pre-incubated with the reaction mixture for at

least 5 min. in a room temperature water bath. The reaction was started by adding glyceraldehyde-3-phosphate to 1.66 mM and quickly mixed by pipeting, and the change in absorbance was recorded at 340 nm using a UV 500 UV/VIS spectrophotometer (Thermo, Waltham, MA). The change in absorbance over 10 sec. was converted into specific activity ($\Delta A/\text{min}\cdot\text{mg}$). Control runs were also performed in the absence of glyceraldehyde-3-phosphate or NAD^+ to rule out the possibility of background activity in the extract. The values were then normalized using the values for reactions without addition of glyceraldehyde-3-phosphate, and calculated as a percentage of wild type for each experiment. Non-hydrolyzable forms of GTP (GppNHp and $\text{GTP}\gamma\text{S}$, Sigma) and GDP ($\text{GDP}\beta\text{S}$, EMD Chemicals) were also added to extracts at 100 μM and incubated 15-60 min. before assay start (Figure 2.4B).

Northern analysis

To obtain cultures for extraction of RNA, 200 mL of VM was inoculated with 1×10^6 conidia/mL from wild-type, $\Delta\text{gna-1}(1\text{B4A})$, and gna-1^* strains and incubated at 30°C with shaking at 200 rpm for 16 hrs. RNA was extracted from each strain using the extraction protocol described above (Gentra). Northern gel: To make the formaldehyde denaturing gel to separate RNA by electrophoresis, 1.5 g of agarose was added to 91 mL of DEPC- H_2O and allowed to cool for 10-20 min. To this mixture 12.5 mL of 10X MOPS (400 mM 3-(N-morpholino)propanesulfonic acid) pH 7.0, 100 mM NaOAc, and 10 mM EDTA) and 20.3 mL a 37% formaldehyde solution was added and the gel was poured. The RNA (20 μg) was prepared by adding 2.5 μL of 10x MOPS, 4.38 μL of

37% formaldehyde, 12.5 μL of formamide, and 1 μL of a 1 mg/mL ethidium bromide solution. The RNA mixture was incubated at 65°C for 15 min. and 5 μL formaldehyde loading buffer (50% glycerol, 1 mM EDTA, pH 8.0, 0.25% bromophenol blue, and 0.25% xylene cyanol FF) was added. The RNA was loaded onto the formaldehyde gel submerged in 1X MOPS and ran at 70 mA for 2-3 hrs., and RNA visualized as described for DNA in Methods above. The gel was washed three times for 10 min. in DEPC- H_2O , for 45 min. in 10X SSC (44.1 g $\text{Na}\cdot\text{C}_6\text{H}_7\text{NaO}_7$ and 87.6 g NaCl in 1 L water), and transferred overnight in 10X SSC to a nylon neutral transfer membrane (GE healthcare, model #N00HY00010). The RNA was then UV cross-linked to the membrane CL-100 Ultraviolet Crosslinker (UVP).

Radiolabeled probe: probes were synthesized using random primer labeling (Promega, Madison, WI) as follows: H_2O was added to 20-200 ng DNA to a final volume of 26 μL , and boiled for 5 min. at 95°C. The tube was cooled immediately on ice and the following were added: 10 μL 5x random primer buffer, 5 μL of a 4 mg/mL solution of acetylated BSA, 3 μL 1x dNTP's (minus dCTP), 1 μL Klenow DNA polymerase, and 5 μL (approximately 50 μCi) ^{32}P -dCTP (MP biomedical, Solon, OH). The reaction was left at room temperature for 1-2 hours, then either used immediately or stored at -20°C. When necessary, unincorporated nucleotides were removed using a Micro-bio Spin 30 Chromatography column according to manufacturer's suggestions (Biorad).

Hybridization and washes: Hybridization solution was made as follows: 500 mL of 1 M solution of Na_2HPO_4 , 2 mL of a 500 mM solution of EDTA, and 70 g SDS were added to approximately 300 mL water and stirred on a hot plate at low heat until components were

dissolved. This solution was cooled to room temperature, 10 g BSA was added, and solution brought up to 1 L with water. The membrane was incubated with 20 mL hybridization solution for 20-60 min. at 65°C in a rotary incubator. The probe was boiled for 5 min. in a 95°C water bath and cooled immediately on ice. The probe was added to the hybridization solution and the membrane was incubated at 65°C overnight. The membrane was washed twice for 10-15 min. with 20 mL of wash I (40 mM Na₂HPO₄, 1 mM EDTA, 5% SDS, and 0.5% BSA in water), and washed twice for 10-15 min. with 20 mL of wash II (40 mM Na₂HPO₄, 1 mM EDTA, and 5% SDS, in water). The membrane was then exposed to film (BioMax XAR, Kodak Company, Rochester, NY).

To construct DNA for the *ccg-7* probe, clone #1/8 from the yeast two-hybrid screen was used to amplify a 460 bp fragment of the 3' end using the high fidelity enzyme Pfu (cloned Pfu polymerase, Agilent technologies-Stratagene, Cedar Creek, TX). The PCR reaction mixture contained 10 µL 10X buffer, 8 µL of 2.5 mM dNTPs, 0.5 µL each of primers *gapdh* ERI fw (5'-AAAAGAATTCGTCGATGGTCCTTCCGCCAAG-3') and *gapdh* BHI rv (5'-AAAGGATCCGTTTAAGCCTTCTTGGCATCGAC-3') at 250 ng/µL, 1 µL template (150 ng/µL), 1 µL Pfu, and 78 µL H₂O. Thermocycler conditions used were: 98°C for 10 min.; 30 cycles of: 98°C for 45 sec., 60°C for 45 sec., and 72°C for 45 sec.; and 72°C for 10 min. The fragment was separated by agarose gel electrophoresis and cut from the gel using a clean razor blade. DNA was purified from this slice of agarose using the QIAEX II kit according to manufacturer's suggestions (Qiagen). This fragment was used as a template for a ³²P-dCTP probe for Northern analysis.

Western analysis

The SDS-PAGE resolving gel was prepared by mixing 6.25 mL 2X buffer A (90.75 g Tris base and 2 g SDS, in water adjusted to pH 8.8), 60 μ L of a 10% ammonium persulfate (APS) solution, 7 μ L Tetramethylethylenediamine (TEMED) and a 6.23 mL mixture of water and 40% bis-acrylamide (37.5:1, EMD chemicals, Gibbstown, NJ) for desired acrylamide percentage. This solution was poured between two sealed glass plates separated by 0.75 mm spacers to about 1/3 of the total volume. After the resolving gel was set (approximately 30 min.), the stacking gel was prepared by mixing 2.5 mL 2x buffer B (90.75 g Tris base and 2 g SDS, in water adjusted to pH 6.8), 2 mL water, 0.5 mL 40% bis-acrylamide, 60 μ L of a 10% ammonium persulfate (APS) solution, and 7 μ L Tetramethylethylenediamine (TEMED), and added to the top of the resolving gel, comb added, and allowed to solidify for 15 min.

Whole cell extracts were obtained from wild-type, Δ *gna-1*(1B4A), and *gna-1*^{Q204L} strains using the same protocol used for the GAPDH enzyme assays. Protein samples (100 μ g each) were denatured by boiling in a 1/10 volume of 10X SDS loading buffer (500 mM Tris-HCl pH 6.8, 20% glycerol, 2% SDS, 1% β -mercaptoethanol, and 0.005% bromophenol blue) for 5 min. The Samples were then resolved on a 10% SDS PAGE gel at 50-70 mA for 2-3 hours in 1X running buffer. To make 10X running buffer, 30 g Tris base, 143.75 g glycine, and 5 g SDS was added to water for a total volume of 1 L. The proteins were then transferred to a nitrocellulose membrane (G.E. Healthcare, Piscataway, NJ; 0.45 micron pore size) using a Bio-rad transblot cel at 225 mA for 2-3 hours in transfer buffer (9 g Tris base, 42.45 g glycine, 2.4 L water, and 600 mL

methanol). Membranes were blocked in 5% milk in TBST (1X TBS pH 7.6, 0.05% Tween-20) for 30-60 min. at room temperature. To make 10X TBS stock, 24.2 g Tris base and 80 g NaCl were added to a final volume of 1 L and adjusted to pH 7.6 with HCl. Membranes were incubated with either a monoclonal mouse antibody directed against GAPDH (Chemicon, Temecula, CA) at 1:200 in 0.1% BSA in TBST (4°C, overnight) or a polyclonal antibody directed against GNA-1 (Ivey et al. 1996) at 1:4000 in 5% milk in TBST (room temperature, 3 hrs). Blots were washed 2-3 times for 5-10 min. with 5% milk in TBST. Both secondary antibodies were horseradish peroxidase conjugates (Biorad) diluted in 5% milk at 1:000 (goat anti-mouse), and 1:8,000 (goat anti-rabbit). Membranes were washed again 2-3 times for 5-10 min. with 5% milk in TBST, and twice with 1X TBS for 5 min. each. Chemiluminescence development was accomplished by mixing approximately 500-1000 μ L each of peroxide solution and enhancer solution in a 1:1 ratio (SuperSignal West Pico Chemiluminescent Substrate, Rockford, IL), adding this solution to the membrane, and incubating for 5 min. with gentle rotation by hand. The luminescent bands were visualized on a Biochemi System imager (UVP, Upland, CA).

Results

Identification of novel GNA-1 interacting proteins

I conducted a yeast two-hybrid library screen in order to identify novel GNA-1 binding proteins in *N. crassa*. RNA was extracted from wild-type tissue (FGSC #2489) from 16 hr submerged culture and 6 day old SCM plates (unfertilized female tissue) and was used to construct a cDNA library using RT-PCR and homologous recombination in yeast (See methods). RNA, mRNA, and cDNA can be visualized in Figure 2.2. Plasmid pGADT7rec was used to create the cDNA library and expresses the cDNA as a fusion to the activation domain of the GAL4 transcription factor (GAL4-AD). This construct carries the ampicillin resistance gene (Amp^R) for selection in *E. coli* and the *LEU2* nutritional marker for selection in yeast. pGBKT7 was used as the bait vector and expresses cDNA as a fusion to the DNA-binding domain of the GAL4 transcription factor (GAL4-DBD). This construct carries the kanamycin resistance gene (Kan^R) for selection in *E. coli* and *TRP1* nutritional marker for selection in yeast.

The library cloned in vector pGADT7rec was transformed into strain AH109 and screened with *gna-1* in pGBKT7 in strain Y187 using a mating strategy. These strains contain mutations in various amino acid biosynthetic genes, which aid in plasmid selection, or reporter genes which have been inserted into the genome. The mutations in the biosynthetic pathway genes confer a phenotype in which the yeast can only grow on medium supplemented with the given amino acid added unless the strain contains a plasmid which expresses the gene. The reporter genes *his-3* and *ade-2* are expressed

when there is a physical interaction between the two candidate proteins (Figure 2.1). A stringent selection (activation of both reporter genes) was used to obtain only strongly interacting proteins. There were 83 total positive clones. Of the 83 clones, 44 were identified as legitimate, a 53% efficiency. The other 39 clones were either self-activating, unable to reconstitute an interaction, or prey that are located inside the mitochondria. The results of the positive clones as well as the mitochondrial clones are shown in Table 2.1.

The 44 legitimate clones accounted for nine proteins. The most frequent protein, glyceraldehyde-3-phosphate dehydrogenase (GAPDH), comprised 41% of the positives. GAPDH is a metabolic enzyme involved in glycolysis, gluconeogenesis, and the pentose phosphate pathway. During glycolysis, GAPDH converts glyceraldehyde-3-phosphate to 1,3 bis-phosphoglycerate, which is one step upstream of the first ATP producing step. GAPDH is allelic with *ccg-7*, which is a clock-controlled gene (Shinohara et al., 1998). Elongation factor-1- α (EF-1 α) comprised 32% of the positive clones. EF-1 alpha is a subunit of the translational machinery in *N. crassa*. Other clones were found in lower abundance, such as the glycolytic enzyme pyruvate kinase (2 clones), a subunit of serine palmitoyl CoA transferase (2 clones), which is involved in sphingolipid synthesis, a protein involved in vitamin B6 synthesis (SNZ-1), 40S ribosomal protein S17 subunit (CRP-3), and a putative Arp2/3 complex 21 kDa subunit. Two proteins were found that have been characterized as hypothetical proteins by the Broad Institute, and a BLAST search to the NCBI protein database (<http://www.ncbi.nlm.nih.gov/BLAST/>) shows similar proteins only in fungi and with unknown function.

Strains with GTP-ase deficient GNA-1 have lower GAPDH enzyme activity

Since GAPDH was shown to interact with GNA-1 in the yeast two-hybrid system, I determined whether this possible interaction has an effect on GAPDH enzymatic activity. GAPDH specific activity ($\Delta A/\text{min}\cdot\text{mg}$) was determined in wild-type (WT, FGSC #2489), $\Delta gna-1$ (1B2a, 1B2A), and $gna-1^{Q204L}$ ($gna-1^*$, GTPase deficient) whole cell extracts. For each experiment, the specific activity of GAPDH in $\Delta gna-1$ and $gna-1^{Q204L}$ strains was normalized by calculating the percent of wild-type for activity.

There appears to be a modest but reproducible effect on GAPDH activity in the activated allele strain (specific activity is 39% lower than wild-type), but not in the $\Delta gna-1$ strain (Figure 2.3A). This data suggests that an abundance of the GTP-bound form of GNA-1 in the cell has a negative effect on GAPDH enzyme activity. Since the GAPDH activity was significantly reduced in the strain that expresses a GTPase deficient $gna-1$ allele, the effects of added non-hydrolysable forms of GTP (GppNHp, GTP γ S) and GDP (GDP β S) was also tested (Figure 2.3B). The addition of analogs did not reduce the GAPDH enzyme activity in wild-type. However, it has been shown using purified G α proteins that GDP dissociation from G α subunits is the rate limiting step for the binding of various guanine nucleotide analogs to G α subunits (Ferguson et al., 1986). This raises the possibility that the analogs may have not bound to GNA-1 in the *Neurospora* cell extract to an extent that they would influence GAPDH activity.

It was previously shown that mRNA and protein levels for *ccg-7* (the gene encoding GAPDH) fluctuate with the *N. crassa* circadian rhythm (Shinohara et al., 1998). I tested whether the effect of the $gna-1^{Q204L}$ allele on GAPDH enzyme activity results from

altered GAPDH protein or mRNA levels. Northern analysis was performed on mRNA isolated from submerged cultures of wild-type, $\Delta gna-1(1B4A)$, and $gna-1^{Q204L}$, using *ccg-7* as a probe. The mRNA level is similar in all three strains (Figure 2.5A), indicating that the allelic state of *gna-1* does not influence transcript levels. Western analysis using anti-GAPDH antibody was also performed on wild-type, $\Delta gna-1(1B4A)$, and $gna-1^{Q204L}$ whole cell extracts (Figure 2.5B). Although the blot has high background, it appears that GAPDH protein levels are similar in all three strains.

Discussion

The change in GAPDH activity in a strain expressing a GTPase-deficient form of GNA-1 is not due to a difference in *ccg-7*/GAPDH mRNA or protein levels. This, along with the yeast two-hybrid data, suggests the possibility of a direct interaction between GNA-1 and GAPDH in *N. crassa*. GAPDH has been shown to be associated with erythroid cell membranes (Allen, 1987), suggesting an interaction between GAPDH and membrane-bound proteins in mammals. The next question to be asked is why these two proteins interact. The fact that GNA-1 only modestly affects GAPDH activity suggests that there may be a non-enzymatic function for the interaction of these two proteins. In mammals, GAPDH has been shown to have many non-glycolytic functions. For instance, GAPDH has been shown to bind AU-rich elements of RNA and regulate mRNA turnover and translation (Nagy, 1995). GAPDH has also been found to play a role in apoptosis (Tarze, 2007). The role of GAPDH in translation could be interesting to pursue because EF-1 α , an elongation factor in translation, and the 40S ribosomal subunit S17 (CRP-3) were both found to interact with GNA-1 in the yeast two-hybrid library screen. One possibility is that these two proteins are part of a complex involved in translational regulation, as there is growing evidence that the actin cytoskeleton and translational machinery work together to localize protein synthesis (Gross, 2005; Kim, 2010). A future project could be to investigate this interaction using *in vivo* localization studies of GNA-1, ARP2/3 complex, and translational machinery in wild-type with the addition of actin and microtubule disrupting chemicals.

Also of interest is the possible interaction of GNA-1 with serine palmitoyl-CoA transferase, which is the first step of sphingolipid biosynthesis. This enzyme is embedded in the membrane of the Endoplasmic Reticulum (ER), and studies show that the catalytic portion of this enzyme faces the cytosol (Mandon et al., 1992). In addition, it has been found that Gpa1p, the GNA-1 homolog in *S. cerevisiae*, binds to an ER associated protein SCP160 (Guo et al., 2003). There is a model proposed that the G α subunit may be palmitoylated and form a heterotrimer with G $\beta\gamma$ on the membrane of the ER (Marrari et al., 2007), however the mechanism is unknown.

Another hypothesis is that the reduction of GAPDH activity by GNA-1 is significant and could function to influence the concentration of metabolites or to sequester metabolites to different parts of the cell. For instance, it has been shown in mammalian brain tissue that GAPDH is responsible for the phosphorylation state of the GABA_A receptor, which is important in neurotransmission (Laschet, 2004). Growth and reproduction require cell division, and since GNA-1 has been shown to be important for both growth and reproduction in *N. crassa*, it is possible that GNA-1 reduces the activity of GAPDH to influence the metabolic state of the cell and favor anabolic processes during growth and reproduction.

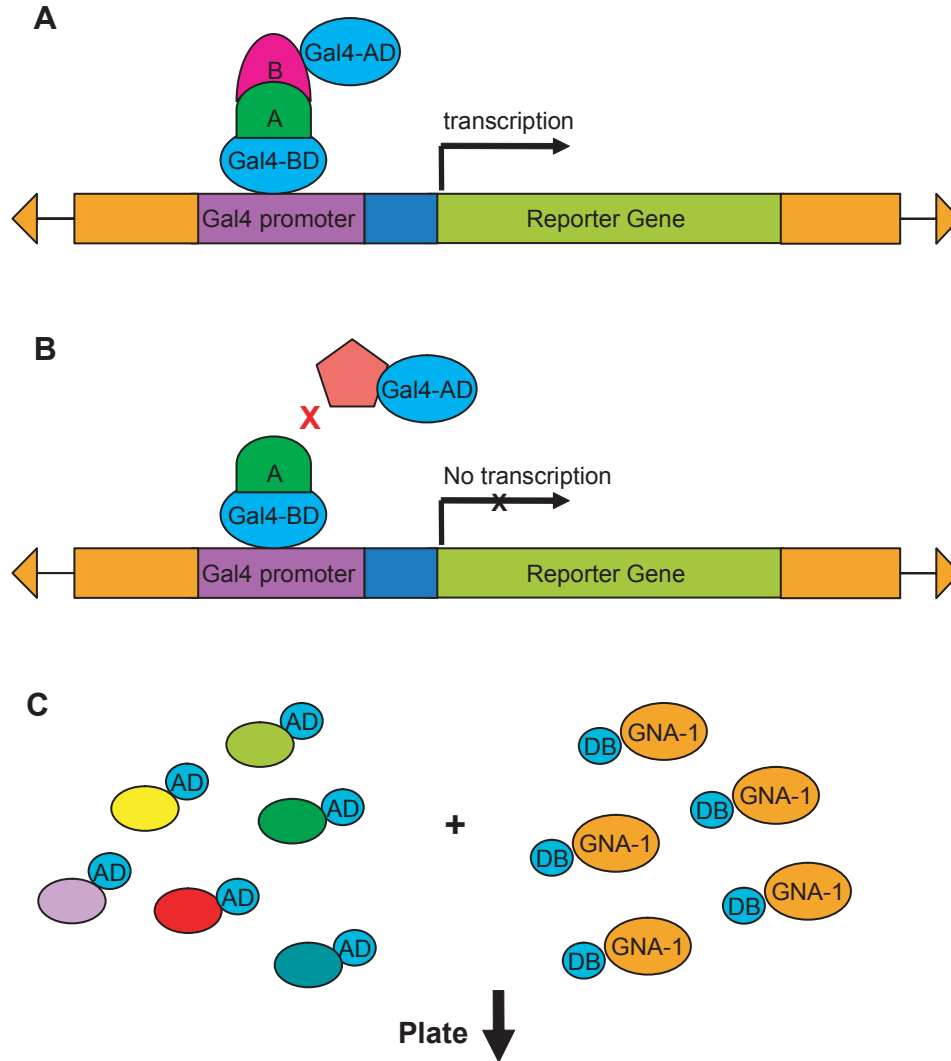


Figure 2.1: Schematic for the yeast two-hybrid assay and cDNA library screening

The yeast two-hybrid system takes advantage of the modular nature of transcription factors, in this case Gal4. The gene for one protein of interest is cloned into the pGBKT7 vector (creates a Gal4 DNA-binding domain (BD) fusion) and the gene for another protein of interest is cloned into pGADT7 (creates a Gal4 activation domain (AD) fusion). These vectors are transformed into yeast which contain the Gal4 promoter fused to several reporter genes. The yeast strains lack the ability to make Tryptophan, Leucine, Adenine, or Histidine. Vectors pGBKT7 and pGADT7 restore Tryptophan and Leucine synthesis, while Adenine and Histidine synthesis is under control of the Gal4 promoter. A) When Protein A and B interact, the AD and DB modules of Gal4 transcription factor are brought together to activate the reporter gene. B) Protein A and Z do not interact, therefore Gal4-AD and Gal4-BD will not come together to activate the reporter gene. C) cDNA was amplified from mRNA isolated from *Neurospora crassa* and cloned into pGADT7. Yeast cells containing *gna-1* cloned into pGBKT7 were mated to yeast cells containing cDNA fragments cloned into pGADT7 and colonies were selected on SC media lacking Tryptophan, Leucine, Adenine, and Histidine (Q.D.O., see methods). Colonies that grew contained potential GNA-1 interactors and were tested further.

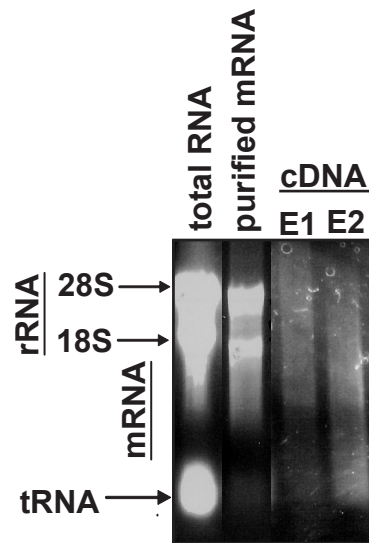


Figure 2.2: RNA, mRNA, and cDNA used for library construction

Total RNA, purified mRNA, and cDNA used for the cDNA library construction. Total RNA was extracted from wild-type (FGSC #2489) 16 hour submerged cultures. The RNA sample was enriched for mRNA; and Reverse transcription and PCR reactions were done to obtain cDNA, which was cloned into library vector pGADT7rec (see chapter 2 methods for more details). E1 and E2 refer to elution #1 and #2 of double-stranded cDNA from the BD Chroma Spin TE-400 column

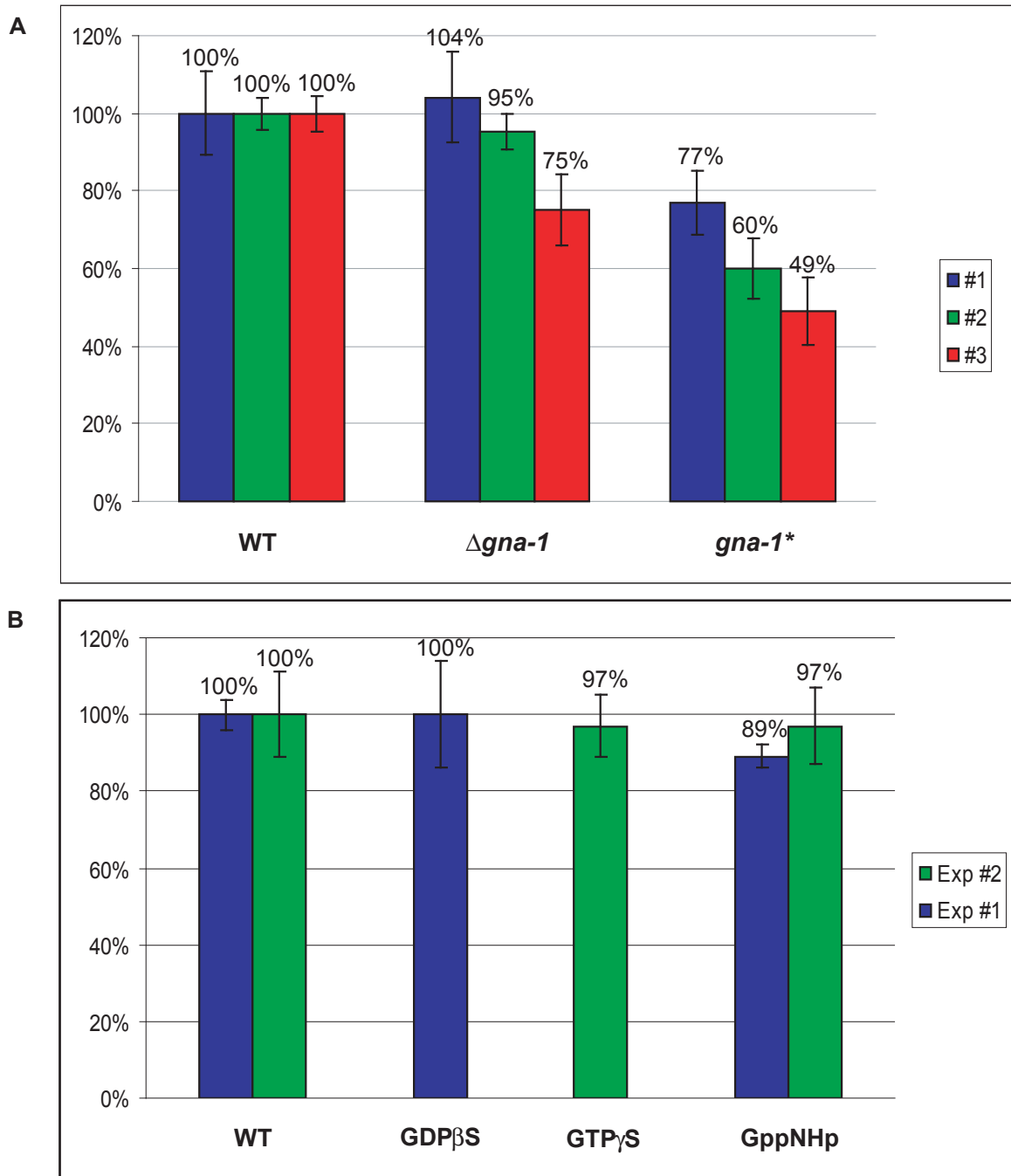


Figure 2.3: GAPDH enzyme activity is reduced in the *gna-1*^{Q204L} strain

A) GAPDH activity in wild-type (WT), $\Delta gna-1$, and *gna-1*^{Q204L} (*gna-1**) whole cell extracts was measured and graphed as a percent of wild-type activity (see methods for details). Exp #1 and #2 uses $\Delta gna-1$ strain 1B2a and Exp #3 uses $\Delta gna-1$ strain 1B4A. B) Effects of the addition of GTP and GDP analogs on GAPDH activity. WT extract from Exp #1 and #2 was assayed for GAPDH activity in the presence of non-hydrolyzable forms of GDP (GDP β S) and GTP (GTP γ S and GppNHp).

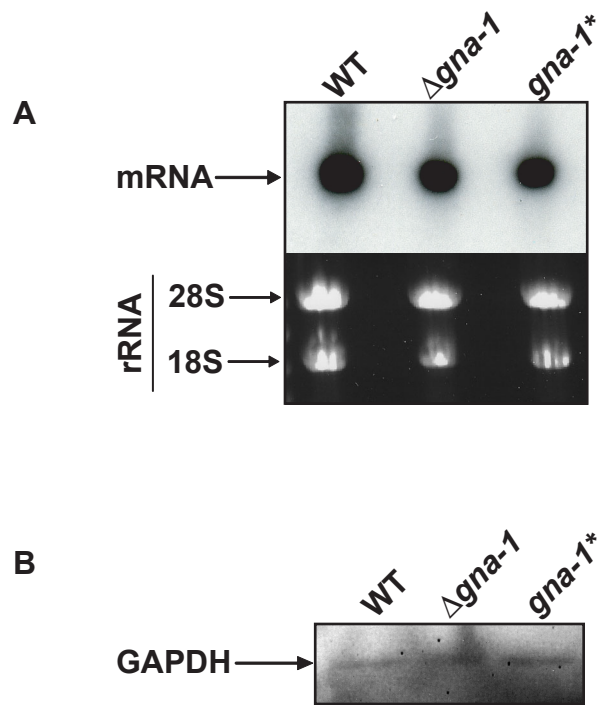


Figure 2.4: mRNA transcript and protein levels of GAPDH (*ccg-7*) in WT, $\Delta gna-1$, and *gna-1 strains** A) Level of *ccg-7* transcripts. Samples containing 20 μ g of total RNA isolated from 16-h submerged cultures were subjected to Northern analysis using a 460bp fragment of the 3' end of *ccg-7* as a probe. Strains used for analysis were wild type (FGSC 2489) and $\Delta gna-1$ (1B4A), and *gna-1** ($\Delta gna-1 gna-1^{Q204L}$). B) GAPDH protein levels. Samples containing 100 μ g of protein from whole cell extracts isolated from 16 hour submerged cultures were subjected to Western analysis using a monoclonal mouse antibody against GAPDH at 1:200.

Table 2.1: Potential GNA-1 interacting proteins from the cDNA library screen

NCU#	Name	Function
01528.4	<i>gpd-1</i> , <i>ccg-7</i>	glyceraldehyde-3-phosphate dehydrogenase; converts glyceraldehyde-3-phosphate to 1,3 bis-phosphoglycerate
02003.4	<i>tef-1</i>	elongation factor 1 alpha; essential for translation
06075.4		pyruvate kinase; converts phosphoenolpyruvate to pyruvate
06870.4		Serine palmitoyltransferase subunit, converts palmitoyl-CoA and serine to 3-ketodihydroshingosine; localized to the ER
06550.4	<i>pdx-1</i>	SNZ1 homolog; involved in vitamin B6 synthesis
07014.4	<i>crp-3</i>	cytoplasmic ribosomal protein-3; 40S ribosomal protein subunit involved in translation
09572.4		ARP2/3 complex 21 kDa subunit homolog; involved in actin nucleation and branching
06609.4		hypothetical protein; conserved in filamentous fungi
04588.4		hypothetical protein; conserved in filamentous fungi
01169.4		24 KDa subunit of NADH dehydrogenase; complex I of the electron transport chain
01666.4		Acetolactate synthase (ALS) small subunit; converts pyruvate acetolactate in mitochondria; bacterial, fungal, and plant specific
01213.4	<i>sod-2</i>	superoxide dismutase; removes superoxide radicals (byproduct of the electron transport chain) in mitochondria

Table 2.1: Potential GNA-1 interacting proteins from the cDNA library screen

To identify potential GNA-1 interacting proteins, *gna-1* cDNA in the GAL4 AD vector was used to screen a *N. crassa* cDNA library in the GAL4 DBD vector using a mating strategy (see methods). DNA was extracted from the colonies that grew on stringent selection media, and *E. coli* was transformed to select for the library vectors. Vectors were verified and sequenced (see methods). Each gene is designated using an NCU#, a unique number given to every gene in *Neurospora crassa* by the Broad Institute (Cambridge, MA), and a *Neurospora crassa* gene name if designated. The function of each gene was determined by identifying homologous proteins with known function through a BLAST search (<http://www.ncbi.nlm.nih.gov/BLAST/>) to the NCBI protein database. Proteins localized to organelles are highlighted in grey.

Chapter 3: Characterization of RIC8 in *Neurospora crassa*

Abstract

In the traditional model for G protein signaling, G protein coupled receptors (GPCRs) act as guanine nucleotide exchange factors (GEFs) for G α subunits. Recently, facilitated GDP/GTP exchange by non-GPCR GEFs, such as the RIC8 protein, has emerged as an important mechanism for G α regulation in animals. RIC8 is present in filamentous fungi, but is absent from the genomes of plants, sequenced protists, and *Saccharomyces cerevisiae*. This Chapter presents the characterization of RIC8 in the model eukaryotic filamentous fungus *Neurospora crassa*. Deletion of *ric8* leads to defects in polar growth and asexual and sexual development in *Neurospora*, similar to those observed for a mutant lacking the G α genes *gna-1* and *gna-3*. A functional and physical interaction between RIC8, GNA-1 and GNA-3 is supported by the observation that GTPase deficient alleles of *gna-1* and *gna-3* rescue many defects of $\Delta ric8$ mutants, that $\Delta ric8$ strains have greatly reduced levels of G protein subunits, and that RIC8 interacts with GNA-1 and GNA-3 in the yeast two-hybrid assay. Hyphae from $\Delta ric8$ mutants have small cell compartments with nuclei that are small and morphologically abnormal, which suggests a role in polar cell growth. The $\Delta ric8$ mutation also influences cAMP signaling. Adenylyl cyclase protein levels are reduced in the $\Delta ric8$ mutant, and the $\Delta ric8$ mutant phenotype can be partially suppressed by a mutation in the protein kinase A regulatory subunit. These results support a role for RIC8 and G proteins in regulation of growth, development, and cAMP signaling in *Neurospora*.

Introduction

Eukaryotic cells sense many hormones, growth factors, neurotransmitters and the presence of light via G protein signaling pathways. The G protein heterotrimer consists of a $G\alpha$ subunit, which binds and hydrolyzes GTP, and of tightly-associated $G\beta$ and $G\gamma$ subunits. G proteins interact with seven-transmembrane helix G protein coupled receptors (GPCRs) to regulate downstream signaling pathways (reviewed in Chapter 1). Recently a non-receptor protein, RIC8, has been implicated as a positive regulator of $G\alpha$ proteins in several animal species, including *Caenorhabditis elegans*, *Drosophila melanogaster* and mammalian cells (rev. in (Wilkie and Kinch, 2005a). RIC8 is required for asymmetric cell division in zygotes and priming of synaptic vesicles in *C. elegans* (Miller and Rand, 2000b-a; Wilkie and Kinch, 2005a). In *Drosophila*, RIC8 is essential for responses to extracellular ligands and for maintenance of polarity during asymmetric cell division in embryogenesis (Hampoelz et al., 2005). $G\alpha$ GEF activity has been demonstrated for the mammalian RIC8 homolog, RIC-8A (Tall et al., 2003a). The data support a mechanism in which RIC-8A binds to the GDP-bound $G\alpha$ in the absence of $G\beta\gamma$ and GDP is then released, forming a stable RIC-8A: $G\alpha$ complex. Subsequently GTP binds the $G\alpha$ protein and RIC-8A is released.

Neurospora crassa possesses three $G\alpha$ subunits (GNA-1, GNA-2 and GNA-3), one $G\beta$ (GNB-1), one $G\gamma$ (GNG-1) and more than 25 putative GPCRs (reviewed in (Li et al., 2007b); see Chapter 1 for more details. Previous results have demonstrated that loss of *gna-1* and *gna-3* or all three $G\alpha$ genes leads to a severe decrease in extension of both basal and aerial hyphae (Kays and Borkovich, 2004a-a). The relatively subtle phenotypes

of GPCR mutants in comparison to strains lacking one or more $G\alpha$ genes (Bieszke et al., 2007; Kim and Borkovich, 2004; Krystofova and Borkovich, 2006; Li and Borkovich, 2006) prompted exploration of possible non-GPCR regulators of G proteins in *Neurospora*. It was recently reported that RIC8 homologues are present in animals and fungi, but not in plants or protists, including *Dicytostelium discoideum* (Wilkie and Kinch, 2005a). Further investigation using BLAST searches of the NCBI database with metazoan RIC8 sequences revealed homologues that are present in *Neurospora* and other fungi, but absent from *S. cerevisiae* (K. Borkovich, G. Turner, and S. Wright, unpublished; See Figure 2.3 for fungal homologues). It has been hypothesized that RIC8 was acquired by animals and certain fungi after the evolution of G proteins and GPCRs and is therefore a fairly recent addition to G protein regulatory pathways (Wilkie and Kinch, 2005a).

The results in this chapter demonstrate that *ric8* is essential for normal growth, asexual sporulation and sexual differentiation in *Neurospora*. Loss of *ric8* yields several phenotypes found in strains lacking *gna-1* and *gna-3*; i.e., extremely impaired growth, shorter aerial hyphae, inappropriate conidiation in submerged culture, loss of female fertility and smaller cell compartments with small, elongated nuclei. The data also show that RIC8 acts upstream of and interacts with certain $G\alpha$ proteins, consistent with a role as a $G\alpha$ GEF in *Neurospora crassa*.

Materials and Methods

Strains and growth conditions

A list of *Neurospora* strains is provided in Table 3.1. Strains were maintained on Vogel's minimal medium (VM; (Vogel, 1964); and all cultures were inoculated with conidia collected from VM agar flasks as indicated in Chapter 2. Synthetic crossing medium (SCM) was used to induce formation of female reproductive structures (protoperithecia; (Vogel, 1964; Westergaard and Mitchell, 1947). For VM plate cultures, VM agar plates overlaid with cellophane were inoculated in the center using 1-2 μL of a 1×10^9 conidia/ μL suspension and incubated for three days at 30°C. Sorbose-containing medium (FGS; VM medium minus sucrose, containing 0.5% sorbose, 0.0125% glucose, and 0.025% fructose) was used to induce colonial growth for isolation of single colonies on plates (Davis and de Serres, 1970). Medium used for phosphinothricin selection is similar to VM medium, except that NH_4NO_3 is excluded from the 50X VM and 0.5% L-Proline is added. After autoclaving phosphinothricin (ignite) is added at 400 $\mu\text{g}/\text{ml}$.

Cloning using restriction enzyme digest and ligation reactions

For all restriction enzyme digest reactions, 1-10 μg DNA from PCR or plasmid was used in a total reaction volume of 60-100 μL reaction containing 2-10 units enzyme, 100 $\mu\text{g}/\text{mL}$ BSA (when needed) and appropriate buffer according to manufacturer's suggestions (New England Biolabs, Ipswich, MA). Reactions were incubated at 37°C for 2-4 hours (or overnight as indicated). In the event of a double digestion, the New

England Biolabs double digest chart was used to choose the best buffer. The reactions were de-salted using the QIAprep miniprep kit or the insert or plasmid was isolated by separating the fragments on a 1% agarose (described in Chapter 2) and cut from the gel using a clean razor blade. DNA was purified from this slice of agarose using the QIAEX II kit according to manufacturer's suggestions (Qiagen). For all ligation reactions, insert and plasmid were added at an approximately 1:1 molar ratio to 1 μ L T4 ligase and 1 μ L ligase buffer in a total volume of 10 μ L (New England Biolabs) and incubated for 2 hours at room temperature or 16 hours at 4°C. One half of the reaction (5 μ L) was used to transform *E. coli* cells by chemical competence transformation as described in Chapter 2.

Isolation and sequencing of the *ric8* gene

The existence of a *ric8* homologue in fungi was suggested by Wilkie and Kinch (Wilkie and Kinch, 2005a). Homology searches (BLAST, (Altschul et al., 1997) of the *N. crassa* genome database at the Broad Institute (Galagan et al., 2003) using the *Xenopus laevis* Ric8 protein sequence (Accession #NP_989159) revealed that the *Neurospora* RIC8 protein corresponds to NCU02788. Data from the Broad Institute database showed there were several cosmids containing the *ric8* gene, including cosmid pMOcosX G19 C10. A *ric8* subclone was generated by digesting cosmid pMOcosX G19 C10 with restriction enzyme *EcoRI*, releasing a 12.6 kb fragment (corresponding to contig 7.7, nucleotides 24473-37042) that was cloned into pGEM4 (Promega, Madison, WI), creating pSM17. The clone was sequenced (Institute for Integrative Genome Biology, Core sequencing facility, University of California, Riverside) using universal

primers supplied by the Core Facility (T7 and SP6) and several gene-specific primers (R8 seq primers; see Table 3.2) to verify that it contained the *ric8* gene.

There are two predicted introns in *ric8*. The presence of the 65 bp 3' predicted intron was confirmed by the sequence of a cDNA clone (NCW06G3T7 cDNA clone W06G3 3'; BROAD). The 56 bp 5' predicted intron and *ric8* transcript expression was verified by RT-PCR. Total RNA was extracted from conidia, 16 hour submerged cultures and 3 day VM plate cultures of wild-type strain 2489, $\Delta ric81a$, and R8GFP (Table 3.1). RNA was extracted using a modified protocol from the Purescript RNA isolation kit (Gentra Systems, Minneapolis, MN), as described in Chapter 2. Semi-quantitative RT-PCR analysis (Kays and Borkovich, 2004a-a) was performed using the Access RT-PCR system (Promega, Madison, WI) with gene-specific primers (R8I1fw and R8I1rv) designed to flank the 5' intron (Table 3.2) according to manufacturers suggestions. A control reaction was also run using 18S rRNA-specific primers (Li and Borkovich 2006). A 50 μ L total volume included 10 μ L DNase treated RNA (2 μ g total) and both AMV reverse transcriptase and Tfl polymerase (Promega). The RT reaction was incubated at 48°C for 45 min., and at 94°C for 2 min. The PCR thermocycling conditions were: 35 cycles of 94°C for 30 sec., 50°C for 1 min., and 68°C for 90 sec.; and a final elongation step of 68°C for 7 min. The samples were subjected to electrophoresis on a 2% agarose gel at 70-80 mA for 2-4 hours. The DNA was visualized as described in Chapter 2. The gel was incubated for 20-45 min. with rotation in denaturation solution (200 mM NaOH, 600 mM NaCl, in water) and again for 20-45 min. in neutralization solution (1 M Tris-Cl pH 7.4, 1.5 M NaCl, in water). The gel was transferred to a nylon

membrane (GE Healthcare) as described in Chapter 2, except that 2X SSC was used in place of 10X SSC. After this point, the membrane was treated the same as for Northern Blotting described in Chapter 2. Probes were amplified using the same PCR reaction and primers as the RT-PCR reactions.

Strain construction

A heterokaryotic transformant containing the *ric8* deletion mutation was obtained from the *Neurospora* genome project (Colot et al., 2006). Briefly, strains with gene deletions ('knockouts') are constructed by replacing the open reading frame of the gene of interest with the *hyg* gene, which confers resistance to the antibiotic hygromycin. This is achieved by using strains which are deficient in the non-homologous end-joining DNA repair pathway, $\Delta mus-51$ and $\Delta mus-52$ (Inuoe). These genes were knocked out using the bar gene, which confers resistance to phosphinothricin (Pall 1993). These strains, which are almost 100% accurate in homologous DNA recombination, are transformed with a piece of DNA ('cassette') containing the *hyg* gene flanked by the 5' and 3' UTR regions of the gene of interest. After transformation, the strain is crossed to wild-type to obtain a homokaryotic strain containing the knockout mutation, but not the *hyg* gene.

I obtained the $\Delta ric8$ heterokaryon transformed by the genome project and crossed it as a male to wild-type strain 74A (female). For genetic crosses, the female was grown on SCM slants for 6 days in the light at 30°C, to induce the formation of protoperithecia (unfertilized female structures). Conidia from the male strain were collected as a suspension in sterile water, and a sterile cotton swab was used to inoculate the female.

The fertilized females were incubated for 10 days to 3 weeks at 25°C in the light, until perithecia were present and ascospore progeny were ejected. These ejected ascospores were collected using a sterile cotton swab and submerged in 500 µL sterile water, washed twice with 500 µL sterile water (pelleted by centrifugation at 3000 RPM for 5 min. in the microcentrifuge), and suspended in a final volume of 500-1000 µL H₂O. A 100 µL aliquot was removed and incubated in a 60°C water bath for 45 min. to activate germination. The activated ascospores were left at room temperature for 5 min. and 4°C for 5 min; then washed once in 100 µL H₂O, re-suspended in 100-200 µL sterile H₂O or 0.1% agar. After discovering that *Δric8* homokaryons were unable to germinate on FGS medium, I plated ascospores on VM plates supplemented with 200 µg/ml hygromycin. Colonies of *Δric8* homokaryons were able to grow to a visible size in 1-2 days. These colonies were individually transferred onto VM+hyg slants, and spot-tested on VM+phosphinothricin medium. *Δric8 his-3* strains were isolated in a similar manner by crossing the *his-3* strain (FGSC 6103) as a male to the *Δric8* heterokaryon as a female and plating the ascospore progeny on VM-hyg plates containing histidine. The progeny were transferred to VM+hyg slants, spot-tested on VM+phosphinothricin to test for phosphinothricin, and spot-tested on VM lacking Histidine to test for *his-3*. Genomic DNA was extracted from these progeny in order to verify the *Δric8* gene replacement using Southern analysis.

Genomic DNA was extracted using the Puregene kit according to manufacturer's protocols (Gentra Systems, Minneapolis, MN). VM liquid (1-2 mL) was inoculated with conidia from each sample and grown for 1-3 days at 200 RPM. Tissue was collected by

vacuum filtration and stored at -20°C until use. Tissue was ground to a powder in liquid nitrogen using a mortar and pestle. Approximately 25 mg ground tissue (2 scoops with a small, flat spatula) was added to 600 µL cell lysis solution and 3 µL of a 20 mg/mL Proteinase K solution in a 2 mL screw cap tube and mixed gently by inverting. The solution was incubated at 55°C for 1 hour to overnight to inactivate DNases. The sample was cooled to room temperature, 200 µL Protein precipitation solution was added, and the solution was mixed by inverting the tube rack 150 times and put on ice for 10-15 min. The sample was then centrifuged at 15,000 RPM at 4°C for 3 min., and the supernatant was removed and put on ice for 10 min. This spin step was repeated once to ensure adequate removal of aggregated protein. To the supernatant, 600 µL isopropanol was added and the solution mixing by inverting the tube rack 50 times. The solution was then centrifuged at 15,000 RPM for 1-3 min. at 25°C. To the supernatant, 600 µL of 70% ethanol was added and the solution was centrifuged at 15,000 RPM for 1 min. at 25°C. The pellet was air dried for 15 min, then completely dried in using a speed vacuum as described in Chapter 2. Genomic DNA resuspended by addition of 100 µL TE buffer and incubation in a 65°C H₂O bath for 1 hour. Genomic DNA was stored at -20°C until use.

For all Southern analyses, 3-6 µL of genomic DNA was digested at 37°C for 12-16 hours with 3-6 units of restriction enzyme in a 15 µL total reaction volume. To confirm the gene replacement of *ric8*, genomic DNA was digested with *NcoI* (New England Biolabs, Ipswich, MA). Digestion reactions were run on a 1% agarose gel and transferred to a nylon membrane as described about for southern analysis of the RT-PCR reaction. The knockout cassette was used as a probe (Colot et al., 2006); and probe

labeling was as described in Chapter 2. Digestion of genomic DNA from wild-type strains with *NcoI* yields hybridizing fragments of 2.4 and 1.7 kb, while digestion of DNA from $\Delta ric8$ mutants with the same enzyme yields hybridizing fragments of 3.0 and 2.1 kb (Figure 3.1B).

For GFP localization studies of RIC8 and to complement the $\Delta ric8$ mutation *in trans*, the *ric8* open reading frame (Hibbett et al.) was cloned into vector pMF272 (Folco et al., 2003). pMF272 contains the *ccg-1* promoter and allows expression of an ORF with a 3' GFP fusion at the *his-3* locus in *Neurospora*. The *ric8* ORF, including introns, was amplified from pSM17 using primers designed to add *XbaI* (5' end, R8 GFP fw) and *BamHI* (3' end, R8 GFP rv) sites to the *ric8* gene (Table 3.2) using Pfu turbo DNA polymerase (Stratagene). The PCR reaction mixture consisted of the same concentration of components as described in the northern probe PCR in Chapter 2, except that the total reaction volume was 50 μ L instead of 100 μ L. Thermocycling conditions were as follows: Initial denaturation of 95°C for 5 min.; 30 cycles of 95°C for 30 sec., 60°C for 30 sec., and 72°C for 3.5 min. (included in thermocycle with longer targets); and a final extension of 72°C for 10 min. This PCR reaction (30 μ L, insert) along with plasmid pGEM7, were digested with *XbaI* for 3 hours at 37°C, de-salted using the QIAprep kit with a 30 μ L elution (described in Chapter 2), and digested again for 2 hours with *BamHI*. The fragments were desalted and equal volumes used in a T4 DNA ligation reaction overnight. This ligation reaction was transformed into *E. coli* using the CaCl₂ mediated method described in Chapter 2, and mixture plated on LB+amp plates. DNA was obtained from clones using the boiling mini-prep method described in Chapter 2, and

screened for the presence of an insert by digestion with *Xba*I and *Bam*HI in *Bam*HI buffer using the same conditions as for Southern analysis, except that reaction time was 2 hours.

Clones with inserts were sequenced as described in Chapter 2. A positive clone was chosen and purified using the QIAprep kit. This clone, along with plasmid pMF272, were digested using the same step-wise digestion as described above except that the *Xba*I reaction was incubated overnight. The clone insert was separated from plasmid by electrophoresis on a 1% agarose gel as described in Chapter 2 and cut from the gel using a clean razor blade. DNA was purified from this slice of agarose using the QIAEX II kit according to manufacturer's instructions (Qiagen). The purified clone insert and digested pMF272 vector were ligated and recovered in *E. coli* as described above.

pSM14 was used to target the *ric8-gfp* fusion to the *his-3* locus of $\Delta ric8 his-3$ strain #3 by homologous recombination (Table 3.1; (Aramayo, 1996). Conidia were collected as described in Chapter two, except the last water wash was replaced by washing twice with 1M cold sorbitol. The conidia were suspended in 500 μ L of 1M sorbitol, and conidia concentrations of 2.5×10^9 /mL or greater were used for all transformations. Aliquots of 40 μ L were transferred to tubes on ice and 3 μ g DNA (pSM14) was added. The mixture was then transferred to a 2mm electroporation cuvette and electroporated at 1800V. The electroporation mixture was plated on VM-hyg plates and colonies were transferred onto VM-hyg slants after 2-3 days incubation at 30°C. Isolates were analyzed for integration of *ric8-gfp* at the *his-3* locus as described above for the analysis of the *ric8* gene deletion mutants. Digestion of genomic DNA with *Hind*III and *Bam*HI yields 5.2 and 4.4 kb hybridizing fragments from the wild-type strain 74A

and 7.2 and 4.1 kb hybridizing fragments from the *ric8-gfp* strain when using the 8.8 kb *HindIII* fragment from pRAUW122 (Aramayo, 1996) as a probe. Transformants with the correct integration event were purified by three rounds of colony isolation from VM-hyg plates.

Predicted GTPase-deficient, constitutively activated alleles of *gna-1* (Q204L; (Yang and Borkovich, 1999), *gna-2* (Q205L; (Baasiri et al., 1997) and *gna-3* (Q208L) were introduced into the $\Delta ric8$ background to determine epistatic relationships between *ric8* and the three G α genes. The vectors made by Svetlana Krystofova and Susan Won will be described elsewhere (Krystofova, Won and Borkovich, unpublished). Briefly, the open reading frames corresponding to the three G α alleles were subcloned into vector pMF272, with eviction of the GFP gene, producing plasmids pSVK51 (*gna-1*^{Q204L}), pSVK52 (*gna-2*^{Q205L}) and pSVK53 (*gna-3*^{Q208L}). These genes are all under control of the *ccg-1* promoter. The plasmids were targeted to the *his-3* locus in $\Delta ric8$ *his-3* #3 and *his-3* control (FGSC 6103) strains as described above, generating strains R8G1*, R8G2* and R8G3*. Digestion of genomic DNA with *HindIII* and *EcoRI* yields 6.0 and 3.6 kb hybridizing fragments from wild-type strain 74A and 3.6, 3.5, and 2.4 kb hybridizing fragments upon integration of *gna-2*^{Q205L} or *gna-3*^{Q208L} into *his-3* strains using the *HindIII* 8.8 kb *his-3* fragment excised from pRAUW122 as a probe. A *HindIII* digest yielded a 9.0 kb hybridizing fragment from wild-type and a 7.0 and 4.1 kb from strains with *gna-1*^{Q204L} integration at the *his-3* locus using the same probe.

To construct a strain containing the *gna-1*^{Q204L} and *gna-3*^{Q208L} alleles in the $\Delta ric8$ background, the insert from plasmid pSVK53 (carrying *gna-3*^{Q208L}) was first introduced into a vector that would allow ectopic integration into the *Neurospora* genome. A 2.2kb fragment from pSVK53 containing the *ccg-1* promoter and *gna-3*^{Q208L} allele was released using a step-wise digestion with *NotI* and *EcoRI* as described for cloning the pSM14. This fragment was cloned by ligation into pBARGEM7-2 digested with the same enzymes. pBARGEM7-2 contains the *bar*⁺ gene, which has a high level of ectopic integration, and confers phosphinothricin resistance (Pall 1993). The resulting vector, pSM23, was transformed into the R8G1* strain using electroporation as described above. Transformants were plated on FGS+hyg plates, individual colonies picked onto VM+hyg slants, and spot tested on VM containing phosphinothricin. Transformants that were resistant to phosphinothricin were analyzed for the ectopic integration of *gna-3*^{Q208L}. Digestion of genomic DNA with *SpeI* and *EcoRI* yields an 8.4 kb hybridizing fragment from wild-type strain 74A and a 2.6 kb hybridizing fragment upon integration of *gna-3*^{Q208L} into the R8G1* strain using the 3.1 kb *NotI-EcoRI* fragment from pSM23 as a probe.

The $\Delta ric8$ *mcb* double mutant (R8 *mcb*, Table 3.1) was generated from a cross with a $\Delta ric8$ helper strain (R8 *a^{ml}*) as a female crossed to the *mcb inl* strain (*mcb*). The *mcb* and *inl* genes are linked, allowing screening for the *mcb* mutation in progeny by spot-testing for growth dependence on inositol. Progeny were plated on VM plates containing hygromycin and inositol to isolate $\Delta ric8$ and $\Delta ric8$ *mcb inl* mutants and spot-tested on VM+hyg to identify $\Delta ric8$ *mcb inl* strains.

Northern and Western analysis

To analyze the G protein transcript levels in the $\Delta ric8$ mutants, samples containing 20 μg of total RNA were subjected to Northern analysis as described in Chapter 2. Probes for Northern detection of *gna-1*, *gna-2*, *gna-3*, and *gnb-1* were amplified as described previously (Krystofova and Borkovich, 2005).

All whole cell extract preparations for Western analysis were as described for the GAPDH enzyme assay using extraction buffer (10mM HEPES pH 7.5, 0.5mM EDTA pH 8.0, 0.5mM PMSF, 1M sorbitol, and 1 $\mu\text{L}/\text{mL}$ fungal protease inhibitor cocktail (Sigma-Aldrich Corp. St. Louis, MO)). For Western analysis of GNA-1, GNA-2, GNA-3 and GNB-1 protein subunits, the particulate fraction was isolated as described previously (Ivey et al., 1996; Kays et al., 2000b; Krystofova and Borkovich, 2005). Briefly, whole cell extracts were centrifuged at 25,000 RPM for 45 min. at 4°C in an Avanti J-25 High-Performance Centrifuge ultracentrifuge using rotor JA 25.5 (Beckman Coulter, Inc., Brea, CA). The pellet (particulate fraction) was re-suspended in extraction buffer and homogenized with 10-12 strokes of a 10 mL dounce homogenizer using a B pestle (Kimble Chase, Vineland, NJ). Protein concentration was determined using the Bradford protein assay (Bio-Rad).

Samples containing 35 μg (50 μg for GNA-3 Westerns) of total protein were denatured by adding a 1/4 volume of 4X Laemmli loading buffer (same as 10X loading buffer in Chapter 2, except at 4X concentration), and heating at 85°C in a water bath in for 5 min. Samples were resolved on a 10% SDS PAGE gel (7.5% for CR-1) and transferred to a nitrocellulose membrane (G.E. Healthcare, Piscataway, NJ; 0.45 μm pore

size). Membranes were blocked in 5% milk in TBST pH 7.6 (3% BSA in PBS for GFP) for 30-60 min. at room temperature, then incubated with polyclonal antibody in blocking buffer for 3 hours at room temperature. The primary polyclonal antibodies raised against GNA-1, GNA-2 and GNB-1 were used at dilutions of 1:1000, GNA-3 at 1:500, and CR-1 at 1:5000 (Ivey et al., 1996; Kays et al., 2000b; Krystofova and Borkovich, 2005). The primary polyclonal antibody against GFP (abcam, Cambridge, MA) was used at a dilution of 1:2000. Both secondary antibodies were horseradish peroxidase conjugates of anti-rabbit antibodies (Bio-Rad) used at a range of 1:4000-1:8000. Chemiluminescence detection reagents (SuperSignal West Pico Chemiluminescent Substrate, Rockford, IL) were used to visualize blots on a Biochemi System imager (UVP, Upland, CA) as described in Chapter 2. Coomassie staining was used visualize total protein on polyacrylamide gels. Gels were soaked in Coomassie stain (0.1% Coomassie Brilliant Blue, 25% Methanol, and 10% glacial acetic acid, in water) for 30-60 min. with rotation. Gels were then soaked in de-stain solution (10% acetic acid and 25% Methanol, in water) for 3 hours to overnight, using kimwipes to soak up exceed dye (Kimberely-Clark, Neenah, WI) and changing solution when needed. Gels were dried between two pieces of cellophane (Biorad).

Phenotypic analysis and microscopy.

Submerged cultures were viewed using a BX41 compound microscope (Olympus America, Center Valley, PA). Protoperithecial development was analyzed by spreading SCM plates with 10 μ L of a conidial suspension and culturing for two weeks at 25°C in

the light. Perithecial formation was assayed by fertilizing strains with conidia of opposite mating type (Strains 2489 (*matA*) or 4200 (*mata*); Table 3.1) followed by incubation for one week at 25°C in the light. Images of plate cultures were obtained by scanning, while sexual structures and colony edges were viewed using a SZX9 stereomicroscope (Olympus). All photos were taken using a C-4040 digital camera (Olympus).

Microscopic observation of GFP fluorescence from the RIC8-GFP fusion protein expressed in submerged and plate culture tissues was achieved using a BX41 fluorescent microscope equipped with a WIB fluorescence cube (excitation 460 to 490 nm; emission 515 to 550 nm) and UM Plan Fluorite objective lenses (Olympus). Confocal images of conidia for the RIC8::GFP strain were obtained using a Leica TCS SP2 confocal microscope with an Argon laser (Institute for Integrative Genome Biology, UC Riverside). For nuclei staining, a stock solution of 100 µg/mL 4',6-diamidino-2-phenylindole (DAPI, MP biomedical) dissolved in water was added to 14 hour submerged cultures at a concentration of 0.8 µg/mL and images were captured using the confocal microscope with a UV laser. For hyphal septa staining, Calcofluor White stain for fungi (Calcofluor White and Evans blue, ENG scientific, Clifton, NJ) was added to 14 hour submerged cultures at 2 µL/500 mL and imaging performed using a BX41 fluorescent microscope equipped with a WU fluorescence cube and UM Plan Fluorite objective lenses (Olympus).

Yeast two hybrid assay

A *ric8* ORF clone lacking introns was constructed using homologous recombination in *S. cerevisiae* (Colot et al., 2006). The two introns were removed separately, creating two halves of the *ric8* gene. All DNA fragments for cDNA were amplified by PCR using Pfu turbo DNA polymerase (Stratagene) according to manufacturers protocols. Thermocycling conditions were as follows: Initial denaturation of 95°C for 5 min., 30 cycles of 95°C for 30 sec., 50-60°C for 30 sec., and 72°C for 30-90 sec. (1 min./kb); and a final extension of 72°C for 10 min. To remove the first intron, the 5' UTR up to the first intron was amplified (574 bp product; primers R8YR11fw and R8YR11rv, Table 3.2) as well as the first part of the second exon (756 bp product; primers R8YR12fw and R8YR12rv), using pSM17 as a template. The second intron was removed by amplifying the last part of the second exon (727 bp product, R8YR21fw, R8YR21rv) and the third exon and 3'UTR (579bp; R8YR22fw, R8YR22rv, Table 3.2).

The two sets of fragments were transformed separately into *S. cerevisiae* strain (Colot et al., 2006; Winston et al., 1995) along with vector pRS416 (Christianson et al., 1992; Gera et al., 2002) gapped with *Xba*I and *Eco*RI, with selection on SC medium lacking uracil. DNA was extracted from transformants (Smash N' Grab, see Methods in Chapter 2) and plasmids were recovered by electroporation into *E. coli* and plating on LB+Amp. The recovered plasmids were sequenced, and it was discovered that the plasmid containing the 5' portion of *ric8* was missing the first 24 nucleotides. Therefore, this construct was re-amplified with a primer that added the nucleotides back (744bp; R8Y2H fw new, R8YR12rv).

PCR was used to amplify the *ric8* cDNA and introduce restriction sites for yeast two-hybrid cloning. The 5' fragment was amplified with primers R8Y2Hfw and R8YR12rv (744bp), introducing the *EcoRI* restriction site 5' to the initiator ATG and extending to include the restriction site *XhoI*. The 3' fragment was amplified with primers R8YR21fw and R8Y2Hrv (836bp), which include the *XhoI* site and insert a *BamHI* site in place of the TGA stop codon. These fragments were digested and ligated into *EcoRI* and *BamHI* digested pGEM4 and clones selected for sequencing. The cDNA from one correct construct was digested using *EcoRI* and *BamHI* and subsequently ligated into *EcoRI* and *BamHI* digested pGAD424 and pGBKT7. These constructs were transformed separately into *S. cerevisiae* strains AH109 and Y187 (see Chapter 2 methods for genotype information and yeast transformation protocol), and plated on either SD/-leu or SD/-trp to yield yeast strains R8-AD and R8-BD. The *gna-1*, *gna-2*, and *gna-3* genes were cloned into pGAD424 and pGBKT7 (Kim and Borkovich, unpublished).

The yeast two-hybrid assay was conducted using a mating method (See Chapter two for details). Strains R8-AD and R8-BD were mated to the G α strains and strains containing pGAD424 and pGBKT7 empty vectors. Mating reactions were plated on SD/DDO to select for diploids. Diploids were then tested on SD/TDO (+3-aminotriazole to eliminate leaky *HIS3* expression), and SD/QDO medium to select for the expression of the *HIS3* and *ADE2* reporter genes. Plates were incubated for 5 days at 30°C. To screen for expression of the reporter gene *lacZ*, a colony lift assay for β -galactosidase activity was performed according to manufacturer's recommendations (Clontech). A sterile

Whatman No. 5 filter was pre-soaked by placing it in 2.5–5 ml of Z buffer/X-gal solution (60 mM Na_2HPO_4 , 40 mM $\text{NaH}_2\text{PO}_4 \cdot \text{H}_2\text{O}$, 10 mM KCl, 1 mM $\text{MgSO}_4 \cdot 7\text{H}_2\text{O}$, 39 mM 2-mercaptoethanol, 1 mg/ml 5-bromo-4-chloro-3-indolyl-Beta-D-galactopyranoside (X-gal), pH 7.0). A dry nitrocellulose circle (Protran[®] BA85, 0.45 μm pore size, Sigma-Aldrich) was placed over the surface of the plate of yeast and gently rubbed with forceps to help the yeast cells cling to the filter. The filter was carefully transferred to a pool of liquid nitrogen, submerging for 10 sec. The filter was then removed from the liquid nitrogen and allowed it to thaw at room temperature, then placed on the presoaked Whatman filter and incubated at room temperature until colonies turned blue.

Results

ric8 isolation, gene structure analysis and protein alignment

RIC8 is found only in fungi and animals (Wilkie and Kinch, 2005a). In fungi, the closest homologue to animal RIC8 is a 53 KDa *Neurospora crassa* protein designated NCU02788.3 (Broad institute). The predicted gene structure in the Broad Institute database was confirmed by sequence analysis and verification of the predicted introns. The presence of the 3' intron was confirmed by cDNA sequence NCW06G3T7 (cDNA clone W06G3 3'; Broad Institute) and the 5' predicted intron was verified by reverse transcriptase-polymerase chain reaction (RT-PCR; Figure 3.1C).

Of the animal RIC8 homologs, *Neurospora* RIC8 is most homologous to *Xenopus tropicalis* Ric-8A and also exhibits significant identity to human RIC-8A (Figure 3.2). Although RIC8 proteins are highly conserved among certain fungi (Figure 3.3), there are no significant ($E < 1e^{-4}$) homologs in the yeast *S. cerevisiae*, and RIC8 is also absent from the genomes of plants and sequenced protists, including *Dictyostelium discoideum*. Four sequenced yeasts possess proteins similar to the *Neurospora* RIC8 homolog (*Yarrowia lipolytica* ($E=9e^{-20}$), *Schizosaccharomyces japonica* ($E=5e^{-20}$), *Schizosaccharomyces pombe* ($E=9e^{-13}$), and *Debaryomyces hansenii* ($E=1e^{-5}$), but not to animal RIC8 proteins. The observation that RIC8 is widely found in filamentous fungi may reflect a role for RIC8 in polar growth in these multicellular organisms.

Epistatic and physical relationships between *ric8* and G α subunits

Since RIC8 has been shown to be a GEF for G α proteins in other systems, we investigated a possible role for *Neurospora* RIC8 as an upstream regulator of the G α subunits GNA-1, GNA-2, and GNA-3. Our laboratory has previously demonstrated that simultaneous loss of *gna-1* and *gna-3* causes severe defects in vegetative growth and sexual structure formation and inappropriate formation of conidia in submerged cultures (Kays and Borkovich, 2004a-a). Loss of *ric8* leads to similar phenotypes in vegetative growth and sexual and asexual development (Figure). During the sexual cycle, $\Delta ric8$ strains do not differentiate protoperithecia and are thus female-sterile (Figure). $\Delta ric8$ mutants have thin basal hyphae that grow extremely slowly and produce short aerial hyphae (Figure 3.4A and Figure 3.10). $\Delta ric8$ mutants also produce short aerial hyphae and inappropriately form conidia in submerged culture (Figure 3.4A). In addition, the submerged culture conidiophores of $\Delta ric8$ mutants are morphologically abnormal. $\Delta ric8$ mutant conidiophores form at a 90 degree angle from the basal hyphae in submerged cultures, whereas conidiophores from previously studied G protein mutants are formed at a less than 90 degree angle in the direction of tip-growth (Figure 3.4A; (Ivey et al., 2002; Kays et al., 2000b; Yang et al., 2002). Complementation of the $\Delta ric8$ mutant with the *ric8-gfp* fusion construct inserted *in trans* is shown in Figure 3.1C.

The shared defects of $\Delta ric8$ and G α mutants prompted me to measure G α protein levels in the $\Delta ric8$ mutant. Loss of *ric8* causes a drastic reduction in protein levels of GNA-1, GNA-2, GNA-3, and GNB-1 (Figure 3.5A), to the point where they cannot be detected by western blot analysis. In contrast, transcript amounts for the respective genes

are similar in wild-type and the $\Delta ric8$ strain (Figure 3.5B), suggesting a post-transcriptional control mechanism. In submerged cultures, loss of *gnb-1* leads to almost undetectable amounts of GNA-1 and levels of GNA-2 are greatly reduced, while GNA-3 protein levels are unaffected (Yang et al., 2002). A similar requirement for *ric8* in maintaining normal levels of a $G\alpha_i$ protein and associated $G\beta$ subunit has been observed in *Drosophila* (Hampoelz et al., 2005). Though a decreased level of GNB-1 in the $\Delta ric8$ mutant could account for low amounts of GNA-1 and GNA-2, the reduction in GNA-3 levels in $\Delta ric8$ mutants can not be explained by the loss of GNB-1. This suggests that GNA-3 stability is regulated by RIC8 independently of GNB-1.

During the G protein cycle, GTP-bound $G\alpha$ is released from $G\beta\gamma$ and the GPCR and is then free to interact with downstream effectors. Hydrolysis of GTP to GDP returns the $G\alpha$ protein to $G\beta\gamma$. Because of these factors, a GTPase-deficient $G\alpha$ allele is constitutively active and independent of $G\beta\gamma$. We therefore transformed activated forms of the three $G\alpha$ genes into the $\Delta ric8$ background under control of the strong *ccg-1* promoter in order to determine whether they would rescue $\Delta ric8$ phenotypes.

Introduction of each $G\alpha$ activated allele into the $\Delta ric8$ background restored the encoded protein to wild-type levels (Figure 3.5A). It could be that the $G\alpha$ activated alleles are more stable than the wild-type alleles, however since the activated alleles are under control of a non-native promoter (*ccg-1*) these effects could be due to a change in expression. The presence of the *gna-1*^{Q204L} and *gna-3*^{Q209L} activated alleles partially rescued the slow growth phenotypes of $\Delta ric8$ (Figure 3.4B). The colony diameter is

about double that of $\Delta ric8$ in the presence of the $gna-1^{Q204L}$ allele, and introducing the $gna-3^{Q209L}$ allele has an even greater effect, with a colony diameter at least three times larger than the $\Delta ric8$ strain. When both $gna-1^{Q204L}$ and $gna-3^{Q209L}$ were introduced into the $\Delta ric8$ background, the phenotype resembled that obtained after transformation with $gna-3^{Q209L}$ alone. Transformation of the $gna-2^{Q205L}$ activated allele into the $\Delta ric8$ background had no effect. Though the strains still exhibited inappropriate conidiation in liquid culture, the abnormal 90° growth of the $\Delta ric8$ conidiophores were restored to that of a $\Delta gna-3$ mutant (less than 90°) with the introduction of $gna-1^{Q204L}$ and $gna-3^{Q209L}$ but not $gna-2^{Q205L}$ (Figure 3.4). Thus, the results from the genetic epistasis experiments suggest that RIC8 acts upstream of and is a positive regulator of GNA-1 and GNA-3, but not GNA-2.

I next investigated the possibility of a physical interaction between the G α proteins and RIC8 using the yeast two hybrid assay. RIC8 was observed to interact with GNA-1 using the ADE2 reporter, and GNA-3 using both the ADE2 and β -galactosidase reporter (Figure 3.6). An interaction between RIC8 and GNA-2 could not be observed using this method. This data suggests that RIC8 may bind to GNA-1 and GNA-3 *in vivo* in *Neurospora*. Interestingly, RIC8 interacts with GNA-1 as a Gal4 DNA binding domain fusion and GNA-3 as a Gal4 activation domain fusion (Figure 3.6; ADE2 reporter). This may indicate a different physical relationship and/or binding site for RIC8 on these two G α subunits. Taken together, these results are consistent with RIC8 functioning as a positive regulator of GNA-1 and GNA-3, but not GNA-2, in *Neurospora*.

Loss of *ric8* affects the cAMP signaling pathway

Adenylyl cyclase has been extensively characterized in eukaryotes and has been shown to be activated and repressed by G protein signaling in various systems (rev in (Neves et al., 2002)). Activated adenylyl cyclase produces cAMP, which binds to the regulatory subunits of protein kinase A (PKA), releasing the catalytic subunits of PKA to phosphorylate a wide variety of target proteins. In the *C. elegans* synaptic signaling pathway, RIC8 has been linked to cAMP metabolism through the identification of mutations that suppress defects of *ric8* loss-of-function mutants (Charlie et al., 2006; Schade et al., 2005). These mutations include dominant activated alleles of *gsa-1* ($G\alpha_s$) and *acy-1* (adenylyl cyclase), and reduction-of-function alleles of *kin-2* (regulatory subunit of PKA) and *pde-4* (cAMP phosphodiesterase). These results suggest that RIC8 is an upstream positive regulator of the cAMP pathway during synaptic signal transmission in *C. elegans*. In *Neurospora*, results suggest that adenylyl cyclase (CR-1) is activated by GTP-bound GNA-1, while GNA-3 is required to maintain normal levels of CR-1 protein (Ivey et al., 1999; Kays et al., 2000b). Furthermore, a mutant allele of the PKA regulatory subunit (*mcb*) that is predicted to lead to hyperactivation of the catalytic subunit is epistatic to *gna-3* and suppresses the Δ *gna-1* mutation (Bruno et al., 1996; Kays and Borkovich, 2004a-a). Consistent with animal systems, cAMP is a major downstream pathway in Heterotrimeric G protein signaling in *Neurospora*.

Based on the known relationship between RIC8 and cAMP metabolism in *C. elegans* as well as the physical and genetic relationship between RIC8, GNA-1 and GNA-3 in *Neurospora*, we investigated whether cAMP signaling is affected in *Neurospora*

$\Delta ric8$ mutants. Levels of the CR-1 adenylyl cyclase are reduced greatly in all strains in the $\Delta ric8$ background (Figure 3.7A), similar to results observed for $\Delta gna-3$ mutants and consistent with low cAMP levels (Kays et al., 2000b). We followed up on this finding by testing the effect of the *mcb* PKA regulatory subunit mutation described above (Strain R8 *mcb*; Table 3.1). The *mcb* mutation partially suppresses the $\Delta ric8$ growth phenotype, as the colony diameter of the $\Delta ric8$ *mcb* strain is at least four times greater than that of the $\Delta ric8$ strain (Figure 3.7B). The short aerial hyphae and hyperconidiation phenotypes of the $\Delta ric8$ mutant also appear to be suppressed in the $\Delta ric8$ *mcb* strain, which is fluffy and less pigmented than the $\Delta ric8$ strain mutation (Figure 3.7B). These results show that RIC8 is important for normal levels of CR-1, and that some $\Delta ric8$ phenotypes may be due to a decrease in PKA signaling.

RIC8 localizes to septa in hyphae and the cytoplasm in conidia

Models of asymmetric cell division that have been theorized are consistent with RIC8 having a dynamic cell localization (Nguyen-Ngoc et al., 2007; Wilkie and Kinch, 2005a). For example, by using a combination of strains which express GFP tagged RIC8 and immuno-staining wild-type cells with anti-RIC8 antibody, it has been shown that RIC8 localize to the cell cortex, the asters of the mitotic spindles, the central spindle, at the nuclear envelope and around the chromatin during various stages of mitosis in early embryonic cell division in *C. elegans* (Couwenbergs et. al. 2004). In order to determine the localization of RIC8 in *Neurospora*, we produced a vector containing a C-terminal GFP fusion of RIC8. This construct, which was transformed into the $\Delta ric8$ *his3* strain,

restored expression of the *ric8* transcript, and restored all $\Delta ric8$ phenotypes, which shows complementation. Production of a full-length RIC8-GFP fusion protein in this strain was observed by Western analysis using whole cell extracts and GFP antiserum (Figure 3.1). Analysis of strains carrying the GFP fusion showed that RIC8 is cytosolic in all tissue types tested except for aerial hyphae (Figure 3.9A). In aerial hyphae, RIC8 is localized to septa, and in conidiophores is dispersed into the cytosol. This could indicate that either RIC8 is needed only for septal formation and dissipates shortly after, or that RIC8 migrates from the septa into mature conidia.

Septal spacing and nuclear morphology in $\Delta ric8$

Filamentous fungi exhibit apical tip growth in which cell division is characterized by formation of cross walls, or septa, that divide individual hyphal compartments (Hunsley and Gooday, 1974). Septa contain a pore that allows nutrients and organelles such as nuclei to move between hyphal compartments. Since septation is an important aspect of hyphal growth in filamentous fungi, we investigated formation in *ric8* mutants. The distance between septa in basal hyphae is approximately half that of wild-type in all strains with the $\Delta ric8$ mutation (Figure 3.8C). In addition, the hyphal diameter in strains lacking *ric8* is more than half the diameter of wild-type (Figure 3.8A). These two parameters contribute to the smaller size of cell compartments in $\Delta ric8$ mutants. Mutation of *gna-3*, but not *gna-1*, affects septa spacing, indicating that normal septal spacing may require both GNA-3 and RIC8 (Figure 3.8C).

Movement of organelles, including nuclei, through the hyphal network is crucial for polar growth in filamentous fungi (McKerracher, 1987). It has been recently determined that fungal nuclei range in shape from round to elongated, and that elongated nuclei are undergoing movement in the direction of hyphal tip growth (Freitag et al., 2004). In submerged cultures, wild-type and $\Delta gna-1$ mutants exhibit normal nuclear size and morphology and elongated nuclei were rarely observed (Figure 3.9B). In contrast, nuclei from the $\Delta ric8$ mutants are small and more than 50% are elongated. Mutation of *gna-3* leads to smaller and more elongated nuclei, although not to the same extent as observed for the $\Delta ric8$ mutant (less than 50% are elongated). This indicates that loss of *ric8* or *gna-3* leads to smaller nuclei and an increase in nuclear movement.

The presence of the *gna-1*^{Q204L} allele does not alter nuclear morphology in the $\Delta ric8$ background (Figure 3.9B). However, introduction of *gna-3*^{Q208L} completely restores nuclei to normal size and reduces the number of abnormal nuclei (less than half are elongated). This result is consistent with regulation of nuclear movement by both RIC8 and GNA-3 in *Neurospora*.

Discussion

The discovery and subsequent study of RIC8 in metazoan cells has shown that this protein is required for major cellular processes, including asymmetric cell division and synaptic signaling. Here we demonstrate that RIC8 is involved in critical functions, including vegetative growth, sexual and asexual sporulation, and nuclear morphology in *Neurospora*. Mutations that activate the GNA-1 and GNA-3 G α proteins in the $\Delta ric8$ background partially restore wild-type phenotypes in the $\Delta ric8$ mutant, and RIC8 interacts with GNA-1 and GNA-3 in the yeast two-hybrid assay. The data suggest that RIC8 participates in pathways involving GNA-1 and GNA-3 to different extents, as only GNA-3 influences adenylyl cyclase levels (see below) and nuclear movement.

Work in *C. elegans* has demonstrated the importance of cAMP metabolism to RIC8-related functions in the synaptic signaling pathway. It is striking that positive regulation of the cAMP pathway by RIC8 is apparently conserved between *C. elegans* and *Neurospora*. In both systems, a mutation in the PKA regulatory subunit suppresses a *ric8* mutation. Importantly, we also demonstrate that loss of RIC8 leads to a reduced level of adenylyl cyclase protein, a finding that has not been previously reported in any system. This observation may explain why a hyperactive allele of adenylyl cyclase was recovered in a *ric8* suppressor screen in *C. elegans* (Schade et al., 2005). Finally, similar to reports in *Drosophila*, RIC8 is also required for normal levels of G proteins in *Neurospora* (Hampoelz et al., 2005). Taken together, these results suggest that maintenance of normal levels of G proteins, adenylyl cyclase (and perhaps other yet-

unknown regulatory components) is an important conserved function of the RIC8 protein and one that directly impacts cAMP signaling.

The only other study of a RIC8 homolog in filamentous fungi has been reported very recently in the fungal rice pathogen *Magnaporthe oryzae* (Li et al 2010).

Magnaporthe RIC8 (MoRic8) was discovered in a screen for non-pathogenic T-DNA insertion mutants. Through localization studies, MoRic8 was shown to be cytosolic and expressed highest during appressorium formation. *Magnaporthe* contains three G α subunits which are homologous to GNA-1 (MagB), GNA-2 (MagC) and GNA-3 (Galagan et al.) (Liu and Dean 1997). It was also shown that MoRic8 binds to MagB, but not MagA or MagC, in the yeast two-hybrid assay; and that addition of exogenous cAMP increases appressorium formation of the MoRic8 gene deletion mutant by 60%, however these appressoria are unable to infect plants (Li et al 2010). Taken together, these results complement the results from my study of RIC8 in *Neurospora crassa*.

Microtubule dynamics are critical for proper asymmetric cell division. In *C. elegans* one-cell embryos, the microtubule associated protein dynein forms a complex with LIN-5 (coiled-coil protein) and GPR-1/2 (Goloco protein) at the minus end of microtubules, and a GDP-bound G α protein (GOA-1 or GPA-1) anchors this complex to the membrane through interactions with GPR-1/2 (Nguyen-Ngoc et al., 2007; Wilkie and Kinch, 2005a). Dynein then ‘walks’ towards the minus end of the microtubule, causing a pulling force. The GEF activity of RIC-8 activates the G α proteins and releases the complex, while RGS-7 accelerates GTPase activity of the G α proteins to re-form the complex. *Neurospora* contains an RGS-7-like protein (Borkovich et al., 2004), dynein

subunits (Borkovich et al., 2004) and more than eight potential LIN-5 homologs. There are no significant homologs of GPR-1/2; however, since this protein is thought to serve as a scaffold, there may be a fungal-specific protein that fulfills the same purpose.

In fungi, microtubules are required for transport of nuclei and other organelles towards the tip of growing hyphae (Xiang X, 2003). In addition to RIC8, another *Neurospora* protein that influences septation and nuclear morphology is RHO-4, a small GTPase that localizes to sites of septation (Rasmussen and Glass, 2005; Rasmussen CG, 2008). Loss of *rho-4* leads to hyphae that are aseptate, possess large, elongated nuclei and contain a reduced number of microtubules that display aberrant morphology at hyphal tips (Rasmussen CG, 2008). The increase in elongated nuclei in both *ric8* and *rho4* mutants, and the observation that *rho4* mutants have microtubule abnormalities suggests that both genes are required for normal nuclear movement along microtubules. The current model for asymmetric division of nuclei in *C. elegans* embryos involves regulation of microtubule organization in order to generate the proper pulling forces (Nguyen-Ngoc et al., 2007). Therefore, a conserved role for *Neurospora* RIC8 in microtubule-based movement of nuclei and links to RHO-4 will be investigated in the future.

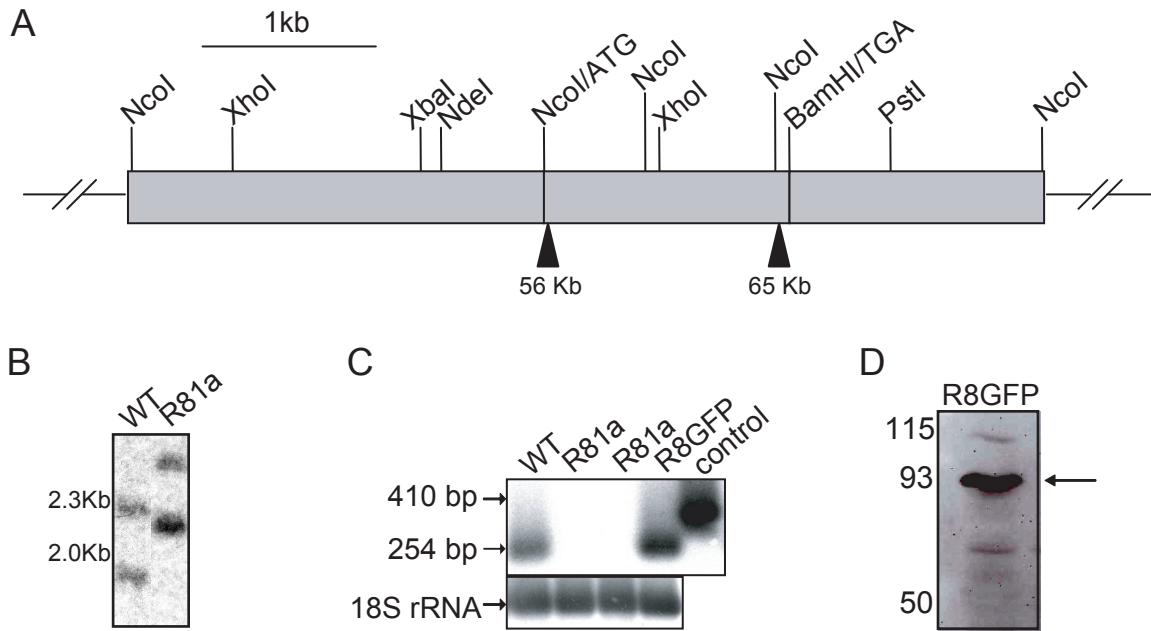


Figure 3.1: *ric8* gene structure, mutant verification, and protein molecular weight

A) The *ric8* genomic region from *Neurospora crassa*. Intron locations (black triangles) and restriction enzyme digestion sites (black lines) are shown. B) Southern verification of gene replacement mutant. Southern analysis was used to verify the $\Delta ric8$ mutation generated by the *Neurospora crassa* genome project using the knockout cassette as a probe. Using restriction enzyme *NcoI*, a digestion pattern of 2.4 Kb and 1.7 Kb is seen for wild-type and 3.0 Kb and 2.1 Kb for the $\Delta ric8$ mutant. C) Intron verification and complementation of the $\Delta ric8$ mutation. Samples containing 2 μ g of total RNA isolated from conidia of wild-type (2489), $\Delta ric8$ (R81a, loaded twice) and R8GFP strains were subjected to RT-PCR with primers designed to flank the first predicted intron of *ric8*. The predicted intron size is 56 bp, making the total size of the RT-PCR fragment 354 bp. The genomic control (410 bp) and probe DNA were amplified by PCR from plasmid pSM2 using the same primers. Expression of the 18S rRNA gene was assessed under identical RT-PCR conditions and used as a control. The complementation of the $\Delta ric8$ mutant *in trans* is shown by RT-PCR (R8G). D) A Western blot showing the expression of a RIC8-GFP fusion protein in *Neurospora* using anti-GFP antiserum. The approximately 93 KDa protein is indicated by the black arrow.

```

NC  ---MASHGVSGEPAKIQAVTILIHKLITELIKSTISLSPDE---RDKALJEEKMYGRDPNADFIYKCGHETITKREAFYSP---*
Xt  ---MDFGILDKIESGOELQKALREYNQNSOCFFNAEQRE-ERKKGELVVKFLNRDLQSCQACLETIRLLSRDKHALSPPTGSAIOLACVAGDY---SEEMEMPRIS
Ce  MSEELHSDLJASIFGCKPAKIEEFFKMFANAWKSFDMANS-AQNELGHRICVYIENG---EPTHWILETIKLISREKDGLEGLNDPLCDKILAAEALSS---NENNS
Dm  ---METEHIKRIEAKADHHPAIIPEENKVALLVFVSFRINDLWHEILWLAIFGLDORLSHLHTCCINVRILIRDEFISIQNYIICEVNTIILKARIEAGSKLKPATPDELKQEBREPEOLEPSQ
Hs  ---MFRVAEAIVTGBEDVIMEALRSYNOBHSQSFIFDACEE-DRRRLAELVSVLECGLPPSHRVIMIQSVRLISRDINCLDPFTSKQSIQALACVADIS---VSEGSVLEHS
*
NC  -SETISRVALRMICNAVLLIPEITRQEFVIGYESKACEIKNENWD---EFTATRVIIESTYGTTVLAKTIDHHILAFESVANLARHARSISEHAKNKTK---PDDM
Xt  PGEVAEALKCGNLIYNSEMAQEVAKELRLVCGFARIKLYNETR---SHESEFFDRLLLFLLTALISVNRKQIAOELFGVSLLDLDALESITALKWSDIYEVVTDRLAPPLGKE
Ce  KTMHILMAEQKCIJNLIHSHQRMREFYANPKTGENIOPFLGFEFENRRKTSSIDMIRLILNIPYQAAEIIWVYHRJAFATATIGREFOKMANDBATIDSLILAVEICTNREB---NSIQ
Dm  AQSEVIAEALKCLGNIVYQSSICRROCIROHCTDAILKRVASS-MR---HFCALIEYDVKLLFLLTALIEPAARSRQIDINGLITWYTKWLDKICEDS---VGBE
Hs  ADMVVIIESEKCLCNILYSSVQMLAAEARLVKILTERGLKFRERS---EPHDVQFFDURLLLFLLTALIEFTVROQIFQLGVRLLTALIEITLCVPE---EGNPPPTIILPSQ
*
NC  -SETISRVALRMICNAVLLIPEITRQEFVIGYESKACEIKNENWD---EFTATRVIIESTYGTTVLAKTIDHHILAFESVANLARHARSISEHAKNKTK---PDDM
Xt  PGEVAEALKCGNLIYNSEMAQEVAKELRLVCGFARIKLYNETR---SHESEFFDRLLLFLLTALISVNRKQIAOELFGVSLLDLDALESITALKWSDIYEVVTDRLAPPLGKE
Ce  KTMHILMAEQKCIJNLIHSHQRMREFYANPKTGENIOPFLGFEFENRRKTSSIDMIRLILNIPYQAAEIIWVYHRJAFATATIGREFOKMANDBATIDSLILAVEICTNREB---NSIQ
Dm  AQSEVIAEALKCLGNIVYQSSICRROCIROHCTDAILKRVASS-MR---HFCALIEYDVKLLFLLTALIEPAARSRQIDINGLITWYTKWLDKICEDS---VGBE
Hs  ADMVVIIESEKCLCNILYSSVQMLAAEARLVKILTERGLKFRERS---EPHDVQFFDURLLLFLLTALIEFTVROQIFQLGVRLLTALIEITLCVPE---EGNPPPTIILPSQ
*
NC  *
Xt  *
Ce  *
Dm  *
Hs  *
NC  EIMALGETIRLILFNVTSKCPSSK--LFCFTAAVPHIVITLISLDLPPPKGTP-PIESGFSPIVNALMNLK---IDSEARSQIYPKDAP---SSELABKTIITLDLSIKKA
Xt  ETERWELIKLRFNIITDLSREVEBDDAALYRHLAAILRODGEF-RTEEFHGHVNLILNLP---FALCLDVLITPVEHQLLRQOG---SVEYMGNNMDIYEVVIO
Ce  DINRATIEAKITFFNFVCHFHG---DVKRAIDHKNAAKTACISLVITDILVQSAIHCISVPH---LPMVLSVTCCKNSCOLLRDKNNCGENEBEKKFFVEELSNMQLTEAIIIMIDKQITKVAI
Dm  QNILICEILKWFNVTSAPDKS--PNIEYETOSIHTIGVLRGDLATEIDRAVWTHANILIANISSCLITELTIFCSNABIESHKEEILLRREODNEKEKQTEAGAGAKPRECCSOCFEAFNRSIDVLIIR
Hs  ETERAMELILKVLRFNIITDLSIKGEVDEBDAALYRHLGTLIRTAGL-RTEEFHGHAVNLIENLPE---LALCLDVLITPVEHQLLRQOG---SSELABKTIITLDLSIKKA
*
NC  *
Xt  *
Ce  *
Dm  *
Hs  *
NC  YSDGELDQAVT---PFLYCTISSIYENAPADSPVDFIRKSS---ILPSEB--ERNKVLGCKDITPAKILANMNLIAPEFAFVSHLIFRNSDKDANKFVENIYGXVYASCFTEQNNIPV
Xt  FLDRLLDRGCHKIR---EFTLTPVNLITLSSRIRHRETRKFLRAK---VLPPIIR--DVKNRPEVGNTRLNKRLIMTHVDIT-DVKHCAAEFLFVLCKBNVSRFVKYTYGNAAGLILAAARGLIA
Ce  LINDAPNQQNPMLSAEASTLTDIICFYQVJARLCTDSKVPYQYRER---VPPVISEVYCKRPEENMTRGELIARIMLES-STKDVAAAEFLIIOKRSVNRMIKXILGSHSAGILANILGIC
Dm  YLRQSTAQAEAS---SHELLSEVILVIVKCARSDRVRVHYLRQE---ILPPIIR--DVSOREPVGEBLRHLCRFTLIFAM-TIRDISABEILFVLCKBNVGRMIKYTYGNAAGLILAAARGLID
Hs  FLERELHKTIRLIK---ESWAPVLSVITTEGARHREPAKFLIAGOWPPPPQVLPPIIR--DVRTPEVCEMIRNKILVRLMTHLDT-DVKRVAAEFLFVLGSESEVRFRIKYTYGNAAGLILAAARGLINA
*
NC  ***
Xt  ***
Ce  ***
Dm  ***
Hs  ***
NC  PEGIGC---DAFKGESSQAGOSRRVAVNEITGQFLDITETFPDPPEMTMEEKREZERLTVIFRRAKLGIVN---VENPVAKAVQEGRFEELPDDDEEDSD---
Xt  GGRREG---YSEDEBDITDEETAEAKENINPVTGRVEEKECF--NPMDGMTEEOKEYEAMKLVNFDKLSLEQILQPMGVISDGRLEPDEPAQKMLQROESDDESDSD---
Ce  QINQPK---FASDSDESTEDNQIKFSVNPVTGAILYPSHGSATFAGSEEOKEYEAMKLVNFDAMNQMMETGIVKRFPTIGDDGKIREVSHVTELLKNAPPEPAPNSDSDEE---
Dm  CRREGTYSDESDSDETEEXKQOQOQINPVTCCVEPESK--SHLDDISEOKEYEAMKLVNITCIRROGGIVAFAMDKDGRFQPELHLLQLELPOOQLDKRRTI---
Hs  GGRREG---CYSEDEBDITDEXKAEKASINPVTGRVVEEKECF--NPMEGMTEEOKEHEAMKLVITMFDKLSRNRVLIQPMGNSPREHITISODAN CETIMEOQLSSDPEPSDPE---

```

Figure 3.2: RIC8 homologues
 ClustalW (<http://www.ch.embnet.org/software/ClustalW.html>) was used to align RIC8 sequences from *N. crassa* (Nc; NCU02788.3), *Homo sapiens* (Hs; accession # NP_068751, E=5e-8), *Xenopus tropicalis* (Xt; accession # NP_989159, E=2e-10), *C. elegans* (Ce; accession # Q9GSX9) and *Drosophila melanogaster* (Dm; accession # Q9W358). Boxshade was used to indicate identical (black) and similar (grey) amino acid residues (http://www.ch.embnet.org/software/BOX_form.html). Astericks (*) indicate conservation of identical amino acid residues in all species.


```

Nc MA---SIGVSGPAKIQAVTTLHKLTEDLKSISLSPE-----ERDKALEELKVKYGRDPRVADPIFTKQGFETLTKHAFDPSSETTSRMALRVLICNA
Pa MN---AKAKTPVAKIDAVKQLGSETEDLETSSIAPORWFIFPAALEIASNKFEIGRESILEETLKIYGRDPNGADPIFTKQGHKTLVRHAFDSTSVNTRSRGAURLICNT
Mg ---MLNNTTKG-----TDKLTLDLKEHMLSSQ-----ERDAALEQULKVKYGRDPRVADPEPIFTKQGHSTLAAHSFDGSDTTSRMALRCLANA
Fg MATLPPAGLPIGTDKLEYIKELINDLSEDI NEELVLPD-----DRAAVLQULKILTRDPRVADPLFTKQGHSTLIRHAFDPESTKSDARVLANA
An ---MDLRILIQGSEKIQVTKLINSLEKDLKINSINSAQ-----RTQILIQLRQYGTSPNAGPIYSKKGHEILSKYCHDGETDVRHIALRCVANA

Nc MLLIPEPTRQRFVDLGYESKACEKLNNDWDEFVATRVIFESTYGTIVDLAKLIDEHHLAE SVVANLARHARSRESEHAKNKTKDPMEIMALGETLRLLEFNVTISKCP SKL
Pa LLLPEPTRORFVDHGYAAKAKASEKLEKEDNSDDEFVAVARILLISTXNTNIDLPKLIHQHGLADSIANHLARHAKRISSTNRSITIAN - PMPMALLETIKLTFNVSQFSPNHL
Mg MLLQFSRQELMDLGVHIIKAKAKLAAASDSDDEFVLSRVLMIAANARNINHEILLHQHGLAEILAAARLESIMRHELPDEDSS---FNMEGMALSETLKMNFAMVTRFCPGQS
Fg MVLKTVTRDIFVAKGFAPNACQGTNGSGFDDDEFNISRILFLSTYGTIVDIKKLIDDEKLAIRIENLARHAK-----ESKAKSDPMQDMALVESAKLLEFNVTIYCPDKS
An LLLDSNWRQLFVDTKCGGRLAEMLKGDSSEHEMVI SRILFLSTYDTNLFNFDLANNHSLGDNINYOILRHSKQPKSGR--KPLSQVDELAFDTLKLVENIAKLFQDLA

Nc DCFIAAVPHIVITLLISLDIPPPKGTPLLESPISPIANALMNIKLDLS---EEARSCLYPKDAPSSIAEKLIITLIDLSLKAYSDQ-ELDATVTPLVCIISSIYENAPADSP
Pa ASFEPAIPHIIITLCSLDLPSPHKTPPLGPPFGFAVNAVILNLDLSI---PTAKYLYPDSSESSFDRLIKLISLSIKAYKNP-DLEQIVTPLVCALSLVYEHAPAS--
Mg TRFACAGHIIITLQORPLPAES---VLDPPFGFIVALCTLDLED---EAITNLFPERDPSLVTSRLLISLDLRALSEFKNGMDPTMTVLAGSLCIIIEAAP--EP
Fg SSFTSALPHI VALLKQDIS---QTKPLDPPVCFIVALANLDVCS---SDCOXSIHPEEDPEKVVSRLLISILDAAAMKNVPM-QLDATVSPLI GVISSVVKHAPDSS-
An PITFESIPYIFKTI SRDIP-----IKPLDGLI GHLINCLSTLDLENKMKPYDGNPIFPTFNQNCNVDKLINLIDCAVSAYEPS-ELETKAIPLFHTLVTIHEVADGDP-

Nc VRDITRKSLLPSEERKNKVLGKGDITPAKLIANVTNP IAPEFARAVSHLLFNISD K DANKFVENI GYGYASGFUFONNIP-VPEGLI--GGDAEK-GES SQAGOSRRAVN
Pa VKQSLKALLPTEKREDALGKADTLQCHLLKMNENPEAPELGGKAI AHLYFDLSNRPDPHKFVKNVGYGYASGFUFONNISFTPEELNKGGETVEGEDG--VREIKRPIIN
Mg VRI SVAQALLPTEDRKEVLGSTEIPSKLLKMTNMAPKSRKAI SHLLFLSLSDR DACKFVEKVG YGYASGFUFENIPVQSALASEGASG-----TMOGRAVN
Fg -KKVTRKLLPTEDRKEVLGKGFALS AKLIIQNFNMP LAPSNGTVIQHLLYDLSENDANKFVENVGYGFASGFUFONNIPVPPSASDPG-----SQKPVN
An -RKNVQWLLLPDINDRDRPIGQSDTILSKLLKLSLTMHYAN-LKVAISELMLFVLSKNAESLTKNI GYGFAGHLASRGMDLIPKSAGEAFATNSQ-----DLNPELIN

* * * * *
Nc PITGQFLDTEITPDVPEMTMEEKERBAERL FVLFERARKLGI VNVENPVAKAMQEGRFEELPDDYEEDSD-----
Pa PITGQFLDTERVSELPBMTDEEKERBAERL FVLFERLKTGIIDVQNPVEQAMRGRFEELPDDK-----
Mg PITGQFLDAEKLSDIPMSQEEKEBAERL FVLFERLKTGVDVQNPVEKAFQEGRVEELEDDEDGDENKKVVEQK
Fg PVTGQHVDAEKPVPEPMTDEEKERBAERL FVLFERLKNITGVDIQNPVEAAMRGRYRELKDDVEVEIEI-----
An PITGQVAAEKEDTCEPMTKEEKERBAERL FVLFERAKANGIIGVENPVTOALREGRLEELPDDISE-----

```

Figure 3.3: RIC8 homologues in other fungi

ClustalW (<http://www.ch.embnet.org/software/ClustalW.html>) was used to align RIC8 sequences from *N. crassa* (Nc; NCU02788.3), *Podospora anserina* (Pa; Pa_1_3900), *Magnaporthe grisea* (Mg; MGG_14008), *Fusarium graminearum* (Fg; FGS_01511), and *Aspergillus nidulans* (An; AN1661.3). Boxshade was used to indicate identical (black) and similar (grey) amino acid residues (http://www.ch.embnet.org/software/BOX_form.html). Astericks (*) indicate conservation of identical amino acid residues in all species.

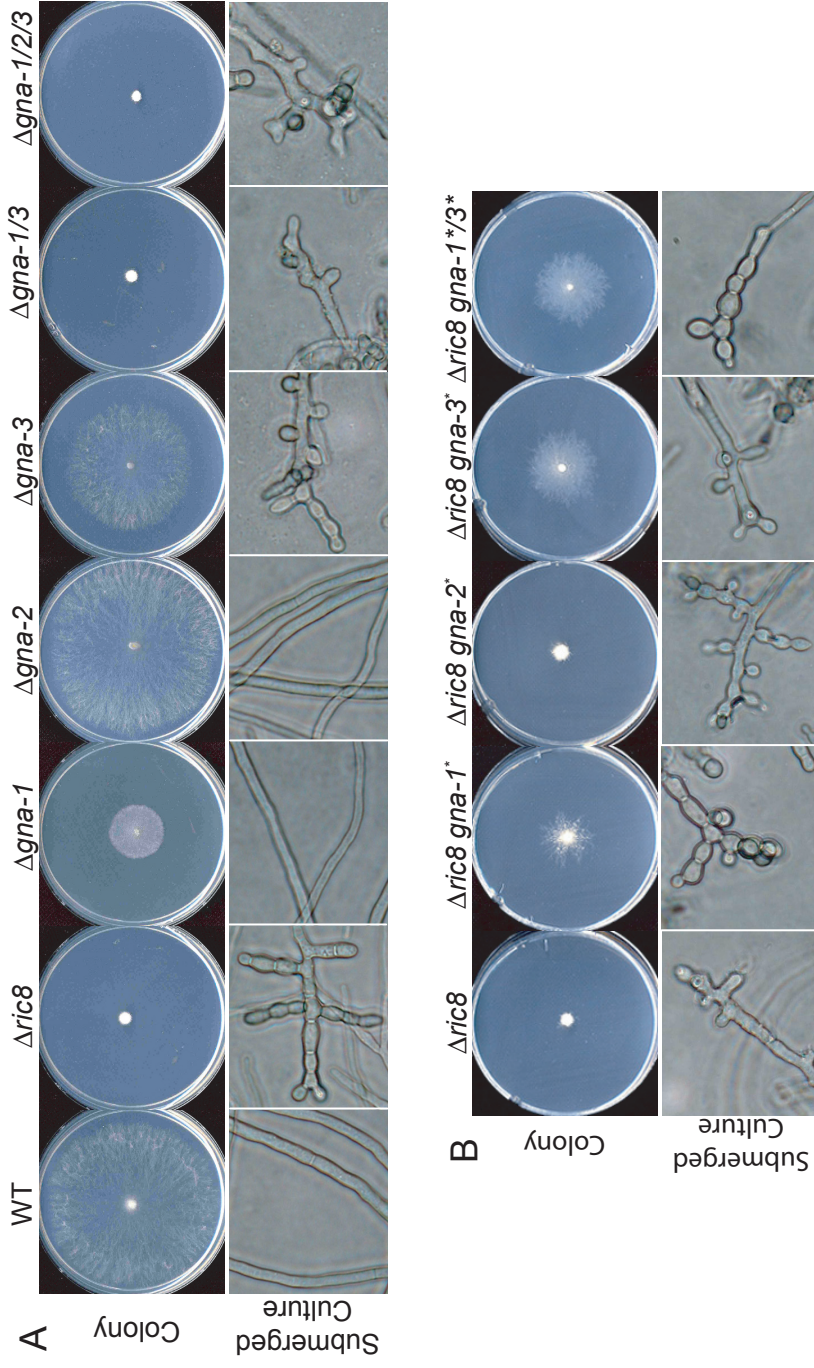


Figure 3.4: Epistatic and physical relationships between *ric8* and *Gα* genes

A) Phenotypes in *Gα* deletion and *Δric8* strains. Strains were inoculated on VM plates and cultured for 1 day at 25°C (Colony) or in 30 ml VM liquid medium for 16 hours at 30°C with shaking (Submerged Culture). Strains used for analysis were wild type (FGSC 2489), *Δric8* (R81a), *Δgna-1* (3B10), *Δgna-2* (a29-1), *Δgna-3* (43c2), *Δgna-1 Δgna-3* (43c2), *Δgna-1 Δgna-2 Δgna-3* ($\Delta gna-1/2/3$, noa), Photos were taken at 400x magnification. B) Phenotypes after introduction of GTPase-deficient, constitutively activated *Gα* alleles (indicated by asterisks; *) into the *Δric8* background. Strains used for analysis were *Δric8* (R81a), *Δric8 gna-1^{Q204L}* (R81*), *Δric8 gna-2^{Q205L}* (R82*) and *Δric8 gna-3^{Q209L}* (R83*) and *Δric8 gna-1^{Q204L} gna-3^{Q209L}* (R81*3*). Culture conditions are as described in A.

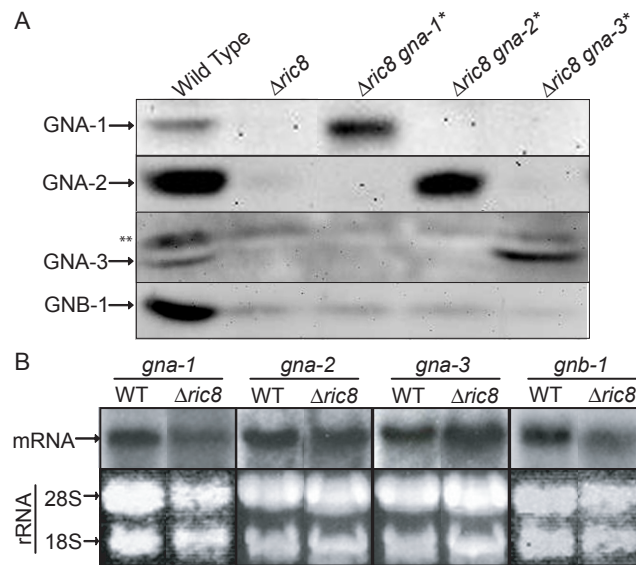


Figure 3.5: Epistatic relationships between $\Delta ric8$ and $G\alpha$ genes

A) $G\alpha$ and $G\beta$ protein levels. Samples containing 100 μ g of protein from particulate fractions isolated from 16 hour submerged cultures were subjected to Western analysis using the GNA-1, GNA-2, GNA-3 and GNB-1 antibodies. The asterisk (*) denotes strains containing activated alleles of $G\alpha$ genes. The double asterisk (**) indicates a background band observed in all GNA-3 Western blots. Strains used for analysis were wild type (FGSC 2489), $\Delta ric8$ (R81a), $\Delta ric8 gna-1^{Q204L}$ (R81*), $\Delta ric8 gna-2^{Q205L}$ (R82*) and $\Delta ric8 gna-3^{Q209L}$ (R83*). B) Levels of $G\alpha$ and $G\beta$ transcripts. Samples containing 20 μ g of total RNA isolated from 16 hour submerged cultures were subjected to Northern analysis using gene-specific open reading frame probes. Strains used for analysis were wild type (FGSC 2489) and $\Delta ric8$ (R81a).

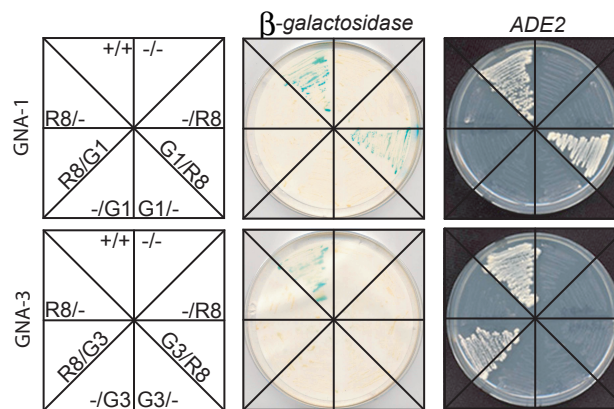


Figure 3.6: RIC8 interacts with GNA-1 and GNA-3 in the yeast two-hybrid assay

Diploid strains contain the GAL4 activation domain (pGAD424) and DNA binding domain (pGBKT7) vectors. The insert in the pGAD424 vector is indicated to the left of the slash (/), while that in the pGBKT7 plasmid is indicated to the right of the slash. G1=GNA-1, G3=GNA-3, R8=RIC8, (-)=no insert in vector, (+)=positive control interactors. β -galactosidase reporter activity: Strains containing vectors with the indicated genes were cultured on medium lacking tryptophan and leucine for three days at 30°C. Plates were scanned 24 hours after the colony lift assay for β -galactosidase. ADE2 reporter growth assay: Strains were grown on medium lacking tryptophan, leucine and adenine for five days and plates were scanned.

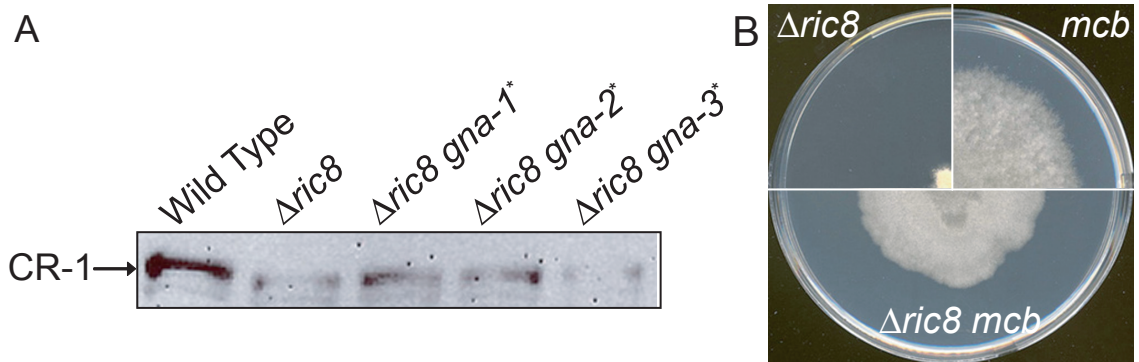


Figure 3.7: Relationship to the cAMP pathway

A) CR-1 (adenylyl cyclase) protein levels. Samples containing 100 μ g of protein from whole cell extracts isolated from 16 hour submerged cultures were subjected to Western analysis using the CR-1 antibody. Strains used for analysis were wild type (FGSC 2489), $\Delta ric8$ (R81a), $\Delta ric8 gna-1^{Q204L}$ (R81*), $\Delta ric8 gna-2^{Q205L}$ (R82*) and $\Delta ric8 gna-3^{Q209L}$ (R83*). B) Effects of the *mcb* mutation. Strains $\Delta ric8$ (R81a), *mcb inl* and $\Delta ric8 mcb inl$ were cultured on VM+inositol plates for three days at 25°C.

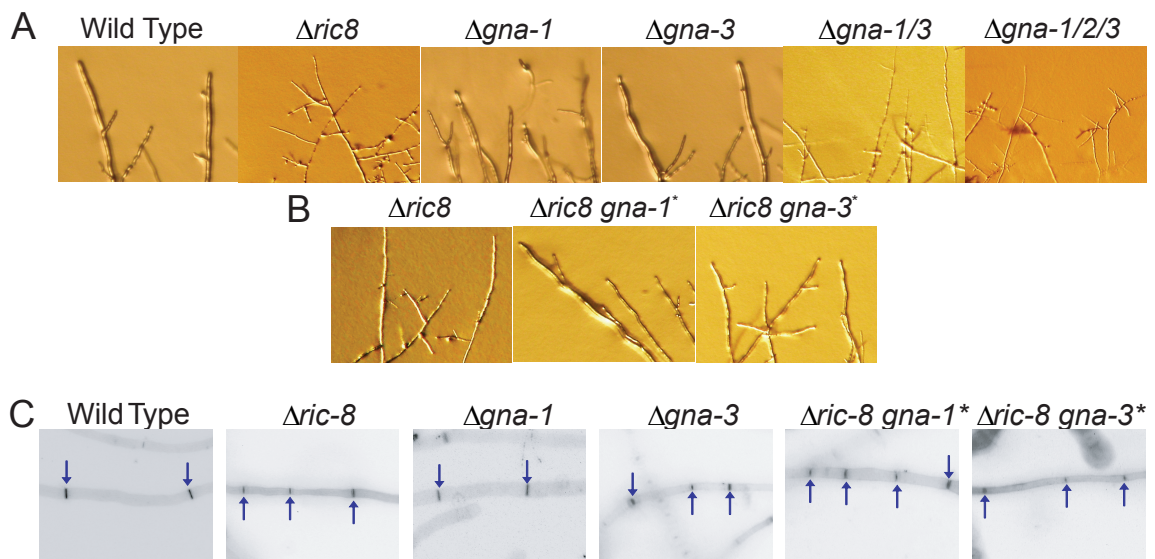


Figure 3.8: Hyphal morphology in $\Delta G\alpha$ and $\Delta ric8$ strains

Strains used were wild-type (FGSC 2489), *Δric8* (R81a), *Δgna-1* (3B10), *Δgna-3* (43c2), *Δgna-1 Δgna-3* (*Δgna-1/3*, g1.3), *Δgna-1 Δgna-2 Δgna-3* (*Δgna-1/2/3*, noa), *Δric8 gna-1^{Q204L}* (R81*), and *Δric8 gna-3^{Q209L}* (R83*). A, B) Colony edge. Strains were inoculated on VM plates and cultured for 1 day at 25°C. A and B were cultured on different days, under the same conditions. Photos were taken at 560x magnification. C) Morphology of septa. Strains were cultured in VM liquid medium for 14 hours at 30°C, with shaking. Septa were visualized by staining cultures with Calcofluor White stain and photos were taken at 400x magnification. Images were inverted to allow better visualization of septa (black). See methods for details regarding microscopy.

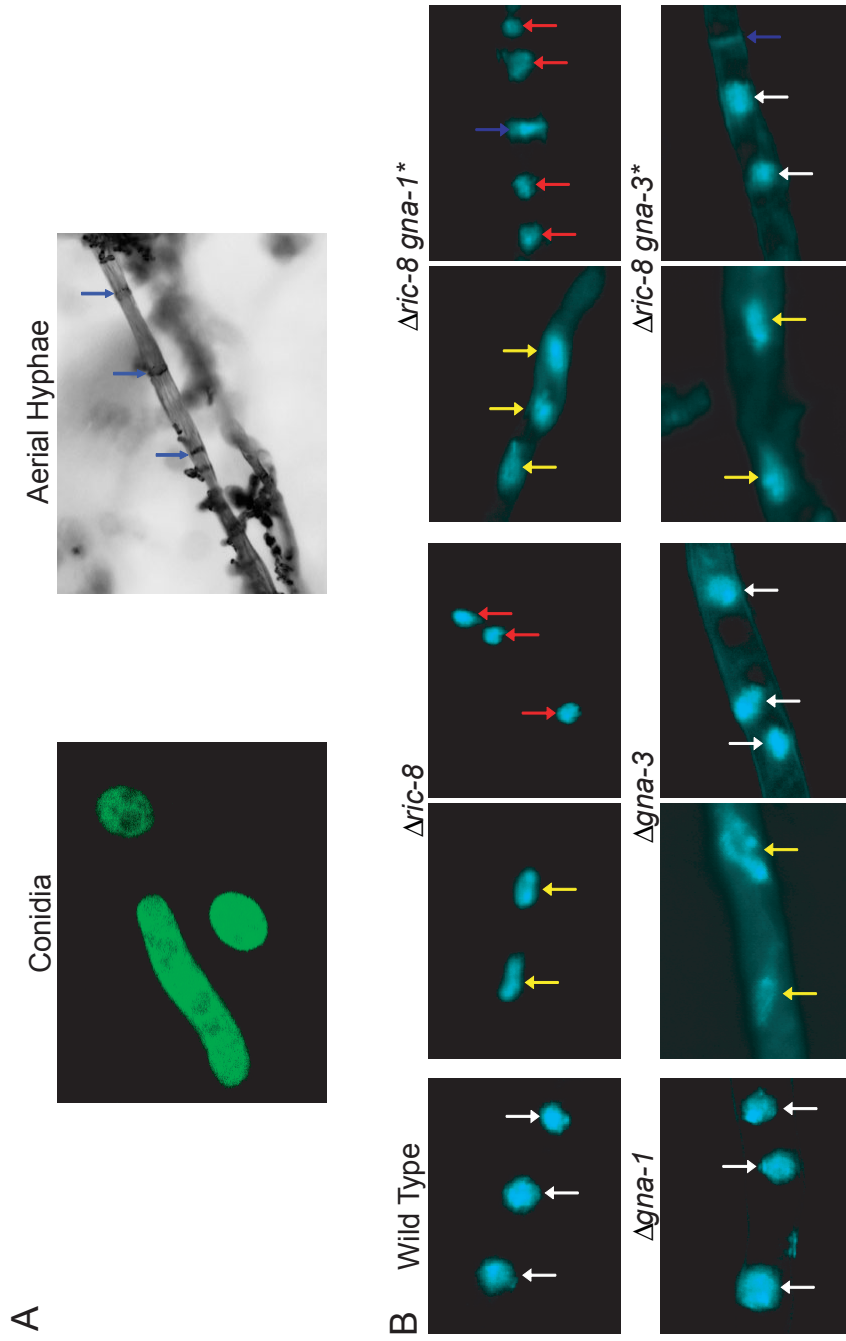


Fig. 3.9: RIC8 localization and nuclear morphology of $\Delta ric-8$ mutants

A) Localization of a RIC8::GFP fusion protein. Left: Conidia were collected from the RIC8::GFP strain and fluorescence visualized with a confocal microscope at 1420x magnification. A conidium and rare arthroconidium are shown. Right: The RIC8::GFP strain was cultured on VM plates for two days at 25°C. RIC8::GFP fluorescence in aerial hyphae was captured in photos taken at 400x magnification. Image was inverted to allow better visualization of septa (black). B) Nuclear morphology. Strains were cultured in VM liquid medium for 14 hours at 30°C, with shaking. Nuclei were visualized by staining with DAPI and images captured using a confocal microscope at 2520x magnification. Yellow arrows denote morphological abnormalities, red arrows point out abnormal nuclear size, white arrows point to normal nuclei, and blue arrows indicate septa. See methods for details regarding microscopy.

Table 3.1. <i>N. crassa</i> strains used in this study		
Strain	Relevant genotype	Source ^a
74A	Wild Type, <i>mat A</i>	FGSC 987
74a	Wild Type, <i>mat a</i>	FGSC 988
2489	Wild Type, <i>mat A</i>	FGSC 2489
4200	Wild Type, <i>mat a</i>	FGSC 4200
his3A	<i>his-3 mat A</i>	FGSC 6103
<i>a^{m1}</i>	<i>a^{m1} ad3B cyh-1</i>	FGSC 4564
R81a	$\Delta ric8::hph^+ mat a$	<i>ric8</i> homokaryon
R81-5a	$\Delta ric8::hph^+ mat a$	<i>ric8</i> homokaryon
R8H3	$\Delta ric8::hph^+ his3 mat A$	<i>ric8</i> heterokaryon X 6103 progeny ^b
R8 <i>a^{m1}</i>	$\Delta ric8::hph^+ a^{m1} ad3B cyh-1$	R8H3, <i>a^{m1}</i> heterokaryon
R8GFP	$\Delta ric8::hph^+ ric8-gfp::his-3^+$	<i>ric8-gfp</i> in $\Delta ric8$ background
R81*	$\Delta ric8::hph^+ gna-1^{Q204L}::his-3^+$	<i>gna-1^{Q204L}</i> in $\Delta ric8$ background
R82*	$\Delta ric8::hph^+ gna-2^{Q205L}::his-3^+$	<i>gna-2^{Q205L}</i> in $\Delta ric8$ background
R83*	$\Delta ric8::hph^+ gna-3^{Q208L}::his-3^+$	<i>gna-3^{Q208L}</i> in $\Delta ric8$ background
R81*3*	$\Delta ric8::hph^+ gna-1^{Q204L}::bar gna-3^{Q208L}::his-3^+$	<i>gna-1^{Q204L}, gna-3^{Q208L}</i> in $\Delta ric8$ background
mcb	<i>mcb inl</i>	FGSC 7094
R8 mcb	$\Delta ric8::hph^+ mcb::inl$	R8 <i>a^{m1}</i> X <i>mcb</i>
3B10	$\Delta gna-1::hph^+ mat a$	<i>gna-1</i> homokaryon
a29-1	$\Delta gna-2::pyrG^+ mat A$	<i>gna-2</i> homokaryon
43c2	$\Delta gna-3::hph^+ mat a$	<i>gna-3</i> homokaryon
RIC8V5	<i>ric8^{V5}::nat mat</i>	V5 epitope-tagged <i>ric8</i> at the native locus
a. FGSC, Fungal Genetics Stock Center, Kansas City, MO, USA.		
b. X denotes a genetic cross		

Table 3.2 Oligonucleotides used in this study

Name	Sequence (5'-3')
R8 seq 4	GATCAGACTGGATGACTCGG
R8 seq 5	GTTTGAGAGGTAAGTACTG
R8 seq 6	GACCTAGGCTATGAGTCCAAG
R7 seq rv	GCCCTGGAGGAACTCAAGGTG
R8I1fw	CACCATGGCCTCAATAGGAGTTTCTGGG
R8I1rv	CAGTTGTCGTTTTTGAGCTTTTCGCAGGCC
R8 GFP fw	TATCTAGAATGGCCTCAATAGGAGTTTCTGGGCCAGGTC
R8 GFP rv	GGGGATCCAGTCCGAATCCTCTTCGTAGTCGTCGGG
R8YR11fw	GTAACGCCAGGGTTTTCCAGTCACGACCGCCTGAGATGTGTTGTATCGAG AG
R8YR11rv	CAGCTTATGAATGAGAGTGGTGACAGCTTGCAACTTGGCTGGCCCAGAAA CTCCTATTGAGG
R8YR12fw	CCAAGTTGCAAGCTGTCACCACTCTCATTCATAAGCTGACCGAGGACCTCA AGAGCAC
R8YR12rv	GCGGATAACAATTTACACAGGAAACAGCCGGCAAGACTGGAGGGTGCCT CCTGGGG
R8YR21fw	GTAACGCCAGGGTTTTCCAGTCACGACCTGCGGTCCCGCATATAGTG
R8YR21rv	CAGGGTTCTCAACATTAACGATTCCCAGCTTCTCGCCCTCTCAAACAAGA CAAACAGTCTCTC
R8YR22fw	GGCGAGGAAGCTGGGAATCGTTAATGTTGAGAACCCTGTTGCCAAGGCGG TTCAGGAG
R8YR22rv	GCGGATAACAATTTACACAGGAAACAGCGGGAGTCGTATACCTCCGCGG AGGAAGGCC
R8Y2Hfw	AATTGAATTCATGGCCTCAATAGGAGTTTCTGGG
R8Y2Hfw-new	AATTGAATCCATGGCCTCAATAGGAGTTTCTGGGCCAGCCAAGTTGCAAGC TGTC
R8Y2Hrv	AATTGGATCCTCAGTCCGAATCCTCTTCGTAGTC
6HG1fw	TTAACATATGCATCATCACCATCACCATGGGGGGATGGGTTGCGGAATGA GTACAGAGG
6HG1rv	TTAAAGATCTTCAAATCAAACCGCAGAGACGCAGG
6HG2fw	TTAACATATGCATCATCACCATCACCATGGGGGGATGTGTTTCGGGGGTGC TGGAAAGG
6HG2rv	TTAAGGATCCTCACAGGATAAGTTGTTTCAGGTTTCGCTGG
6HG3fw	TTAACATATGCATCATCACCATCACCATGGGGGGATGGGCGCATGCATGA GCAAGAACG
6HG3rv	TTAAGGATCCTCATAGAATACCGGAGTCTTTAAGGGCG
6HR8 NdeI fw	AATTCATATGGCCTCAATAGGAGTTTCTGGGC
6HR8 BamHI rv	AATTGGATCCTCAGTCCGAATCCTCTTCGTAGTCG

Chapter 4: Expression and purification of RIC8 and G α subunits and their use in GTP binding assays

Abstract

The non-receptor guanine nucleotide exchange factor (GEF) Ric8 plays a role in asymmetric cell division and neural signaling in animals. A homologue of this protein in *N. crassa*, RIC8, is involved in regulation of growth, development, and cAMP signaling. Experiments were conducted to test the GTP binding of *N. crassa* G α proteins *in vitro*, and the effects of RIC8 on this binding. RIC8 and G α proteins were epitope-tagged with maltose-binding protein (MBP) or hexahistidine (6H) and partially purified from *E. coli*. GNA-1 was the only MBP-tagged G α exhibiting GTP binding, which was increased by MBP-tagged RIC8. However, all three hexahistidine-tagged G α proteins exhibit GTP binding with GNA-1 having the greatest affinity for GTP. 6H-tagged RIC8 increases the GTP binding of GNA-1 and possibly GNA-3, though more studies need to be conducted with more highly purified proteins. This work suggests that *N. crassa* RIC8 functions as a GEF for G α proteins, similar to its role in animal systems.

Introduction

Heterotrimeric G protein signaling is essential for eukaryotic organisms to sense changes in their environment. In the traditional model of G protein signaling, heterotrimeric G α proteins are activated by G protein-coupled receptors in response to an extracellular ligand. However, a non-receptor protein, RIC8, has recently been shown to be a positive regulator of G α proteins in animals (rev. in (Wilkie and Kinch, 2005b). RIC8 is involved in specialized developmental stages in animals, such as asymmetric cell division and neural signaling. RIC8 acts as a guanine nucleotide exchange factor (GEF) by accelerating GTP binding to the G α subunit.

RIC-8 was shown to bind to and function as a GEF for GOA-1 using GST pull-down assays and GTP binding assays. RIC-8 was also shown to bind to G α_i in a *Drosophila* embryonic cell line by immunoprecipitation of RIC8 using both RIC8 and G α_i antibodies (Hampoelz et al.). In addition, the mammalian RIC8 homolog, Ric-8A, was shown to bind to and function as a GEF for mammalian G α_q , G α_{i1} , and G α_o , but not G α_s (Tall et al., 2003b). This Chapter outlines efforts to show that *N. crassa* RIC8 can bind to and act as a GEF for the G α proteins GNA-1, GNA-2, and GNA-3.

Materials and Methods

E. coli vector and strain construction

E. coli strains expressing maltose binding protein (MBP) fusions were made by Regina Inchausti with guidance from Sara Wright and Katherine Borkovich. Expression of MBP fusion proteins from vector pMalC₂X (New England Biolabs) uses the IPTG-inducible ptac promoter, which is a hybrid promoter composed of the -35 region of the *trp* promoter and the -10 region of the *lac* promoter/operator (Marsh, 1986). The cDNA from *ric8*, *gna-1*, *gna-2*, and *gna-3* were cloned into pMalC₂X to create plasmids pRI1, pRI2, pRI3, and pRI4, using the same cloning protocols described in Chapter 3. The cDNA inserts from the yeast two-hybrid vectors described in Chapter 2 and vector pMAC₂X were isolated using restriction enzyme double digests with *Bam*HI and *Eco*RI (*ric8*, *gna-2* and *gna-3*), or a step-wise digestion with *Pst*I and *Eco*RI (*gna-1*). The fragments were isolated by gel extraction, and cloned into pMALC₂X using ligation as described in Chapter 3.

Colonies were checked for the presence of an insert by digesting 3-6 μ L of boiling mini-prep extracted DNA (described in Chapter 2) at 37°C for 2-4 hours with 3-6 units of the restriction enzymes used for cloning in a 15 μ L total reaction volume. Colonies containing inserts were cultured and plasmids recovered using the QIAprep mini-prep kit described in Chapter 2. Plasmid DNA was transformed using chemical competent transformation into *E. coli* strain K12 ER2508 (New England Biolabs), which lacks the *lon* protease and does not produce any native MBP protein.

For construction of N-terminal poly-histidine tagged versions of RIC8 and G α proteins, cDNAs were amplified from the yeast two-hybrid vectors described in Chapter 2 (GNA-2 and RIC8) or from the MBP fusion vectors described above (GNA-1 and GNA-3) using the high fidelity Phusion polymerase (New England Biolabs). For amplification of the G α genes, primer pairs (6HG1fw/6HG1rv, 6HG2fw/6HG2rv, and 6HG3fw/6HG3rv; Table 3.2) were used which introduce sequences encoding six histidine residues (denoted as 6H) at the 5' end of the gene and restriction sites for cloning into pET11a (Novagen, Gibbstown, NJ). The *ric8* primers (HISR8 NdeI fw/HISR8 BamHI rv; Table 3.2) were designed to clone *ric8* into pET16b (Novagen), which contains an N-terminal HIS sequence containing 10 histidine residues. The PCR reaction mixtures contained 10 μ L 5X Phusion HF buffer, 4 μ L of 2.5 mM dNTPs, 1 μ L of each primer, 100 μ M each (2 μ M final concentration), 1 μ L template (100-300 ng/ μ L), 1 μ L Phusion™ DNA Polymerase, and 32 μ L water. Thermocycler conditions used were: 98°C for 1 min.; 30-35 cycles of: 98°C for 30 sec., 50-60°C for 30 sec., and 72°C for 60-90 sec. (1 min./kb); and 72°C for 10 min. Fragments were purified using agarose gel extraction (Qiagex II) and cloned into pGEM vectors (Promega). For the G α PCR products, 3' adenine residues were added to facilitate cloning into pGEM-T (has 3' thymidine overhangs) using Taq polymerase (Fisher BioReagents, Fairlawn, NJ) with the following reaction conditions: 7 μ L purified PCR product, 1 μ L Fisher 10X reaction buffer, 0.4 μ L dATPs, 0.6 μ L water, and 1 μ L Fisher Taq polymerase. This reaction was incubated at 70°C for 30 min. For ligation into pGEM-T, 2 μ L of this reaction was added to 1 μ L pGEM-T, 1 μ L T4 DNA ligase, 5 μ L 2X ligase buffer, and 1 μ L water and

incubated at 4°C overnight. The *ric8* cDNA was cloned into *EcoRV*-digested pGEM5, which leaves blunt ends for cloning of a blunt ended Pfu PCR product. The ligation reactions were transformed into *E. coli* and constructs checked for the presence of a correct insert using the same methods described for analyzing the MBP constructs.

Inserts with the correct sequences were isolated using restriction enzymes *NdeI* and *BglIII* (*gna-1*) or *NdeI* and *BamHI* (*gna-2*, *gna-3*, and *ric8*) using the step-wise digestion described in Chapter 2. The purified inserts and *NdeI* and *BamHI* digested pET11a (*Gα*) or pET16b (*ric8*) were ligated and recovered in *E. coli* strain DH5α as described in Chapter 2 to create plasmids pRI10, pRI11, pRI12, and pSM31. *E. coli* strain BL21(DE3) was used to express the HIS-tagged proteins. This strain lacks the *lon* protease and the *ompT* outer membrane protease, which can degrade proteins during purification. The DE3 refers to the strain being lysogenic for λ -DE3, which encodes the T7 RNA polymerase under the control of the lacUV5 promoter (Studier and Moffatt, 1986).

Purification of MBP-tagged RIC8 and Gα proteins from *E. coli*

The cultures were inoculated by adding 1-2 mL of an overnight culture of each strain to 50-100 mL LB+amp+0.2% glucose and then incubated at 37°C for 2 hours at 225 RPM. Expression of the fusion protein was induced by adding 300 μM IPTG (isopropyl β-D-1-thiogalactopyranoside; Sigma) and incubating for 4 hours at 30°C and 225 RPM. Cells were centrifuged in a Beckman J2-21 refrigerated centrifuge using rotor JA 25.5 at 5,000 RPM for 10 min. and pellets stored at -20°C.

Cell pellets were resuspended in 10 mL extraction buffer (20 mM Tris-Cl pH 7.5, 200 mM NaCl, 1 mM EDTA, 1 mM DTT, and 1 mM PMSF) and subjected to sonication (3-4 pulses, 15-30 sec. each with 30-60 sec. rests, on ice). Cell extracts were centrifuged at 14,000 RPM for 15 min. at 4°C. MBP fusion proteins were purified using an amylose resin, which consists of poly-maltose chains attached to agarose beads (New England Biolabs). A bead volume of 2-3 mL was incubated with the extracts for 1 hour at 4°C in a 15 mL falcon tube using an orbital shaker (Nutator). This slurry was added to a Poly-prep column (Bio-rad), and 5 mL extraction buffer was used to wash the falcon tube and the solution was added to the column. The column was washed four times with 5 mL extraction buffer and the MBP-tagged protein was eluted in 1 mL fractions of extraction buffer +10 mM maltose. The protein concentration of each elution was determined using the Bradford protein assay with BSA as a standard, and fractions with the highest concentrations were pooled. The protein was transferred to an Amicon Ultra 30 column (Millipore, Billerica, MA) and spun for 25 min. at 4000 RPM in a 5810R centrifuge at 4°C (Eppendorf North America, Hauppauge, NY). Exchange buffer (200 mM HEPES pH 7.5, 100 mM NaCl, 10% glycerol, 1 mM EDTA, and 1 mM DTT) was added to the concentrated protein (500-1000 μ L) in 2 mL portions and centrifuged for 4-10 min. This was repeated until a total of 5-6 mL exchange buffer was passed through the column. The protein (500 μ L) was divided into 20 μ L aliquots and stored at -80°C. Western analysis of the MBP-tagged proteins was performed generally as described in Chapter 2 for GAPDH. The anti-MBP polyclonal antibody raised in rabbit (New England Biolabs) and secondary goat anti-rabbit (Bio-rad) antibody were used at 1:10,000.

The MBP tag was removed by cleaving an engineered protease site (Ile-(Glu or Asp)-Gly-Arg) between MBP and the G α protein using factor Xa protease (1 $\mu\text{g}/\mu\text{L}$; New England Biolabs). MBP-GNA-1 was tested for cleavage by adding increasing amounts of the protease (0.1 μL , 1 μL , or 1 μL + 0.01% SDS) to 50 μL of protein eluted from the amylose resin (15 μg) and incubated for 3 hours at room temperature. Addition of SDS is thought to increase the activity of factor Xa in some instances. The reaction was then tested on a larger volume using MBP-tagged RIC8, GNA-1 and GNA-3 using 150 μL (150 μg) protein, 3 μL factor Xa, and 3 μL of a 100 mM CaCl₂ solution and incubated for 5 hours at room temperature. The reactions were frozen at -20°C until further use. The thawed, cleaved protein mixtures were added to a 100 μL bed volume of amylose resin in exchange buffer; and microcentrifuge tubes containing the cleaved proteins were rinsed with an additional 150 μL exchange buffer and added to the beads. The beads were incubated on ice for 15-20 min. with occasional mixing. The tubes were centrifuged for 30 sec. at 15,000 RPM to pellet the beads, and the supernatant, along with 3 mL exchange buffer, was added to an Amicon Ultra 30 column and centrifuged as described above. The samples were exchanged with an additional 3 mL exchange buffer with 1 mM PMSF, and concentrated to 500 μL .

Purification of HIS-tagged RIC8 from *E. coli*

For expression of HIS-RIC8, one colony of each strain was inoculated into 5 mL LB+amp and cultured at 225 RPM for 12-16 hours at 37°C. Two mL of each culture was inoculated into 100 mL LB+amp in a 250 mL baffled flask and grown at 225 RPM for 2.5 hours at 37°C. RIC-8 expression was induced by adding 100 µM IPTG and incubating at for an additional 5 hours at 150 RPM and 30°C. The cells were centrifuged at 4,000 RPM in an Avanti J-26 XP floor centrifuge using rotor JS-4.0 for 10 min. at 4°C, and pellets stored at -20°C.

To a frozen cell pellet, 10 mL His-Pur Lysis buffer (50 mM NaH₂PO₄ pH 7.4, 300 mM NaCl, 10 mM imidazole [Sigma], 10% glycerol, 0.1 mM PMSF) and 0.2 mg/mL lysozyme was added and incubated for 20 min. on ice. The cell suspension was then sonicated 2-4 times at 30% power for 15-30 sec. with 1 min. rests on ice. The extract was centrifuged at 25,000 RPM using rotor JA-25.5 at 4°C for 20 min. The supernatant was added to a 2 mL bed volume of His-Pur Cobalt beads (Thermo Scientific, Rockford, IL) and incubated for 1 hour at 4°C with nutation. The slurry was centrifuged at 700 x g for 30 seconds at 4°C in an IEC Centra CL3 centrifuge with an IEC 243 rotor, the supernatant removed, and transferred to a poly-prep column using 5 mL wash buffer (lysis buffer containing 20 mM imidazole). The column was washed with 10-20 mL wash buffer (until protein concentration is near zero as determine using the Bradford protein assay). Protein was eluted in 1mL fractions with lysis buffer containing increasing amounts of imidazole: 50, 75, and 100 mM (3 mL of each concentration).

For further purification, the peak fractions from the nickel or cobalt columns were applied to an ion-exchange column. Two to three fractions from the HisPur elution and 6-8 mL IE buffer (50 mM Tris-Cl pH 7.4, 1 mM EDTA pH 8.0, 1 mM DTT, 10% glycerol, 0.1 mM PMSF) were combined and then loaded onto a 7ml column packed with Macro-Prep High Q Support (Bio-Rad) using a peristaltic pump (Gilson Inc., Middleton, WI) at approximately 1 mL/min flow rate. The column was washed with 10-20 mL IE buffer and protein eluted with a linear gradient of 300-500 mM NaCl in 2 mL fractions. Fractions with the highest protein concentration (between 300-325 mM NaCl) were pooled and subjected to concentration and buffer exchange as described for MBP tagged proteins.

Purification of Hexa-Histidine tagged G α proteins from *E. coli*

For expression of 6H-G α proteins, 2-3 large colonies were used to inoculate 20 mL LB+amp and grown at 37°C for 16-20 hours at 225 RPM. The 20 mL culture was used to inoculate 1 L LB+amp in a 2.8 L Fernback flask, and incubated at 37°C for 2 hours at 225 RPM. Protein expression was induced by the addition of 10 μ M IPTG and incubation for an additional 6 hours at 25°C and 100 RPM. The cells were centrifuged at 5,000 RPM for 10 minutes at 4°C, and pellets stored at -20°C. To a frozen cell pellet, 10 mL His-Pur Lysis buffer (50 mM NaH₂PO₄ pH 7.4, 300 mM NaCl, 10 mM imidazole, 10% glycerol, 0.1 mM PMSF) and 0.2 mg/mL lysozyme was added and incubated for 20 min. on ice. The cell suspension was then sonicated 4-6 times at 30% for 15 sec. with 45-60 sec. rests, and centrifuged at 20,000 RPM for 20 min. at 4°C. The supernatant was

added to a 3 mL bed volume of His-Pur Cobalt beads and incubated for 1 hour at 4°C with orbital mixing. The beads were centrifuged at 2,000 RPM for 2 min. at 4°C. The supernatant was then removed and 5mL lysis buffer was added to the beads in order to transfer them to a poly-prep column. The column was washed with an additional 5 mL lysis buffer. Protein was eluted the same way as the HIS-RIC8 protein, and fractions with the highest protein concentration (between 50-75 mM imidazole) were pooled and subjected to concentration and buffer exchange as described for MBP tagged proteins. Western analysis of the 6H-tagged proteins was as described in Chapter 2 for GAPDH. The anti-hexahistidine monoclonal antibody raised in mouse (Invitrogen) was used at 1:2000 and secondary goat anti-mouse (Bio-rad) was used at 1:10,000.

To attempt further purification of 6H-GNA-3, separation on a DEAE ion-exchange column was used after separation on the His-Pur column. The 6H-GNA-3 protein was induced in 6 L LB+amp with 30 μ M IPTG at 25°C for nine hours as described above. Whole cell extracts were obtained as described above, except that 20 mL extraction buffer was used. The His-Pur resin was prepared by pouring a total bed volume of 6 mL into a glass Econo-column (Bio-rad) attached to a Minipuls 3 peristaltic pump (Gilson Inc., Middleton, WI). The extract was loaded onto the column at approximately 1 mL/min flow rate. The column was washed with 20 mL His-Pur wash buffer and protein eluted with a linear gradient of 20-220 mM imidazole (total volume 50 mL) in low salt buffer (50 mM NaH₂PO₄ pH 7.4, 300 mM NaCl, 10 mM imidazole, 10% glycerol) using a 100 mL gradient maker (C.B.S. Scientific Company, Del Mar, CA) and 1 mL fractions collected using a fraction collector (Model 2110, Bio-Rad). Fractions

with the highest protein concentration (fractions 8-12, as determined by a Bradford protein assay) were pooled and an equal volume of IE buffer was added for a final NaCl concentration of 20 mM. The protein was loaded onto a packed Macro-Prep DEAE Support (Bio-Rad) and fractions collected using a similar protocol to the His-Pur elution, except that the gradient used was 20-220 mL NaCl in IE buffer.

To attempt further purification of 6H-GNA-1, HT Hydroxyapatite and Affi-gel blue resins (Bio-Rad) were tested. Two or three colonies of *E. coli* cells expressing 6H-GNA-1 were used to inoculate 150 mL LB+amp and grown at 37°C for 16-20 hours at 225 RPM. This culture was used to inoculate four 2.8 L Fernbach flasks (30 mL culture per flask) containing 1.5 L LB+amp. The flasks were incubated at 37°C for 2 hours at 225 RPM. The cells were induced by the addition of 30 μM IPTG and incubated for 12 hours at 25°C and 100 RPM. The cells were centrifuged at 4,000 RPM for 10 min. at 4°C, and pellets stored at -20°C. To the cell pellet, 60 mL HA lysis buffer (20 mM NaH₂PO₄ pH 7.4, 10 mM NaCl, and 10% glycerol) containing 300 μL bacterial protease inhibitor cocktail (Sigma) and 0.1 mg/mL lysozyme was added and the mixture incubated 30 min. on ice. Cells were sonicated twice for 30 sec. with 1-2 min. rests on ice. The extract was centrifuged at 20,000 RPM for 20 min. at 4°C. The hydroxyapatite resin was prepared by loading a total bed volume of 3 ml into a glass Econo-column (Bio-rad) attached to a peristaltic pump and washed with lysis buffer at approximately 1 mL/min. The supernatant (60 mL) was loaded onto the HA column and the column was washed with HA lysis buffer until no protein was detectible in the elutions (approximately 100 mL). A 40 mL linear gradient of 20-200 mM NaH₂PO₄ in lysis buffer with 25 μM GDP was

applied to the column using a 100 mL gradient maker and 1 mL fractions collected using a fraction collector. A GTP binding assay was performed on even numbered fractions between 4-54 using 10 μ L protein in a 20 μ L total volume for approximately 60 min. (see full protocol below). Fractions with the highest GTP binding were pooled (9 mL) and incubated with 1 mL bed volume His-Pur cobalt resin and processed as described above. Affigel blue resin (1 mL) was added to a poly-prep column and washed with approximately 10 mL HA lysis buffer. Fractions 5-7 from the cobalt resin contained the highest protein concentration and were poured over the Affigel blue resin and flow through was collected.

To improve cell lysis, strain BL21(DE3) containing the plasmid pLysS was transformed with pRI10. pLysS expresses the T7 lysozyme, a natural inhibitor of T7 RNA polymerase which reduces background. T7 lysozyme also makes the cells more susceptible to lysis. One colony was used to inoculate 4 mL of LB+amp+cam and incubated at 37°C with shaking at 225 RPM overnight. The culture was washed once with LB medium, resuspended in LB medium, and used to inoculate 100 mL LB+amp+cam. The cells were grown at 37°C for 3 hours at 225 RPM. Protein expression was induced by the addition of 50 μ M IPTG and incubation for a total of nine hours at 25°C and 100 RPM. Aliquots were taken at 0, 1, 2.5, 6, and 9 hours post induction to identify optimum expression. The 1-mL aliquots were centrifuged at 15,000 RPM for 10-15 sec. and pellets stored at -20°C. 125 μ L 1X Laemmli buffer (Chapter 3) was added and samples were subjected to Western analysis as described above.

GTP binding assays

GTP binding assays were modeled after experiments in Tall et. al. 2003. Binding assays were carried out in exchange buffer, with a total reaction volume of 20 μ L. Purified proteins (13-1225 nM of tagged G α proteins and/or 200 nM tagged RIC8 protein) and 10 mM MgSO₄ in a total volume of 18 μ L were incubated on ice until reaction start. Reactions were initiated by adding 2 μ L of a 1:1 mixture of 40 μ M GTP γ S and 1 μ Ci/ μ L GTP γ ³⁵S (Perkin Elmer, Waltham MS) and incubated at 30°C for up to 60 min. Reactions were stopped with 100 μ L cold stop solution (20 mM Tris-Cl pH 8.0, 100 mM NaCl, 2 mM MgSO₄, 1 mM GTP). Reactions were filtered on 0.45 μ M HA mixed cellulose membranes (Millipore) by vacuum filtration and washed 3 times with 5 mL cold wash solution (50 mM TrisCl pH 8.0, 100 mM NaCl, and 2 mM MgSO₄). These filters separate protein-bound GTP γ ³⁵S from free GTP γ ³⁵S by allowing the free GTP γ ³⁵S to flow through. Filters were allowed to dry completely in scintillation tubes in a chemical hood. Scintillation fluid (Scintiverse BD cocktail, Fisher Scientific, 4-5 mL) was added and counted for 1-2 min. per sample using a Beckman LS 6500 liquid scintillation counter.

Immuno-precipitation of tagged RIC8 protein from *N. crassa*

An *N. crassa* strain containing a C-terminal V5-tagged version of RIC8 (RIC8V5; Table 3.1) was constructed by Patrick Schacht (unpublished) using a knock-in approach at the native locus. RIC-8-V5 was immuno-precipitated using magnetic Dynabeads

Protein A (Invitrogen) coupled to Mouse anti-V5 tag antibody (Invitrogen). The Dynabeads were prepared by adding 50 μL (1.5 mg) to a microcentrifuge tube and pelleting the magnetic beads using a Magna GrIP™ Rack (Millipore) and the supernatant removed. A mixture of 10 μL (5 μg) anti-V5 antibody and 190 μL 1X PBS were added to the beads and incubated for 1 hour at 4°C with nutation. The beads were washed once with 200 μL 1X PBS. Conidia collected from wild-type (FGSC #2489) and RIC8V5 strains were inoculated in 200 mL VM liquid medium in a 500 mL baffled flask at 3×10^6 conidia per mL and cultured as described for the GAPDH assays in Chapter 2. The tissue was collected and whole cell extract obtained using the same protocols in Chapter 2, except that the extraction buffer contained 50 mM TrisCl pH 7.5, 1 mM EDTA pH 8.0, 6 mM MgSO_4 , 0.5 mM PMSF, 1 $\mu\text{L}/\text{mL}$ fungal protease inhibitor cocktail, and 20 μM GDP. Extracts were centrifuged at 5,000 RPM for 10 min. at 4°C, and 0.5% Triton X-100 (EMD chemicals) or 1% lauryl maltoside (n-Dodecyl β -D-maltoside; Sigma) were added to 5 mL fractions of the supernatant and nutated for 1.5 hours at 4°C to solubilize membrane associated proteins. The extracts were then centrifuged at 20,000 RPM for 45 min. at 4°C to remove the insoluble fraction. Solubilized extract (3 mg) was added to the Dynabeads and incubated for 2 hours at 4°C with orbital shaking. The beads were washed twice with 100 μL 1X PBST. For elution, 100 μL 1X PBS and 20 μL 4X Laemmli buffer were added and incubated for 10 min. at 85°C. For all experiments, 50 μL fractions were subjected to western blotting as described in Chapter 2. Primary antibody (Mouse anti-V5) was used at 1:2000 in 5% BSA in TBST at 4°C overnight.

Secondary antibody (Goat anti-mouse, Bio-Rad) was used at 1:2000 as described for the GAPDH western in Chapter 2.

RIC8-V5 was also immunoprecipitated using anti-V5 antibody raised in mouse (Sigma) or goat (Bethyl laboratories, Montgomery, TX) coupled to agarose beads. Whole cell extracts from wild-type (FGSC #2489) and RIC8V5 strains obtained using the same protocol as above, except that the extraction buffer was composed of 1X PBS, 6 mM MgSO₄, 0.5 mM PMSF, 1 μL/mL fungal protease inhibitor cocktail, and 20 μM GDP. Lauryl Maltoside (1%) was added to 4.5 mg extract and incubated at 4°C for 2 hours with nutation. Samples were centrifuged at 15,000 RPM for 15 min. at 4°C. To 20 μL beads, 1.8 mg supernatant was added and incubated for 2.5 hours at 4°C with nutation. The beads were pelleted by centrifugation at 2,000 RPM for 1 min. in a microcentrifuge. The beads were washed three times with 1X PBS, and protein elution and western analysis was the same as above. Alternatively, tissue cultured on VM plates with cellophane overlay for 4 days at 30°C were collected, ground in liquid N₂, and 10 mL extraction buffer was added (20 mM TrisCl pH 7.5, 100 mM NaCl, 1 mM EDTA, 1 mM EGTA, 10% glycerol, 0.5% Triton X-100 or 1% CHAPS detergent, 1 mM DTT, 1 mM PMSF, and 1 μL/mL fungal protease inhibitor cocktail). Tissue was sonicated three times for 30 sec. with 1 min. rests, and centrifuged at 15,000 RPM for 10 min. at 4°C. The supernatant was subjected to immunoprecipitation and western analysis as described.

Results

RIC8 acts as a GEF for GNA-1 and GNA-3 *in vitro*

MBP and HIS- tagged G α and RIC8 proteins were purified from *E. coli* and assayed for binding of GTP γ ³⁵S. MBP fusions of RIC8, GNA-1, GNA-2 and GNA-3 were expressed in *E. coli* strain K12 ER2508 and isolated using an amylose resin (Figure 4.1). The extra band above MBP-GNA-2 (Figure 4.1B) is marked as (*) and indicates a protein product that was most likely produced from an inefficient stop codon. The *gna-2* native stop codon is UAG, though *E. coli* prefer UGA or UAA (Alff-Steinberger and Epstein, 1994). MBP-GNA-2 was therefore not used for GTP binding assays. A western blot was also performed for RIC8, GNA-1, and GNA-3 MBP tagged proteins using the anti-MBP antibody to ensure correct size of the MBP tagged proteins (Figure 4.1C). Purified and concentrated MBP-tagged RIC8, GNA-1, and GNA-3 used for GTP binding assays can be seen on a Coomassie stained gel in Figure 4.1A. MBP-GNA-1 and MBP-GNA-3 GTP binding assays with and without MBP-RIC8 were conducted by Katherine Borkovich. MBP-GNA-1 is able to bind GTP, and this binding is increased 8.5 times at 30 min. and 6.9 times at 60 min. by the addition of MBP-RIC8 (Figure 4.3A). MBP-GNA-3 is not able to bind GTP (Figure 4.3B), which could be due to the large MBP tag.

With the help of Regina Inchausti, I therefore constructed vectors that would express hexa-histidine (6H) tagged versions of all three G α subunits in *E. coli* strain BL21(DE3). The stop codon for *gna-2* was changed to TGA to prevent read-through. Proteins were purified on a His-Pur cobalt resin, which binds to the 6H tag, and the

elution fractions were concentrated on an Amicon Ultra 30 column. The total protein from each purification was electrophoresed on a 10% polyacrylamide gel with BSA standards to determine the protein concentration for each G α subunit (Figure 4.2A). Due to the high background, the presence of each protein was also determined by western blot using anti-hexa-histidine or anti-GNA-2 antibodies (Figure 4.2C). 6H-GNA-1, GNA-2, and GNA-3 GTP binding assays were conducted with and without MBP-RIC8 by Sara Wright. 6H-GNA-1 is able to bind GTP, and this binding is increased 4.5 times at 30 min. and 2.8 times at 60 min. by the addition of MBP-RIC8 (Figure 4.4A). 6H-GNA-2 is able to bind GTP, though this binding is only increased by about 1.1 times with the addition of MBP-RIC8 (Figure 4.4B). Unlike MBP-GNA-3, 6H-GNA-3 is able to bind GTP, though this binding is reduced to background with the addition of MBP-RIC8 (Figure 4.4C). The binding of GTP by all three G α proteins normalized to 600nM protein shows that 6H-GNA-1 has the highest affinity for GTP (Figure 4.4D). Since MBP-RIC8 had a negative effect on the GTP binding of 6H-GNA-3, I decided to purify a HIS-tagged version of RIC8 to use in GTP binding assays to see if the MBP tag was affecting the GEF activity of RIC8. HIS-RIC8 was purified by affinity chromatography (His-Pur resin) and isoelectric charge (DEAE column) and therefore was close to 100% pure (Figure 4.2B and C). 6H-RIC8 increases the GTP binding of 6H-GNA-1 by 2.1 times at 2 min., and 1.4 times at 5 and 30 min. (Figure 4.5A). Preliminary results show that 6H-GNA-3 binding of GTP may be increased by the addition of HIS-RIC8 (Figure 4.5B) though the error bars overlap so this cannot be stated definitively.

Additional Purification of MBP-tagged proteins

In an attempt to remove the MBP protein for GTP binding assays, protein purified from the amylose resin was cleaved with factor Xa protease. After cleavage, the expected size of the MBP protein is approximately 45 kDa, G α proteins are approximately 40 kDa, and the RIC8 protein is approximately 53 kDa. This cleavage reaction works very well with a ratio of 1 μ g Factor Xa for 15 μ g protein (Figure 4.6A). However, a much larger amount of purified proteins is needed for the GTP binding assays. Attempts to scale up this reaction using less Factor Xa were not as successful, as MBP was only partially cleaved from GNA-1 and GNA-3 and RIC8 appeared to be degraded after treatment (Figure 4.6B). Additionally, separation of the MBP protein using the amylose resin results in a loss of the desired protein (Figure 4.6C). This could be due to a number of factors, including protein degradation and aggregation.

Additional purification of 6H-G α proteins

As seen in Figure 4.2A, the approximate concentration of the 6H-tagged G α proteins was only about 10% of the total protein. I therefore tried using a second set of resins to purify the G α proteins. First I used ion-exchange chromatography to separate 6H-GNA-3 from the background bands. This resulted in a loss of detectible protein, as 6H-GNA-3 could not even be detected in a western blot (Figure 4.7A). I also tried purification of 6H-GNA-1 using a hydroxyapatite resin followed by His-Pur cobalt resin. Hydroxyapatite is described as a ‘pseudo-affinity’ resin because it is selectable for a specific range of proteins, but also separates proteins in a salt gradient, similar to ion-

exchange. I used a small scale GTP binding assay to determine which fractions contained 6H-GNA-1 (fractions 20-28; Figure 4.7B shows a Coomassie-stained gel for the odd fractions). I pooled the fractions, incubated with His-Pur resin, and eluted the same as previous experiments. In the elutions, there appeared to be a large background band above 6H-GNA-1 (Figure 4.7C). This band is reduced by pouring the extracts over 1-mL affigel blue resin, but there is also a reduction in 6H-GNA-1, as seen in the GNA-1 western (Figure 4.7C). Although these methods may be working somewhat to improve purity of the 6H tagged G α proteins, so much protein is lost during the purification process that there is not enough left to use for the GTP binding assay. Therefore, to improve the purity of heterologously expressed G α proteins I need to increase the expression and solubility of these proteins to increase the amount of starting material. One problem could be the amount of soluble protein obtained from *E. coli* cells. In order to check whether or not this is a cell lysis issue, I attempted to increase the lysis of *E. coli* strain BL21(DE3) by introducing plasmid pLysS. Figure 4.7F shows that 6H-GNA-1 is expressed well in this strain, though attempts to purify soluble protein were unsuccessful. It also appears that the maximum amount of protein expression is seen at a shorter time, therefore decreasing the induction time may increase solubility.

Immunoprecipitation of V5-RIC8 from *Neurospora crassa*

In an attempt to see if RIC8 can bind G α proteins in *N. crassa*, I attempted to coimmunoprecipitate *N. crassa* G α subunits using a V5 epitope tagged RIC8 strain engineered by Patrick Schacht. This strain expresses a V5-RIC8 fusion from the native

promoter, thus preventing non-specific interactions due to over-expression. Immunoprecipitation was conducted using Dyna-beads protein A (magnetic beads linked to protein A) coupled to anti-V5 antibody or anti-V5 antibody coupled to agarose beads. The antibody coupled to the Dynabeads and conjugated to the agarose beads from Sigma were raised in goat, therefore our goat anti-mouse secondary antibodies were reacting to the heavy chain of the antibody, as seen in Figure 4.8. The antibody coupled to the agarose beads from Bethyl, however, were raised in rabbits and therefore these beads will be used for further studies. Both submerged culture tissue and VM plate tissue have been tested in this immunoprecipitation (Figure 4.8); however, attempts to pull-down the $G\alpha$ subunits have not been successful.

Discussion

Results in this Chapter show that *N. crassa* GNA-1, GNA-2, and GNA-3 subunits bind GTP, however I was only able to demonstrate GEF activity of RIC8 for GNA-1. The main experimental issue is obtaining a large amount of soluble protein to use for the GTP binding assays. The MBP tagged G α proteins are very soluble, however MBP-GNA-3 is unable to bind GTP. This could be due to steric hinderance of the large MBP tag, which could be blocking the guanine-nucleotide binding pocket of on GNA-3. probably because of interference from the large MBP tag. Attempts to remove the MBP tag were successful but the amount of enzyme needed to cleave the MBP tag was not practical, therefore a smaller tag was used (6H). Since 6H-GNA-1 seems to have a higher affinity for GTP than the other 6H tagged G α proteins (Figure 4.4D) this may be why I was able to see a significant effect of GTP binding by the addition of 6H-RIC8. A small amount of GTP binding was seen for 6H-GNA-2 and 6H-GNA-3, however there was no significant change upon addition of HIS-RIC8. Because of the purification difficulties and small amount of protein expression using the 6H tag, a different tag may need to be used to facilitate further purification of *N. crassa* G α subunits from *E. coli*. Preliminary data shows that RIC8 has GEF activity toward GNA-1 and possibly GNA-3; though more research needs to be done to determine the fold stimulation of GTP binding.

V5 tagged RIC8 was successfully purified from *N. crassa* whole cell extracts (Figure 4.8), but attempts to coimmunoprecipiate G α subunits has been unsuccessful to date. This could be due to a number of factors, including transient or weak binding between RIC8 and G α proteins, or the dynamic sub-cellular localization of RIC8, as has

been observed in animals. For example, during *C. elegans* embryonic cell division, RIC8 is not present in the interphase nuclei, localizes around kinetochore microtubules at the onset of mitosis, and becomes dispersed about the cytosol during anaphase (Hess et al., 2004). In addition, RIC8 may have many binding partners and therefore the amount of G α proteins bound to RIC8 at any given time could be low. One way to solve this is to immunoprecipitate the G α protein and to test for the presence of RIC8. Unfortunately attempts at immunoprecipitation were unsuccessful using the current *N. crassa* G α antibodies in our lab. However, experiments are underway to make a strain expressing tagged versions of both RIC8 and G α proteins in order to immunoprecipitate G α proteins from *N. crassa*.

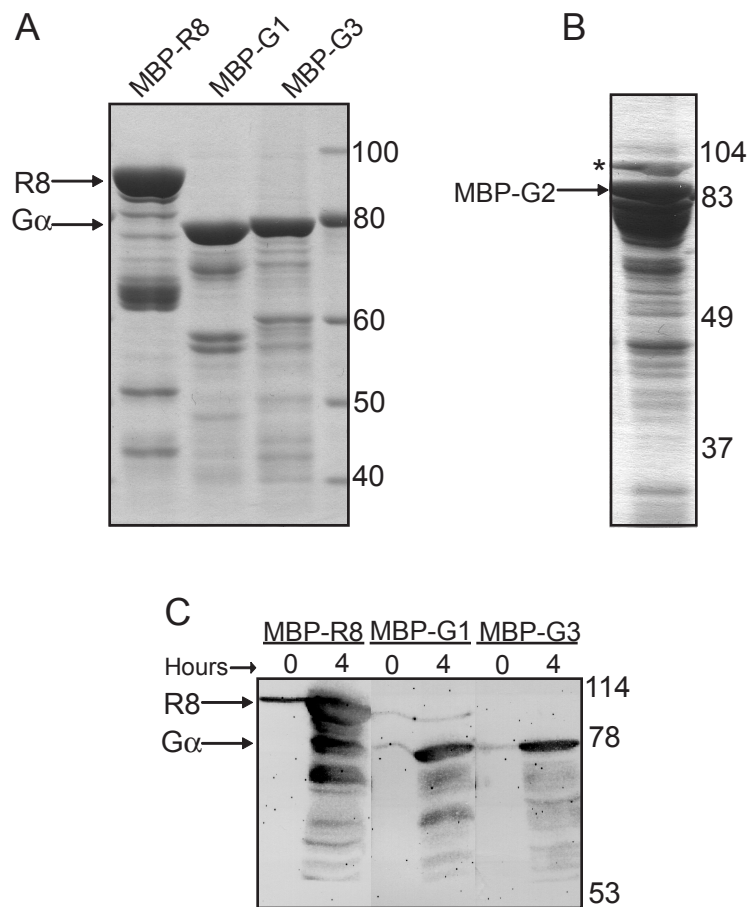


Figure 4.1: Purification of MBP tagged G α and RIC8 proteins from *E. coli*

MBP tagged RIC8 and G α proteins were expressed in *E. coli* strain K12 ER2508 and purified on an amylose resin. RIC8 is denoted as R8 and G α proteins as G1, G2, and G3. A) Purified MBP tagged R8, G1, and G3 proteins used for GTP binding assays. MBP-RIC8 is approximately 98kDa and MBP-G α proteins are approximately 85kDa. B) Purified MBP tagged G2. The extra band above MBP-G2 is marked as (*) and indicates an inefficient stop codon. MBP-G2 was therefore not used for binding assays. C) Western blot of purified MBP tagged proteins. Hours shown indicate T=0 and T=4 hours after induction with IPTG.

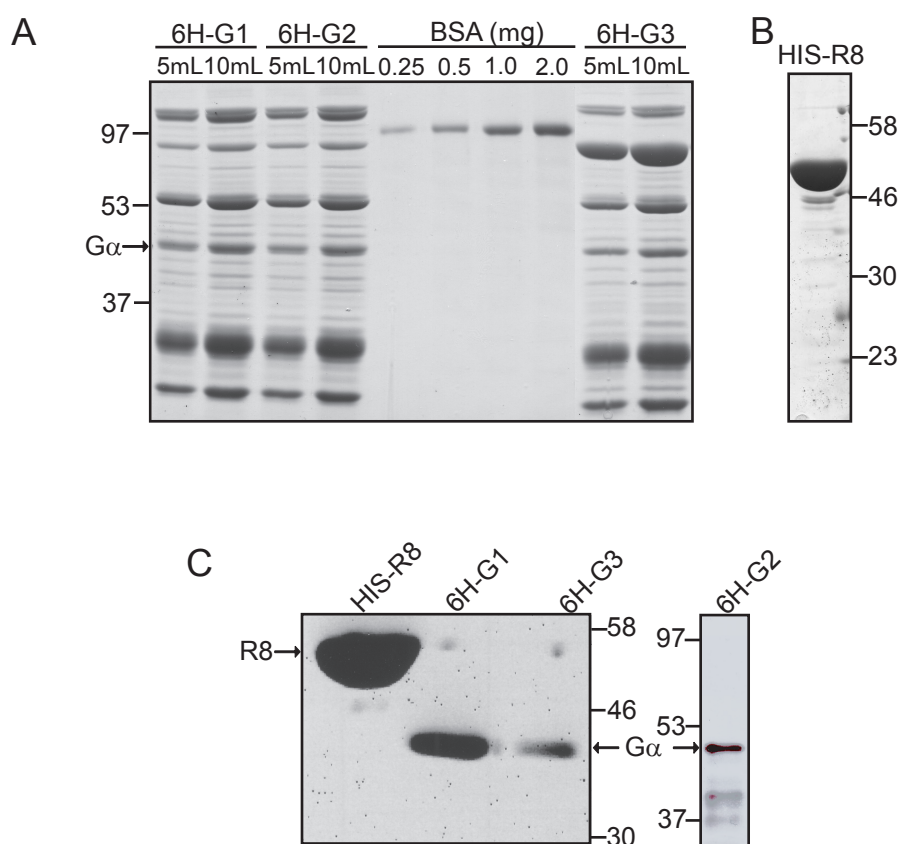


Figure 4.2: Purification of poly-histidine tagged $G\alpha$ and RIC8 proteins from *E. coli*
Poly-histidine tagged versions of RIC8 (10 histidines, HIS) and $G\alpha$ (6 histidines, 6H) were expressed in *E. coli* strain BL21(DE3). RIC8 is denoted as R8 and $G\alpha$ proteins as G1, G2, and G3. A) Total protein from His-Pur cobalt resin elution of 6H- $G\alpha$ proteins concentrated on an Amicon Ultra 30 column. Because of the high background, 5 and 10 μ L of 6H- $G\alpha$ proteins used for GTP binding assays and known amounts of BSA were ran to determine protein concentration. B) Total protein from His-Pur cobalt resin elution of HIS-R8 proteins concentrated on an Amicon Ultra 30 column. B) Western blot of HIS-R8, 6H-G1, and 6H-G3 proteins from A using anti-hexa-histidine antibody (left) and Western blot of 6H-G2 eluted from the His-Pur cobalt resin using anti-GNA-2 antibody (right).

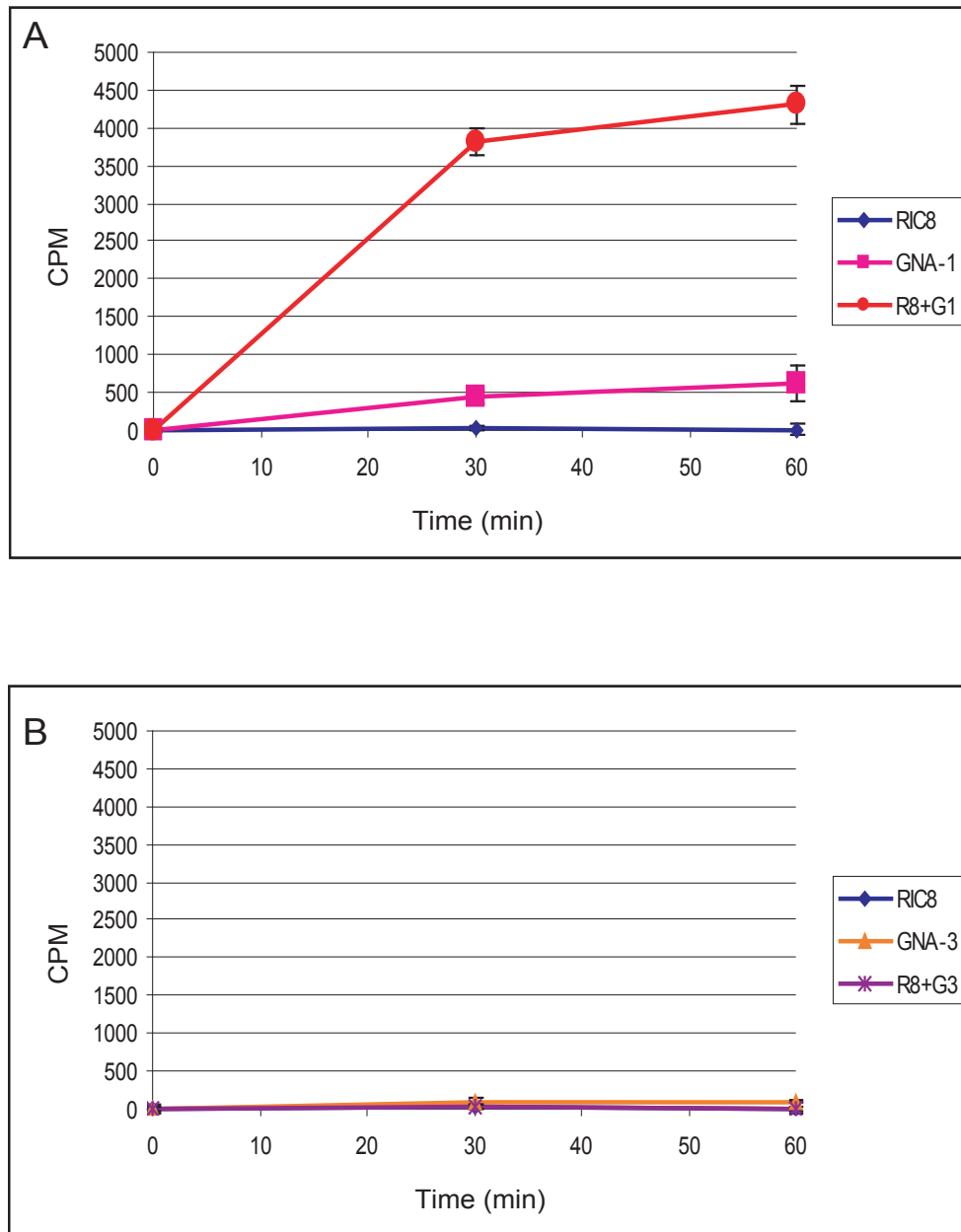


Figure 4.3: GTP binding of G α subunits and GEF activity of RIC8

A) and B) MBP-G α with and without the addition of MBP-RIC8 were assayed for binding of GTP γ ³⁵S. Proteins were incubated on ice in a total volume of 18 μ L in exchange buffer and 10mM MgSO₄. Reactions were started by adding 2 μ L of 1:1 mixture of 40 μ M GTP γ S and 1 μ Ci/ μ L GTP γ ³⁵S and incubated at 30°C for up to 60 minutes. The concentration of MBP-RIC8 used was 200nM and MBP-G α 's was 700nM. Error bars represent +/- 1 standard deviation. CPM=counts per minute.

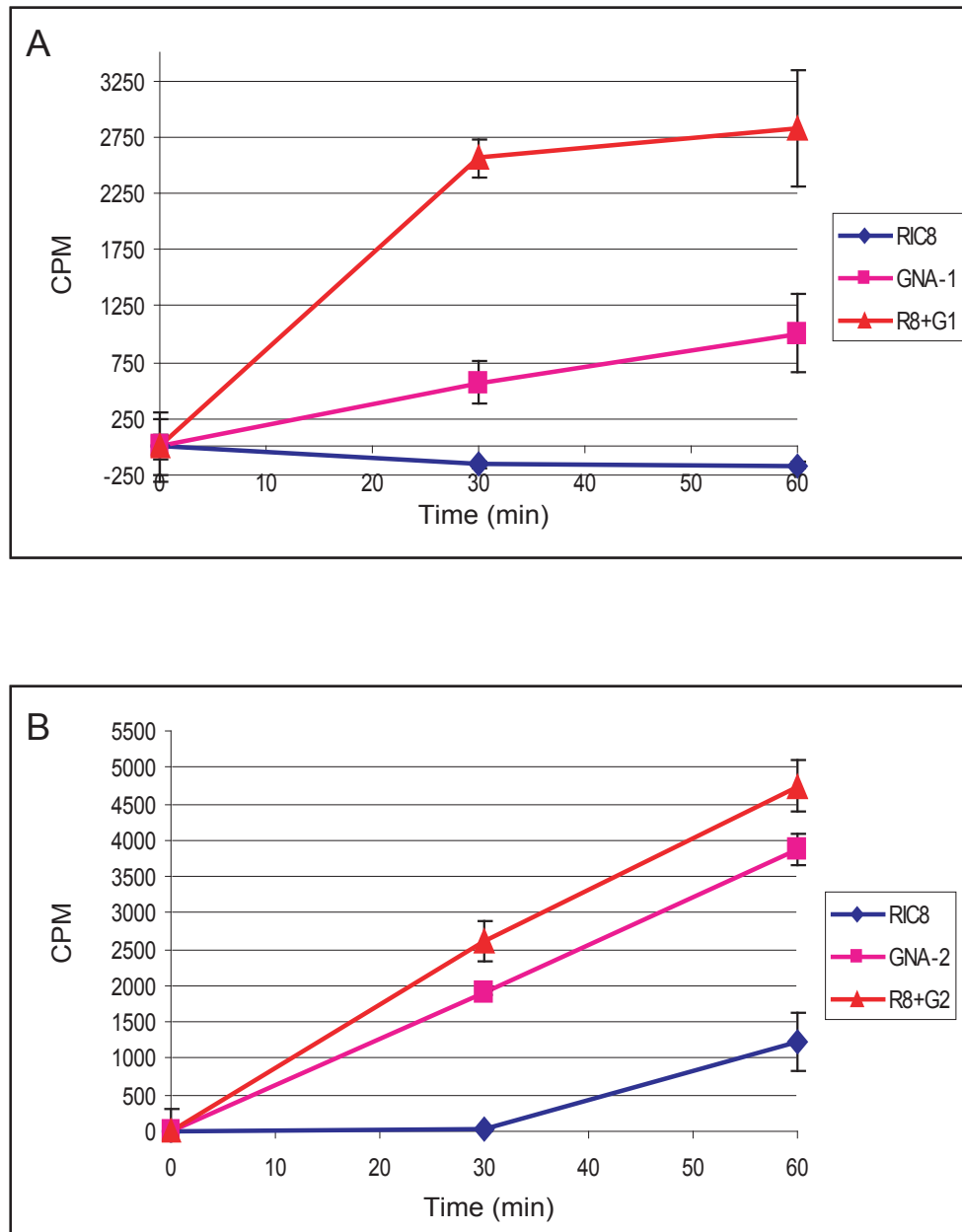


Figure 4.4: GTP binding of G α subunits and GEF activity of RIC8

A) Hexa-histidine (6H) tagged GNA-1 (13.75nM) with and without the addition of MBP-RIC8 (200nM) was assayed for binding of GTP γ ³⁵S. Proteins were incubated on ice in a total volume of 18 μ L in exchange buffer and 10mM MgSO₄. Reactions were started by adding 2 μ L of 1:1 mixture of 40 μ M GTP γ S and 1 μ Ci/ μ L GTP γ ³⁵S and incubated at 30°C for up to 60 minutes. B) Hexa-histidine (6H) tagged GNA-2 (787.5nM) with and without the addition of MBP-RIC8 (200nM) was assayed for binding of GTP γ ³⁵S as described in A). Error bars represent +/- 1 standard deviation. CPM=counts per minute.

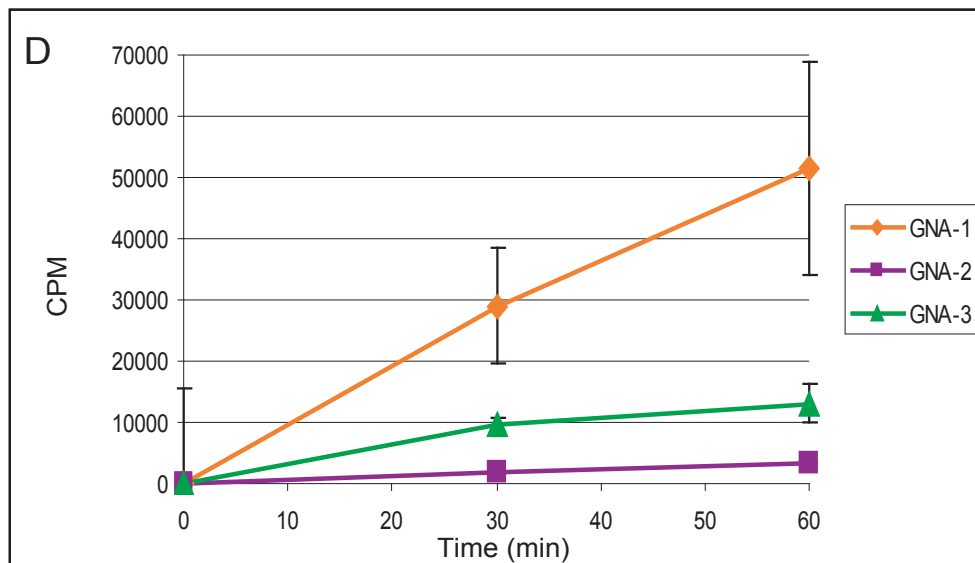
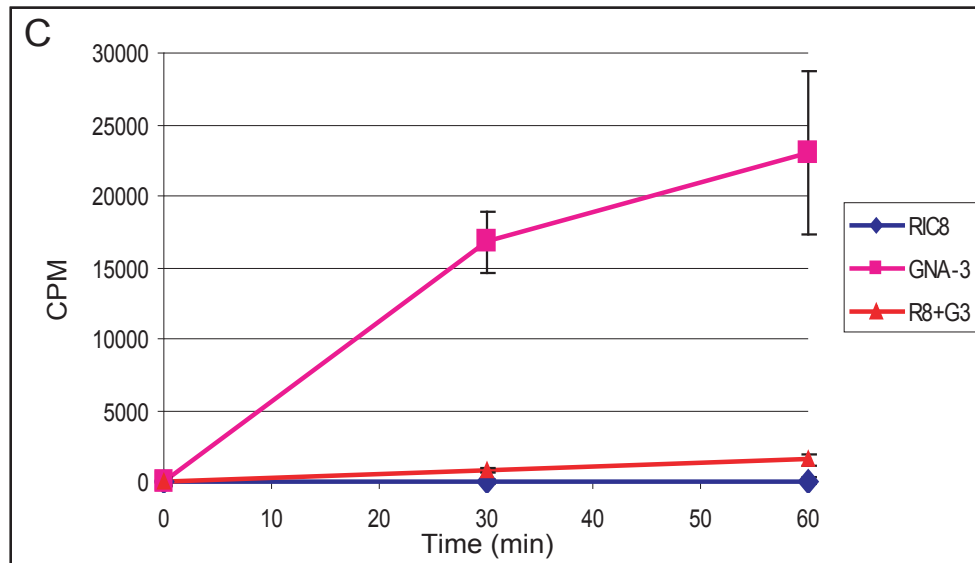


Figure 4.4: GTP binding of G α subunits and GEF activity of RIC8

C) Hexa-histidine (6H) tagged GNA-3 (1225nM) with and without the addition of MBP-RIC8 (200nM) was assayed for binding of GTP γ^{35} S. Proteins were incubated on ice in a total volume of 18 μ L in exchange buffer and 10mM MgSO $_4$. Reactions were started by adding 2 μ L of 1:1 mixture of 40 μ M GTP γ S and 1 μ Ci/ μ L GTP γ^{35} S and incubated at 30°C for up to 60 minutes. D) Values for A, B, and C GTP γ^{35} S binding assays normalized to 700nM 6H-G α . Error bars represent +/- 1 standard deviation. CPM=counts per minute.

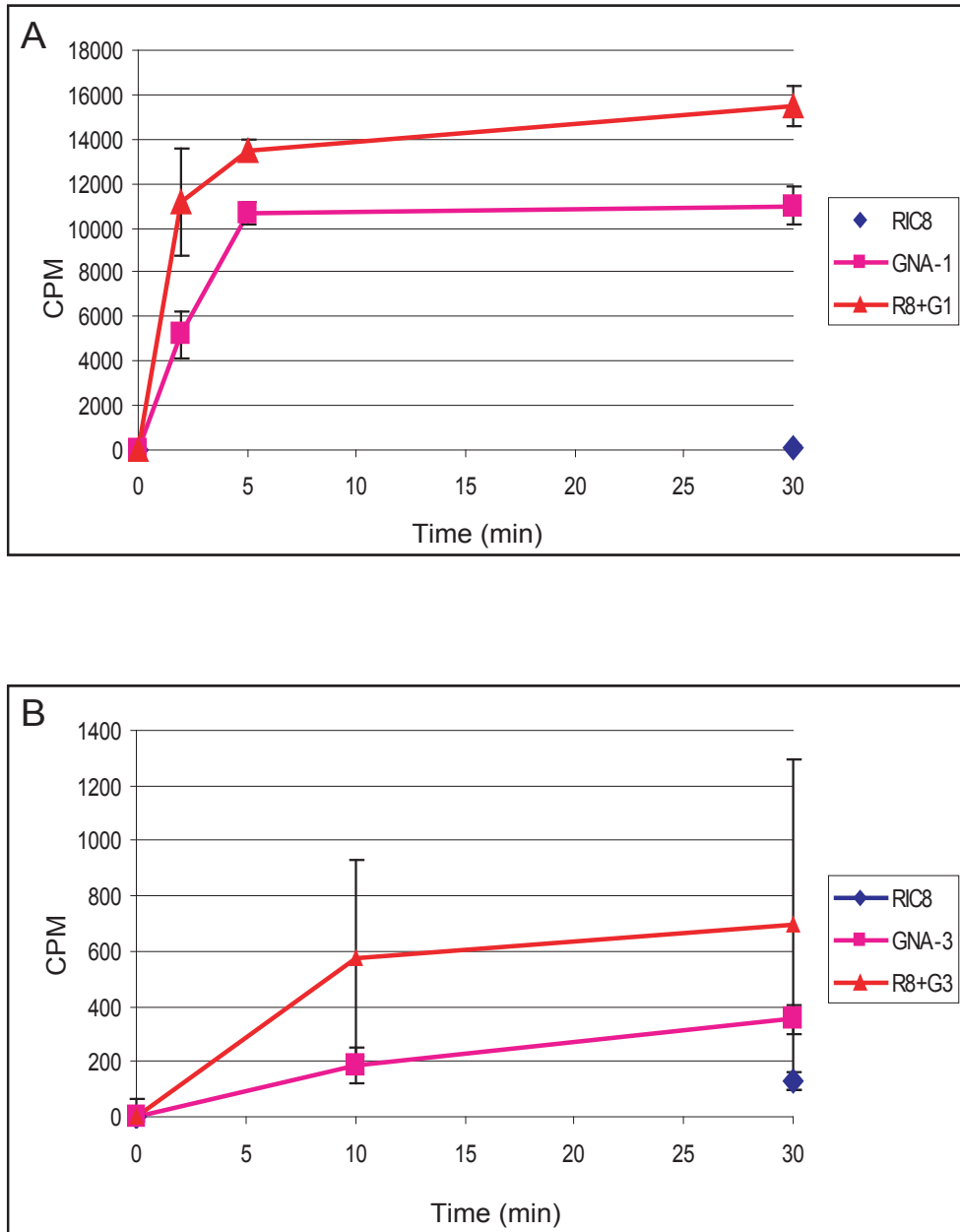


Figure 4.5: GTP binding of 6H-G α subunits and GEF activity of HIS-RIC8

A) and B) Hexa-histidine (6H) tagged GNA-1 (70 nM) and GNA-3 (350 nM) with and without the addition of HIS-RIC8 (200 nM) was assayed for binding of GTP γ ³⁵S. Proteins were incubated on ice in a total volume of 18 μ L in exchange buffer and 10 mM MgSO₄. Reactions were started by adding 2 μ L of 1:1 mixture of 40 μ M GTP γ S and 1 μ Ci/ μ L GTP γ ³⁵S and incubated at 30°C for up to 30 min. Error bars represent +/- 1 standard deviation. CPM=counts per min.

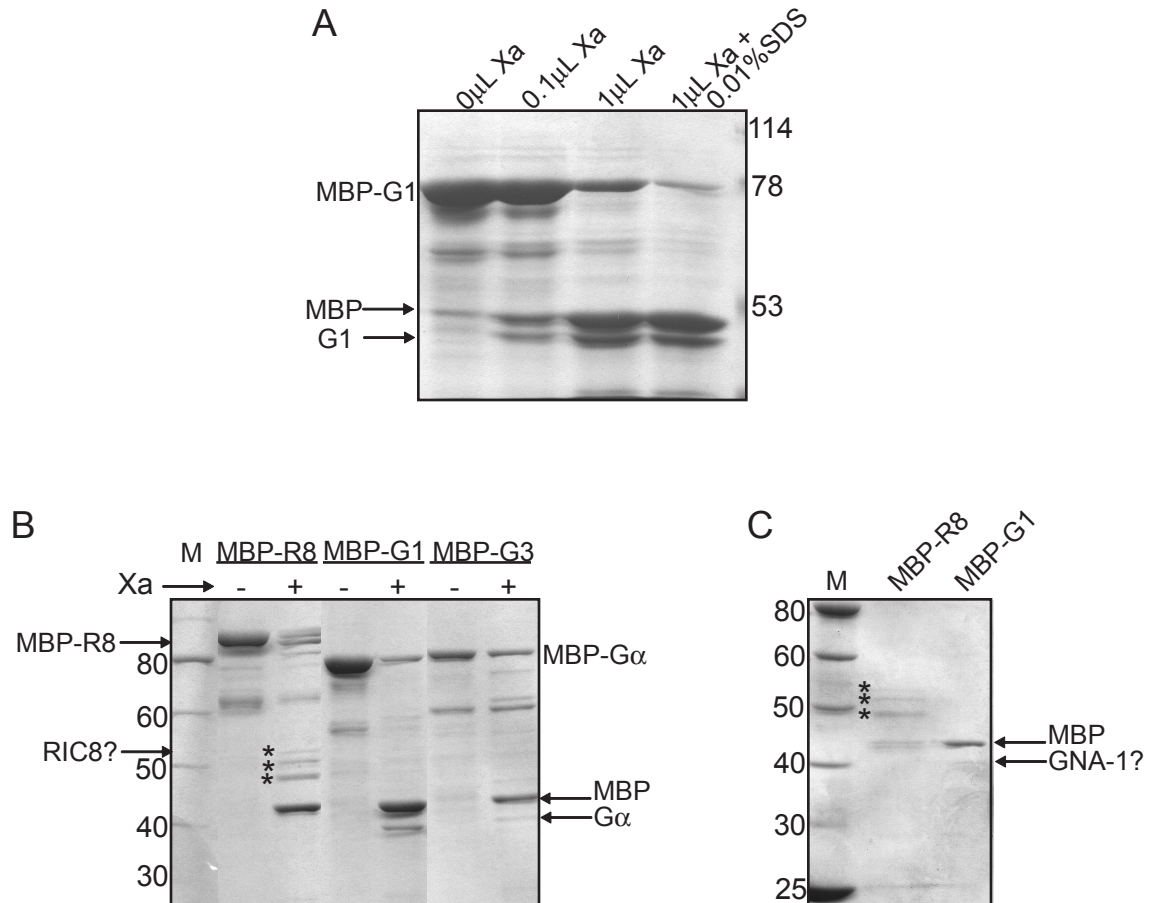


Figure 4.6: Removal of MBP tag from RIC8, GNA-1, and GNA-3

Cleavage of the MBP tag using factor Xa. MBP protein is approximately 35 kDa, Gα proteins are approximately 40 kDa, and RIC8 is approximately 53 kDa. A) A small scale cleavage reaction using 15 μg His-Pur purified MBP-GNA-1 and various amounts of Factor Xa. SDS is thought to increase the activity of factor Xa in some situations. Full cleavage is visible at 1 μg of enzyme. B) Scale up of cleavage reaction using 150 μg purified MBP tagged RIC8, GNA-1, and GNA-3 and 3 μg Factor Xa. Note that the cleavage reaction is not 100% efficient, and that there are multiple bands around the size of RIC8 (*), indicating degradation. C) Reactions from B) purified on an amylose resin. MBP protein is still present in the sample and GNA-1 is barely visible. There are multiple bands for RIC8, suggesting degradation. GNA-3 sample was lost during concentration due to experimental error and is therefore not shown. M=marker.

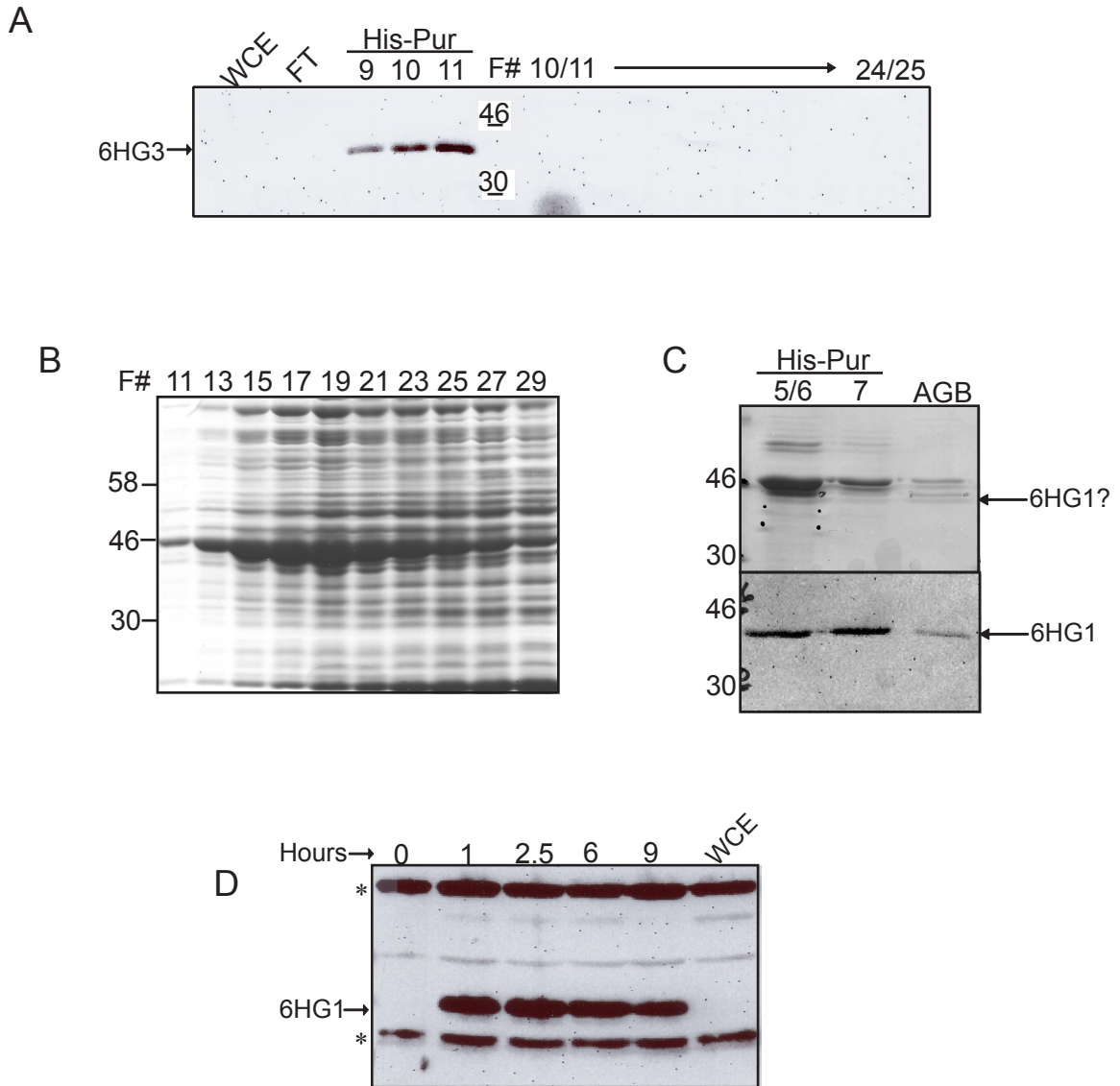


Figure 4.7: Additional purification steps for 6H tagged G α proteins

A) Fractions obtained from purification of 6H-G3 on a His-Pur cobalt resin were further purified using ion-exchange chromatography (DEAE column). Proteins were eluted using a 20-220 mM NaCl linear gradient, and fractions were subjected to western blot using the anti-hexa-histidine antibody. Two fractions (25 μ L each) were run per lane. F# = fraction # B) 6H-GNA-1 purified using hydroxyapatite resin. Proteins were eluted using a 20-200 mM phosphate gradient and odd number fractions were visualized using SDS-PAGE and coomassie staining. C) Fractions 20-28 from B) were purified using the His-Pur resin. Elutions 5, 6, and 7 from this resin were pooled and poured over affigel blue resin. Purification steps were visualized using SDS-PAGE and coomassie staining and western analysis using anti-GNA-1 antibody. D) Time course of 6H-G1 expression using BL21(DE3) transformed with plasmid pLysS. Hours shown indicate time after induction. WCE=whole cell extract on cell pellet collected after 9 hours.

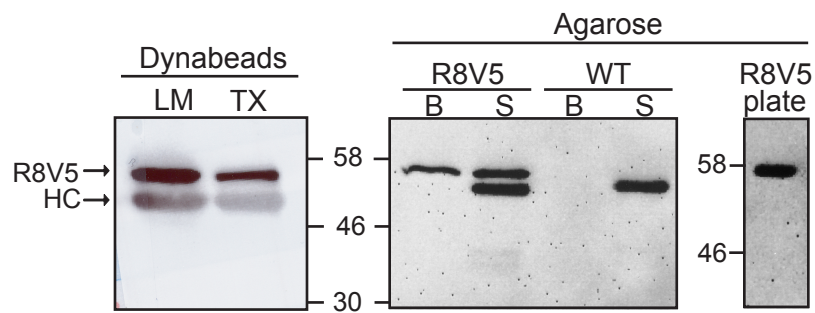


Figure 4.8: Immuno-precipitation of RIC8-V5 from *Neurospora crassa*

RIC8 protein was immuno-precipitated using a C-terminal V5 epitope tagged RIC8 strain generated by Patrick Schacht. Anti-V5 anti-sera coupled to either Dynabeads protein A or agarose (Bethyl or Sigma) was incubated with whole cell extracts of submerged or VM plate culture for 1 hour, washed, eluted by boiling, and visualized by western analysis. Extracts treated with detergent are indicated as LM (lauryl maltoside), or TX (Triton X-100). B= beads from Bethyl, S= beads from Sigma, HC=Heavy chain.

Table 4.1 Oligonucleotides used in this study

Name	Sequence (5'-3')
6HG1fw	TTAACATA TGCA TCA CCATCA CCA TGGGGGGA TGGGTTGCCGGA A TGAG TACAGAGG
6HG1rv	TTAAAGATCTTCAA AATCAA ACCCGCA GA GACGCAGG
6HG2fw	TTAACATA TGCA TCA CCATCA CCA TGGGGGGA TGTGTTCCGGGGGTCGT GGAAAGG
6HG2rv	TTAAGGATCCTCACAGGA TAAGTTGTTTCA GGTTCGGCTGG
6HG3fw	TTAACATA TGCA TCA CCATCA CCA TGGGGGGA TGGGCCGCA TGCA TGAG CAAGA ACG
6HG3rv	TTAAGGATCCTCATAGAA TACCAGGAGTCTTTAAGGGCG
HISR8 NdeI fw	AATTCA TATGGCCTCAA TAGGA GTTCTCTGGGC
HISR8 BamHI rv	AATTGGA TCCTCAGTCCGA ATCCTCTTCCGTAGTCCG

Chapter 5: Conclusions

This dissertation shows the characterization of a novel GEF for filamentous fungi, RIC8. *N. crassa* RIC8 is involved in essential functions including asexual and sexual sporulation, vegetative growth, cell and nuclear morphology, and movement. RIC8 also regulates G α subunits, most likely through protein stability and/or localization, and GEF activity. A study in *M. oryzae* published this year shows that MoRic8 is essential for virulence, is expressed highly in the appressorium and is cytosolic, and binds to G α subunit MagB (Li et al., 2010). This is similar to results in *N. crassa*, which is expected given the high conservation among RIC8 homologs in filamentous fungi.

RIC-8 has been shown to be an important GEF for G α subunits in animals. RIC-8 was first discovered in *C. elegans*, where it is important in embryogenesis and neural signaling (Miller et al., 2000a; Miller and Rand, 2000b-b; Reynolds et al., 2005; Schade et al., 2005). A model for asymmetric division of the *C. elegans* one-cell embryo involves RIC-8, G α subunits, an RGS protein, microtubules, and dynein (Nguyen-Ngoc et al., 2007; Wilkie and Kinch, 2005a). During mitosis, a two scaffolding proteins, GPR-1/2 and LIN-5, are localized to the cell cortex at the posterior end of the cell. LIN-5 binds to dynein, which possesses microtubule minus end motility, and can pull the astral microtubule toward the complex. The complex is membrane bound by GDP-bound G α , which binds to GPR1/2, causing the pull of astral microtubules toward the posterior cortex by dynein. RIC-8 and RGS-7 regulates the guanine nucleotide binding state of the

G α subunit, and when G α is GTP bound it releases the GPR-1/2 complex and the microtubule. This oscillation continues until mitosis is complete, giving two asymmetric daughter cells (Nguyen-Ngoc et al., 2007; Wilkie and Kinch, 2005a).

Neurospora crassa extends hyphae through tip-growing polar growth, which relies on the constant trafficking of macromolecules and organelles to the growing tip through microtubules (Riquelme et al., 1998; Seiler et al., 1999). The organelles, eg. nuclei, are transported to the growing tip through microtubules (long distance) and actin filaments (localized, short distance). It is thought that nuclei with an elongated morphology are actually in the process of moving, as they are occasionally observed in wild-type (Freitag et al., 2004). Therefore, RIC8 could possibly work in a similar complex to that in *C. elegans*, and the *ric8* gene deletion mutant, which contains many elongated nuclei, may be defective in microtubule organization. Elongated nuclei are also observed in mutants lacking *rho-4*, which encodes a small GTPase. Loss of *rho-4* also leads to hyphae that are aseptate and contain a reduced number of microtubules that display aberrant morphology at hyphal tips (Rasmussen et al., 2008). The role for RIC8 in nuclear movement and possibility of a link to RHO-4 needs to be investigated further.

RIC8 in *N. crassa* is shown to be in the GNA-1 and GNA-3 signaling pathways and may act as a GEF for both subunits. A screen for potential GNA-1 interacting proteins uncovered some very interesting proteins that may be involved in some of the same processes as RIC8. Microtubules and actin are the two main components of the cytoskeleton, and the Arp2/3 complex is responsible for actin branching. EF1 α in yeast

was found to play a role in actin organization, which suggests that these proteins may be acting through GNA-1.

A future experiment to test this theory would be to test interactions between these proteins *in vivo*. This can be accomplished through Bimolecular fluorescence complementation (BIFC), which involves fusing one half of a fluorescent protein to one protein of interest and the other half to another protein of interest. If the two proteins of interest interact, the fluorescent protein will be re-constituted and fluorescence can be visualized. This is useful not only to visualize the interaction between two proteins but also to visualize the cellular localization where this interaction occurs. Actin and microtubule disrupting chemicals such as cytochalasin-A and benomyl can also be used to test the effects of the cytoskeleton on this interaction.

In Chapter 3, I show that the protein levels of the G α subunits are decreased dramatically in the plasma membrane fraction in the $\Delta ric8$ mutant, and that overexpression of the GTPase deficient alleles of the G α subunits partially recover wild-type phenotypes in the $\Delta ric8$ mutant. It would be useful to overexpress the native alleles of *gna-1*, *gna-2*, and *gna-3* to see if this is due to the overexpression of the G α subunits or the GTPase deficiency. The $\Delta ric8$ mutant also has low levels of the G β protein, and it has been previously shown that the loss of G β leads low levels of the G α subunits. It would therefore be interesting to see if overexpression of the *gnb-1* allele will be able to restore any of the G α protein levels in the $\Delta ric8$ mutant. If RIC8 is acting as a GEF for the G α subunits, it would also be useful to overexpress RIC8 in various strains to see if any phenotypes of G α activated alleles can be seen.

In this dissertation, I describe one of the first reports of the function of a RIC8 homolog in filamentous fungi, and potential interactors of GNA-1. These discoveries open up a whole new set of very interesting research questions, and the information gained from the study of RIC8 in *N. crassa* is very beneficial to understanding the function of RIC8 in all organisms. Future investigations will focus on uncovering conserved and/or divergent functions for RIC8 and G α proteins during polar cell growth and microtubule dynamics in *Neurospora* and animals.

References

- Afshar, K., Willard, F.S., Colombo, K., Johnston, C.A., McCudden, C.R., Siderovski, D.P., and Gonczy, P. (2004). RIC-8 is required for GPR-1/2-dependent G α function during asymmetric division of *C. elegans* embryos. *Cell* 119, 219-230.
- Alexopoulos, C.J., Mims, C.W., and Blackwell, M. (1996). *Introductory mycology*, 4th edn (New York, Wiley).
- Alff-Steinberger, C., and Epstein, R. (1994). Codon preference in the terminal region of *E. coli* genes and evolution of stop codon usage. *J Theor Biol* 168, 461-463.
- Allen, R.T., KA; Hoch, JA (1987). Identification of the 37-KDa protein displaying a variable interaction with the erythroid cell-membrane as glyceraldehyde-3-phosphate dehydrogenase. *Journal of Biological Chemistry* 262, 649-653.
- Altschul, S.F., Madden, T.L., Schaffer, A.A., Zhang, J., Zhang, Z., Miller, W., and Lipman, D.J. (1997). Gapped BLAST and PSI-BLAST: a new generation of protein database search programs. *Nucleic Acids Res* 25, 3389-3402.
- Aramayo, R. (1996). Gene replacement at the *his-3* locus of *Neurospora crassa*. *Fungal Genetics Newsletter* 43, 9-13.
- Baasiri, R.A., Lu, X., Rowley, P.S., Turner, G.E., and Borkovich, K.A. (1997). Overlapping functions for two G protein α subunits in *Neurospora crassa*. *Genetics* 147, 137-145.
- Banuett, F. (1995). Genetics of *Ustilago maydis*, a fungal pathogen that induces tumors in maize. *Annu Rev Genet* 29, 179-208.
- Beadle, G.W., and Tatum, E.L. (1941). Genetic Control of Biochemical Reactions in *Neurospora*. *Proc Natl Acad Sci U S A* 27, 499-506.
- Bennett, J.W. (1998). *Mycotechnology: the role of fungi in biotechnology*. *J Biotechnol* 66, 101-107.
- Bieszke, J.A., Li, L., and Borkovich, K.A. (2007). The fungal opsin gene *nop-1* is negatively-regulated by a component of the blue light sensing pathway and influences conidiation-specific gene expression in *Neurospora crassa*. *Curr Genet* 52, 149-157.
- Bistis, G.N., Perkins, D.D., and Read, N.D. (2003). Different cell types in *Neurospora crassa*. *Fungal Genet Newsl* 50, 17-19.

- Bolker, M. (1998). Sex and crime: heterotrimeric G proteins in fungal mating and pathogenesis. *Fungal Genet Biol* 25, 143-156.
- Borkovich, K.A., Alex, L.A., Yarden, O., Freitag, M., Turner, G.E., Read, N.D., Seiler, S., Bell-Pedersen, D., Paietta, J., Plesofsky, N., *et al.* (2004). Lessons from the genome sequence of *Neurospora crassa*: tracing the path from genomic blueprint to multicellular organism. *Microbiol Mol Biol Rev* 68, 1-108.
- Bozkurt, G., Stjepanovic, G., Vilardi, F., Amlacher, S., Wild, K., Bange, G., Favaloro, V., Rippe, K., Hurt, E., Dobberstein, B., *et al.* (2009). Structural insights into tail-anchored protein binding and membrane insertion by Get3. *Proceedings of the National Academy of Sciences* 106, 21131-21136.
- Bruno, K.S., Aramayo, R., Minke, P.F., Metzzenberg, R.L., and Plamann, M. (1996). Loss of growth polarity and mislocalization of septa in a *Neurospora* mutant altered in the regulatory subunit of cAMP-dependent protein kinase. *Embo J* 15, 5772-5782.
- Buss, J.E., Mumby, S.M., Casey, P.J., Gilman, A.G., and Sefton, B.M. (1987). Myristoylated α subunits of guanine nucleotide-binding regulatory proteins. *Proc Natl Acad Sci U S A* 84, 7493-7497.
- Chang, M.H., Chae, K.S., Han, D.M., and Jahng, K.Y. (2004). The GanB $G\alpha$ -protein negatively regulates asexual sporulation and plays a positive role in conidial germination in *Aspergillus nidulans*. *Genetics* 167, 1305-1315.
- Charlie, N.K., Thomure, A.M., Schade, M.A., and Miller, K.G. (2006). The Dunce cAMP phosphodiesterase PDE-4 negatively regulates $G\alpha_s$ -dependent and $G\alpha_s$ -independent cAMP pools in the *Caenorhabditis elegans* synaptic signaling network. *Genetics* 173, 111-130.
- Chen, J.G., Willard, F.S., Huang, J., Liang, J., Chasse, S.A., Jones, A.M., and Siderovski, D.P. (2003). A seven-transmembrane RGS protein that modulates plant cell proliferation. *Science* 301, 1728-1731.
- Chien, C.B., PL; Sternglanz, R; Fields, SJ (1991). The two-hybrid system: a method to identify and clone genes for proteins that interact with a protein of interest. *Proc Natl Acad Sci USA* 88, 9578-9582.
- Christianson, T.W., Sikorski, R.S., Dante, M., Shero, J.H., and Hieter, P. (1992). Multifunctional yeast high-copy-number shuttle vectors. *Gene* 110, 119-122.
- Clapham, D.E., and Neer, E.J. (1997). G protein $\beta\gamma$ subunits. *Annu Rev Pharmacol Toxicol* 37, 167-203.

- Colot, H.V., Park, G., Turner, G.E., Ringelberg, C., Crew, C.M., Litvinkova, L., Weiss, R.L., Borkovich, K.A., and Dunlap, J.C. (2006). A high-throughput gene knockout procedure for *Neurospora* reveals functions for multiple transcription factors. *Proc Natl Acad Sci U S A* 103, 10352-10357.
- Cooper, D.M. (2003). Regulation and organization of adenylyl cyclases and cAMP. *Biochem J* 375, 517-529.
- Davis, R.H. (2000). *Neurospora* : contributions of a model organism (New York, Oxford University Press).
- Davis, R.H., and de Serres, F.J. (1970). Genetic and microbiological research techniques for *Neurospora crassa*. In *Methods in Enzymology*, T. Herbert, and T. Celia White, eds. (Academic Press), pp. 79-143.
- De Wolf, E.D., Madden, L.V., and Lipps, P.E. (2003). Risk assessment models for wheat fusarium head blight epidemics based on within-season weather data. *Phytopathology* 93, 428-435.
- Dean, R.A., Talbot, N.J., Ebbole, D.J., Farman, M.L., Mitchell, T.K., Orbach, M.J., Thon, M., Kulkarni, R., Xu, J.R., Pan, H., *et al.* (2005). The genome sequence of the rice blast fungus *Magnaporthe grisea*. *Nature* 434, 980-986.
- Doehlemann, G., Molitor, F., and Hahn, M. (2005). Molecular and functional characterization of a fructose specific transporter from the gray mold fungus *Botrytis cinerea*. *Fungal Genet Biol* 42, 601-610.
- Dower, W.J., Miller, J.F., and Ragsdale, C.W. (1988). High efficiency transformation of *E. coli* by high voltage electroporation. *Nucleic Acids Res* 16, 6127-6145.
- Ferguson, K.M., Higashijima, T., Smigel, M.D., and Gilman, A.G. (1986). The influence of bound GDP on the kinetics of guanine nucleotide binding to G proteins. *J Biol Chem* 261, 7393-7399.
- Fields, S.S.O. (1989). A novel genetic system to detect protein-protein interactions. *Nature* 340, 245-246.
- Folco, H.D., Freitag, M., Ramon, A., Temporini, E.D., Alvarez, M.E., Garcia, I., Scazzocchio, C., Selker, E.U., and Rosa, A.L. (2003). Histone H1 is required for proper regulation of pyruvate decarboxylase gene expression in *Neurospora crassa*. *Eukaryot Cell* 2, 341-350.
- Fredriksson, R., Lagerstrom, M.C., Lundin, L.G., and Schioth, H.B. (2003). The G-protein-coupled receptors in the human genome form five main families. Phylogenetic analysis, paralogon groups, and fingerprints. *Mol Pharmacol* 63, 1256-1272.

- Freitag, M., Hickey, P.C., Raju, N.B., Selker, E.U., and Read, N.D. (2004). GFP as a tool to analyze the organization, dynamics and function of nuclei and microtubules in *Neurospora crassa*. *Fungal Genet Biol* 41, 897-910.
- Galagan, J.E., Calvo, S.E., Borkovich, K.A., Selker, E.U., Read, N.D., Jaffe, D., FitzHugh, W., Ma, L.J., Smirnov, S., Purcell, S., *et al.* (2003). The genome sequence of the filamentous fungus *Neurospora crassa*. *Nature* 422, 859-868.
- Galagan, J.E., Calvo, S.E., Cuomo, C., Ma, L.J., Wortman, J.R., Batzoglou, S., Lee, S.I., Basturkmen, M., Spevak, C.C., Clutterbuck, J., *et al.* (2005). Sequencing of *Aspergillus nidulans* and comparative analysis with *A. fumigatus* and *A. oryzae*. *Nature* 438, 1105-1115.
- Gera, J.F., Hazbun, T.R., and Fields, S. (2002). Array-based methods for identifying protein-protein and protein-nucleic acid interactions. *Methods Enzymol* 350, 499-512.
- Grigston, J.C., Osuna, D., Scheible, W.R., Liu, C., Stitt, M., and Jones, A.M. (2008). D-Glucose sensing by a plasma membrane regulator of G signaling protein, AtRGS1. *Febs Lett* 582, 3577-3584.
- Gronover, C.S., Kasulke, D., Tudzynski, P., and Tudzynski, B. (2001). The role of G protein α subunits in the infection process of the gray mold fungus *Botrytis cinerea*. *Mol Plant Microbe Interact* 14, 1293-1302.
- Gross, S.K., TG (2005). Translation elongation factor 1A is essential for regulation of the actin cytoskeleton and cell morphology. *Nature Structural and Molecular Biology* 12, 772-778.
- Guo, M., Aston, C., Burchett, S.A., Dyke, C., Fields, S., Rajarao, S.J., Uetz, P., Wang, Y., Young, K., and Dohlman, H.G. (2003). The yeast G protein alpha subunit Gpa1 transmits a signal through an RNA binding effector protein Scp160. *Mol Cell* 12, 517-524.
- Hamm, H.E. (1998). The many faces of G protein signaling. *J Biol Chem* 273, 669-672.
- Hampoelz, B., Hoeller, O., Bowman, S.K., Dunican, D., and Knoblich, J.A. (2005). *Drosophila* Ric-8 is essential for plasma-membrane localization of heterotrimeric G proteins. *Nat Cell Biol* 7, 1099-1105.
- Han, K.H., Seo, J.A., and Yu, J.H. (2004). Regulators of G-protein signalling in *Aspergillus nidulans*: RgsA downregulates stress response and stimulates asexual sporulation through attenuation of GanB ($G\alpha$) signalling. *Mol Microbiol* 53, 529-540.
- Hanahan, D. (1983). Studies on transformation of *Escherichia coli* with plasmids. *J Mol Biol* 166, 557-580.

- Hawksworth, D.L. (2001). The magnitude of fungal diversity: the 1.5 million species estimate revisited. *Mycological Research* 105, 1422-1432.
- Hess, H.A., Roper, J.C., Grill, S.W., and Koelle, M.R. (2004). RGS-7 completes a receptor-independent heterotrimeric G protein cycle to asymmetrically regulate mitotic spindle positioning in *C. elegans*. *Cell* 119, 209-218.
- Hibbett, D.S., Binder, M., Bischoff, J.F., Blackwell, M., Cannon, P.F., Eriksson, O.E., Huhndorf, S., James, T., Kirk, P.M., Lucking, R., *et al.* (2007). A higher-level phylogenetic classification of the Fungi. *Mycol Res* 111, 509-547.
- Hicks, J.K., Yu, J.H., Keller, N.P., and Adams, T.H. (1997). *Aspergillus* sporulation and mycotoxin production both require inactivation of the FadA G α protein-dependent signaling pathway. *Embo J* 16, 4916-4923.
- Hill, C., Goddard, A., Davey, J., and Ladds, G. (2006). Investigating RGS proteins in yeast. *Semin Cell Dev Biol* 17, 352-362.
- Hochberg, M.L., and Sargent, M.L. (1974). Rhythms of enzyme activity associated with circadian conidiation in *Neurospora crassa*. *J Bacteriol* 120, 1164-1175.
- Hoffman, C.W., F (1987). A ten-minute DNA preparation from yeast efficiently releases autonomous plasmids for transformation of *Escherichia coli*. *Gene* 27, 267-272.
- Horvitz, H.R., and Herskowitz, I. (1992). Mechanisms of asymmetric cell division: two Bs or not two Bs, that is the question. *Cell* 68, 237-255.
- Hull, C.M., and Heitman, J. (2002). Genetics of *Cryptococcus neoformans*. *Annu Rev Genet* 36, 557-615.
- Hunsley, D., and Gooday, G.W. (1974). The structure and development of septa in *Neurospora crassa*. *Protoplasma* 82, 125-146.
- Ivey, F.D., Hodge, P.N., Turner, G.E., and Borkovich, K.A. (1996). The G α_i homologue *gna-1* controls multiple differentiation pathways in *Neurospora crassa*. *Mol Biol Cell* 7, 1283-1297.
- Ivey, F.D., Kays, A.M., and Borkovich, K.A. (2002). Shared and independent roles for a G α_i protein and adenylyl cyclase in regulating development and stress responses in *Neurospora crassa*. *Eukaryot Cell* 1, 634-642.
- Ivey, F.D., Yang, Q., and Borkovich, K.A. (1999). Positive regulation of adenylyl cyclase activity by a G α_i homolog in *Neurospora crassa*. *Fungal Genet Biol* 26, 48-61.

James, T.Y., Kauff, F., Schoch, C.L., Matheny, P.B., Hofstetter, V., Cox, C.J., Celio, G., Gueidan, C., Fraker, E., Miadlikowska, J., *et al.* (2006). Reconstructing the early evolution of Fungi using a six-gene phylogeny. *Nature* *443*, 818-822.

Jean-Baptiste, G., Yang, Z., and Greenwood, M.T. (2006). Regulatory mechanisms involved in modulating RGS function. *Cell Mol Life Sci* *63*, 1969-1985.

Johnston, C.A., Taylor, J.P., Gao, Y., Kimple, A.J., Grigston, J.C., Chen, J.-G., Siderovski, D.P., Jones, A.M., and Willard, F.S. (2007). GTPase acceleration as the rate-limiting step in *Arabidopsis* G protein-coupled sugar signaling. *Proceedings of the National Academy of Sciences* *104*, 17317-17322.

Jones, M.B., Siderovski, D.P., and Hooks, S.B. (2004). The G $\beta\gamma$ dimer as a novel source of selectivity in G-protein signaling: GGL-ing at convention. *Mol Interv* *4*, 200-214.

Kasahara, S., Wang, P., and Nuss, D.L. (2000). Identification of *bdm-1*, a gene involved in G protein β -subunit function and α -subunit accumulation. *Proc Natl Acad Sci U S A* *97*, 412-417.

Kays, A.M., and Borkovich, K.A. (2004a-a). Severe impairment of growth and differentiation in a *Neurospora crassa* mutant lacking all heterotrimeric G alpha proteins. *Genetics* *166*, 1229-1240.

Kays, A.M., and Borkovich, K.A. (2004a-b). Severe impairment of growth and differentiation in a *Neurospora crassa* mutant lacking all heterotrimeric G α proteins. *Genetics* *166*, 1229-1240.

Kays, A.M., and Borkovich, K.A. (2004b). Signal transduction pathways mediated by heterotrimeric G proteins. In *The Mycota R. Brambl, and G.A. Marzluf, eds. (Berlin-Heidelberg, Springer-Verlag), pp. 175–207.*

Kays, A.M., Rowley, P.S., Baasiri, R.A., and Borkovich, K.A. (2000a). Regulation of conidiation and adenylyl cyclase levels by the G α protein GNA-3 in *Neurospora crassa*. *Mol Cell Biol* *20*, 7693-7705.

Kays, A.M., Rowley, P.S., Baasiri, R.A., and Borkovich, K.A. (2000b). Regulation of conidiation and adenylyl cyclase levels by the G α protein GNA-3 in *Neurospora crassa*. *Mol Cell Biol* *20*, 7693-7705.

Kim, H., and Borkovich, K.A. (2004). A pheromone receptor gene, *pre-1*, is essential for mating type-specific directional growth and fusion of trichogynes and female fertility in *Neurospora crassa*. *Mol Microbiol* *52*, 1781-1798.

Kim, S.C., PA (2010). Emerging role for the cytoskeleton as an organizer and regulator of translation. *Nature Reviews: Molecular Cell Biology* *11*, 75-81.

- Krohn, M., Kleber, A., Schaffar, G., Dechert, U., and Eck, J. (2008). Now we are talking sense! Functional approaches to novel nutraceuticals and cosmeceuticals. *Biotechnol J* 3, 1147-1156.
- Kronstad, J.W., and Staben, C. (1997). Mating type in filamentous fungi. *Annu Rev Genet* 31, 245-276.
- Krystofova, S., and Borkovich, K.A. (2005). The heterotrimeric G-protein subunits GNG-1 and GNB-1 form a G $\beta\gamma$ dimer required for normal female fertility, asexual development, and G α protein levels in *Neurospora crassa*. *Eukaryot Cell* 4, 365-378.
- Krystofova, S., and Borkovich, K.A. (2006). The predicted G-protein-coupled receptor GPR-1 is required for female sexual development in the multicellular fungus *Neurospora crassa*. *Eukaryotic Cell* 5, 1503-1516.
- Kues, U., and Liu, Y. (2000). Fruiting body production in Basidiomycetes. *Appl Microbiol Biotechnol* 54, 141-152.
- Kulkarni, R.D., Thon, M.R., Pan, H., and Dean, R.A. (2005). Novel G-protein-coupled receptor-like proteins in the plant pathogenic fungus *Magnaporthe grisea*. *Genome Biol* 6, R24.
- Lafon, A., Han, K.H., Seo, J.A., Yu, J.H., and d'Enfert, C. (2006). G-protein and cAMP-mediated signaling in *aspergilli*: a genomic perspective. *Fungal Genet Biol* 43, 490-502.
- Laschet, J.M., F; Kurcewicz, I; Bureau, MH; Trottier, S; Jeanneteau, F; Griffon, N; Samyn, B; Van Beeumen, J; Louvel, J; Sokoloff, P; Pumain, R (2004). Glyceraldehyde-3-phosphate dehydrogenase is a GABA(A) receptor kinase linking glycolysis to neuronal inhibition. *Journal of Neuroscience* 24, 7614-7622.
- Lee, B.N., and Adams, T.H. (1994). Overexpression of flbA, an early regulator of *Aspergillus* asexual sporulation, leads to activation of brlA and premature initiation of development. *Mol Microbiol* 14, 323-334.
- Legras, J.L., Merdinoglu, D., Cornuet, J.M., and Karst, F. (2007). Bread, beer and wine: *Saccharomyces cerevisiae* diversity reflects human history. *Mol Ecol* 16, 2091-2102.
- Li, L., and Borkovich, K.A. (2006). GPR-4 is a predicted G-protein-coupled receptor required for carbon source-dependent asexual growth and development in *Neurospora crassa*. *Eukaryot Cell* 5, 1287-1300.
- Li, L., Shen, G., Zhang, Z.-G., Wang, Y.-L., Thompson, J.K., and Wang, P. (2007a). Canonical Heterotrimeric G Proteins Regulating Mating and Virulence of *Cryptococcus neoformans*. *Mol Biol Cell* 18, 4201-4209.

- Li, L., Wright, S.J., Krystofova, S., Park, G., and Borkovich, K.A. (2007b). Heterotrimeric G protein signaling in filamentous fungi. *Annu Rev Microbiol* 61, 423-452.
- Li, Y., Yan, X., Wang, H., Liang, S., Ma, W.B., Fang, M.Y., Talbot, N.J., and Wang, Z.Y. (2010). MoRic8 Is a novel component of G-protein signaling during plant infection by the rice blast fungus *Magnaporthe oryzae*. *Mol Plant Microbe Interact* 23, 317-331.
- Mandon, E.C., Ehses, I., Rother, J., van Echten, G., and Sandhoff, K. (1992). Subcellular localization and membrane topology of serine palmitoyltransferase, 3-dehydrosphinganine reductase, and sphinganine N-acyltransferase in mouse liver. *J Biol Chem* 267, 11144-11148.
- Marrari, Y., Crouthamel, M., Irannejad, R., and Wedegaertner, P.B. (2007). Assembly and trafficking of heterotrimeric G proteins. *Biochemistry-Us* 46, 7665-7677.
- Marsh, P. (1986). Ptac-85, an E. coli vector for expression of non-fusion proteins. *Nucleic Acids Res* 14, 3603.
- McCudden, C.R., Hains, M.D., Kimple, R.J., Siderovski, D.P., and Willard, F.S. (2005). G-protein signaling: back to the future. *Cell Mol Life Sci* 62, 551-577.
- McKerracher, L.a.H., IB (1987). Cytoplasmic migration and intracellular organelle movements during tip growth of fungal hyphae. *Exp Mycol* 11.
- Miller, K.G., Emerson, M.D., McManus, J.R., and Rand, J.B. (2000a). RIC-8 (Synembryn): a novel conserved protein that is required for $G\alpha_q$ signaling in the *C. elegans* nervous system. *Neuron* 27, 289-299.
- Miller, K.G., Emerson, M.D., and Rand, J.B. (1999). $G\alpha_o$ and Diacylglycerol Kinase Negatively Regulate the $G\alpha_q$ Pathway in *C. elegans*. 24, 323-333.
- Miller, K.G., and Rand, J.B. (2000b-a). A role for RIC-8 (Synembryn) and GOA-1 (G(o)alpha) in regulating a subset of centrosome movements during early embryogenesis in *Caenorhabditis elegans*. *Genetics* 156, 1649-1660.
- Miller, K.G., and Rand, J.B. (2000b-b). A role for RIC-8 (Synembryn) and GOA-1 ($G\alpha_o$) in regulating a subset of centrosome movements during early embryogenesis in *Caenorhabditis elegans*. *Genetics* 156, 1649-1660.
- Moore, D., and Frazer, L.N. (2002). Essential fungal genetics (New York, Springer).
- Mukhopadhyay, R., Ho, Y.-S., Swiatek, P.J., Rosen, B.P., and Bhattacharjee, H. (2006). Targeted disruption of the mouse *Asna1* gene results in embryonic lethality. *Febs Lett* 580, 3889-3894.

- Nagy, E.R., WFC (1995). Glyceraldehyde-3-phosphate dehydrogenase selectively binds AU-rich RNA in the NAD⁺ binding region (Rossmann Fold). *Journal of Biological Chemistry* 270, 2755-2763.
- Neves, S.R., Ram, P.T., and Iyengar, R. (2002). G protein pathways. *Science* 296, 1636-1639.
- Nguyen-Ngoc, T., Afshar, K., and Gonczy, P. (2007). Coupling of cortical dynein and G α proteins mediates spindle positioning in *Caenorhabditis elegans*. *Nat Cell Biol* 9, 1294-1302.
- Nishimura, A., Okamoto, M., Sugawara, Y., Mizuno, N., Yamauchi, J., and Itoh, H. (2006). Ric-8A potentiates Gq-mediated signal transduction by acting downstream of G protein-coupled receptor in intact cells. *Genes Cells* 11, 487-498.
- Odds, F.C., Brown, A.J., and Gow, N.A. (2004). *Candida albicans* genome sequence: a platform for genomics in the absence of genetics. *Genome Biol* 5, 230.
- Oldham, W.M., and Hamm, H.E. (2008). Heterotrimeric G protein activation by G-protein-coupled receptors. *Nat Rev Mol Cell Biol* 9, 60-71.
- Palczewski, K., Kumasaka, T., Hori, T., Behnke, C.A., Motoshima, H., Fox, B.A., Le Trong, I., Teller, D.C., Okada, T., Stenkamp, R.E., *et al.* (2000). Crystal structure of rhodopsin: A G protein-coupled receptor. *Science* 289, 739-745.
- Pandit, A., and Maheshwari, R. (1996). A Demonstration of the Role of *het* Genes in Heterokaryon Formation in *Neurospora* under Simulated Field Conditions. *Fungal Genet Biol* 20, 99-102.
- Rasmussen, C.G., and Glass, N.L. (2005). A Rho-type GTPase, *rho-4*, is required for septation in *Neurospora crassa*. *Eukaryot Cell* 4, 1913-1925.
- Rasmussen, C.G., Morgenstein, R.M., Peck, S., and Glass, N.L. (2008). Lack of the GTPase RHO-4 in *Neurospora crassa* causes a reduction in numbers and aberrant stabilization of microtubules at hyphal tips. *Fungal Genet Biol* 45, 1027-1039.
- Rasmussen CG, M.R., Peck S, Glass NL. (2008). Lack of the GTPase RHO-4 in *Neurospora crassa* causes a reduction in numbers and aberrant stabilization of microtubules at hyphal tips. *Fungal Genet Biol* 45, 1027-1039.
- Reynolds, N.K., Schade, M.A., and Miller, K.G. (2005). Convergent, RIC-8-dependent G α signaling pathways in the *Caenorhabditis elegans* synaptic signaling network. *Genetics* 169, 651-670.

- Riquelme, M., Reynaga-Pena, C.G., Gierz, G., and Bartnicki-Garcia, S. (1998). What determines growth direction in fungal hyphae? *Fungal Genet Biol* 24, 101-109.
- Romo, X., Pasten, P., Martinez, S., Soto, X., Lara, P., de Arellano, A.R., Torrejon, M., Montecino, M., Hinrichs, M.V., and Olate, J. (2008). xRic-8 is a GEF for $G\alpha_s$ and participates in maintaining meiotic arrest in *Xenopus laevis* oocytes. *J Cell Physiol* 214, 673-680.
- Rosenbaum, D.M., Rasmussen, S.G.F., and Kobilka, B.K. (2009). The structure and function of G-protein-coupled receptors. *Nature* 459, 356-363.
- Ross, E.M., and Wilkie, T.M. (2000). GTPase-activating proteins for heterotrimeric G proteins: regulators of G protein signaling (RGS) and RGS-like proteins. *Annu Rev Biochem* 69, 795-827.
- Schade, M.A., Reynolds, N.K., Dollins, C.M., and Miller, K.G. (2005). Mutations that rescue the paralysis of *Caenorhabditis elegans ric-8* (synembryon) mutants activate the $G\alpha_s$ pathway and define a third major branch of the synaptic signaling network. *Genetics* 169, 631-649.
- Schwarzott, D., Walker, C., and Schussler, A. (2001). Glomus, the largest genus of the arbuscular mycorrhizal fungi (Glomales), is nonmonophyletic. *Mol Phylogenet Evol* 21, 190-197.
- Seiler, S., Plamann, M., and Schliwa, M. (1999). Kinesin and dynein mutants provide novel insights into the roles of vesicle traffic during cell morphogenesis in *Neurospora*. *Curr Biol* 9, 779-785.
- Shear, C.L., and Dodge, B.O. (1927). Life histories and heterothallism of the red bread-mold fungi of the *Monilia sitophila* group *Journal of Agricultural Research* 34, 1019-1042.
- Shen, G., Wang, Y.-L., Whittington, A., Li, L., and Wang, P. (2008). The RGS Protein Crg2 Regulates Pheromone and Cyclic AMP Signaling in *Cryptococcus neoformans*. *Eukaryotic Cell* 7, 1540-1548.
- Shimizu, K., and Keller, N.P. (2001). Genetic involvement of a cAMP-dependent protein kinase in a G protein signaling pathway regulating morphological and chemical transitions in *Aspergillus nidulans*. *Genetics* 157, 591-600.
- Shinohara, M.L., Loros, J.J., and Dunlap, J.C. (1998). Glyceraldehyde-3-phosphate dehydrogenase is regulated on a daily basis by the circadian clock. *J Biol Chem* 273, 446-452.

- Siderovski, D.P., and Willard, F.S. (2005). The GAPs, GEFs, and GDIs of heterotrimeric G-protein α subunits. *Int J Biol Sci* 1, 51-66.
- Simon, M.I., Strathmann, M.P., and Gautam, N. (1991). Diversity of G proteins in signal transduction. *Science* 252, 802-808.
- Slessareva, J.E., Routt, S.M., Temple, B., Bankaitis, V.A., and Dohlman, H.G. (2006). Activation of the phosphatidylinositol 3-kinase Vps34 by a G protein α subunit at the endosome. *Cell* 126, 191-203.
- Smith, S.E., and Read, D.J. (2008). *Mycorrhizal symbiosis*, 3rd edn (Amsterdam ; Boston, Academic Press).
- Springer, M.L. (1993). Genetic control of fungal differentiation: the three sporulation pathways of *Neurospora crassa*. *Bioessays* 15, 365-374.
- Stajich, J.E., Berbee, M.L., Blackwell, M., Hibbett, D.S., James, T.Y., Spatafora, J.W., and Taylor, J.W. (2009). The fungi. *Curr Biol* 19, R840-845.
- Stefanovic, S., and Hegde, R.S. (2007). Identification of a Targeting Factor for Posttranslational Membrane Protein Insertion into the ER. *Cell* 128, 1147-1159.
- Studier, F.W., and Moffatt, B.A. (1986). Use of bacteriophage T7 RNA polymerase to direct selective high-level expression of cloned genes. *J Mol Biol* 189, 113-130.
- Tall, G.G., and Gilman, A.G. (2005). Resistance to inhibitors of cholinesterase 8A catalyzes release of $G\alpha_i$ -GTP and nuclear mitotic apparatus protein (NuMA) from NuMA/LGN/ $G\alpha_i$ -GDP complexes. *Proc Natl Acad Sci U S A* 102, 16584-16589.
- Tall, G.G., Krumins, A.M., and Gilman, A.G. (2003a). Mammalian Ric-8A (synembryn) is a heterotrimeric $G\alpha$ protein guanine nucleotide exchange factor. *J Biol Chem* 278, 8356-8362.
- Tall, G.G., Krumins, A.M., and Gilman, A.G. (2003b). Mammalian Ric-8A (synembryn) is a heterotrimeric $G\alpha$ protein guanine nucleotide exchange factor. *J Biol Chem* 278, 8356-8362.
- Tarze, A.D., A; Le Bras, M; Maillier, E; Molle, D; Larochette, N; Zamzami, N; Jan, G; Kroemer, G; Brenner, C (2007). GAPDH, a novel regulator of the pro-apoptotic mitochondrial membrane permeabilization. *Oncogene* 26, 2606-2620.
- Temple, B.R., and Jones, A.M. (2007). The plant heterotrimeric G-protein complex. *Annu Rev Plant Biol* 58, 249-266.

- Tonissou, T., Koks, S., Meier, R., Raud, S., Plaas, M., Vasar, E., and Karis, A. (2006). Heterozygous mice with Ric-8 mutation exhibit impaired spatial memory and decreased anxiety. *Behav Brain Res* 167, 42-48.
- Turner, G.E., and Borkovich, K.A. (1993). Identification of a G protein α subunit from *Neurospora crassa* that is a member of the G_i family. *J Biol Chem* 268, 14805-14811.
- Venter, J.C., Adams, M.D., Myers, E.W., Li, P.W., Mural, R.J., Sutton, G.G., Smith, H.O., Yandell, M., Evans, C.A., Holt, R.A., *et al.* (2001). The sequence of the human genome. *Science* 291, 1304-1351.
- Vogel, H. (1964). Distribution of Lysine Pathways among Fungi - Evolutionary Implications. *American Naturalist* 98, 435-446.
- Wang, P., Cutler, J., King, J., and Palmer, D. (2004). Mutation of the regulator of G protein signaling Crg1 increases virulence in *Cryptococcus neoformans*. *Eukaryot Cell* 3, 1028-1035.
- West, R.E., Jr., Moss, J., Vaughan, M., Liu, T., and Liu, T.Y. (1985). Pertussis toxin-catalyzed ADP-ribosylation of transducin. Cysteine 347 is the ADP-ribose acceptor site. *J Biol Chem* 260, 14428-14430.
- Westergaard, M., and Mitchell, H.K. (1947). *Neurospora-V* - a Synthetic Medium Favoring Sexual Reproduction. *Am J Bot* 34, 573-577.
- Wilkie, T.M., and Kinch, L. (2005a). New roles for G α and RGS proteins: communication continues despite pulling sisters apart. *Curr Biol* 15, R843-854.
- Wilkie, T.M., and Kinch, L. (2005b). New roles for Galpha and RGS proteins: communication continues despite pulling sisters apart. *Curr Biol* 15, R843-854.
- Winston, F., Dollard, C., and Ricupero-Hovasse, S.L. (1995). Construction of a set of convenient *Saccharomyces cerevisiae* strains that are isogenic to S288C. *Yeast* 11, 53-55.
- Woodard, G.E., Huang, N.N., Cho, H., Miki, T., Tall, G.G., and Kehrl, J.H. (2010). Ric-8A and G α_i Recruit LGN, NuMA, and Dynein to the Cell Cortex to Help Orient the Mitotic Spindle. *Mol Cell Biol*.
- Xiang X, P.M. (2003). Cytoskeleton and motor proteins in filamentous fungi. *Curr Opin Microbiol* 6, 628-633.
- Xue, C., Hsueh, Y.P., Chen, L., and Heitman, J. (2008). The RGS protein Crg2 regulates both pheromone and cAMP signalling in *Cryptococcus neoformans*. *Mol Microbiol* 70, 379-395.

- Yang, Q., and Borkovich, K.A. (1999). Mutational activation of a $G\alpha_i$ causes uncontrolled proliferation of aerial hyphae and increased sensitivity to heat and oxidative stress in *Neurospora crassa*. *Genetics* 151, 107-117.
- Yang, Q., Poole, S.I., and Borkovich, K.A. (2002). A G-protein β subunit required for sexual and vegetative development and maintenance of normal $G\alpha$ protein levels in *Neurospora crassa*. *Eukaryot Cell* 1, 378-390.
- Yu, J.H., Wieser, J., and Adams, T.H. (1996). The *Aspergillus* FlbA RGS domain protein antagonizes G protein signaling to block proliferation and allow development. *Embo J* 15, 5184-5190.
- Zaichick, S.V., Metodiev, M.V., Nelson, S.A., Durbrovskyi, O., Draper, E., Cooper, J.A., and Stone, D.E. (2009). The Mating-specific $G\alpha$ Interacts with a Kinesin-14 and Regulates Pheromone-induced Nuclear Migration in Budding Yeast. *Mol Biol Cell* 20, 2820-2830.
- Zheng, B., Ma, Y.C., Ostrom, R.S., Lavoie, C., Gill, G.N., Insel, P.A., Huang, X.Y., and Farquhar, M.G. (2001). RGS-PX1, a GAP for $G\alpha_s$ and sorting nexin in vesicular trafficking. *Science* 294, 1939-1942.
- Zozulya, S., Echeverri, F., and Nguyen, T. (2001). The human olfactory receptor repertoire. *Genome Biol* 2, RESEARCH0018.

Appendix 1: Construction of an *E. coli* strain for the expression of a full length *N. crassa* adenylyl cyclase protein, CR-1

Overview

In order to obtain purified, full-length CR-1 protein, cDNA was constructed using homologous recombination in yeast and cloned into the *E. coli* expression vector pET22b. This construct adds a hexa-histidine (6H) tag to the C-terminus of the protein. Attempts to express this construct in *E. coli* results in a degraded product, and the protocol needs to be optimized by testing different strains, temperatures, and IPTG concentrations to prevent this degradation. The *cr-1* cDNA can also be used for further experiments, such as the yeast two-hybrid assay.

Methods and Results

An *NdeI* fragment of genomic DNA including the *cr-1* gene was previously cloned into pGEM5 to produce pDIV6 (Ivey et al. 2002). The *cr-1* genomic DNA is 8.8kb in length and contains three introns and four exons (Figure A1.1A). A construct containing the first 375 base pairs of *cr-1* lacking the first intron was constructed previously in our lab (Ivey et al., 2002). This construct, pDIV13, is in the pSP72 vector background (Promega) and contains an engineered *NdeI* site at the ATG and continues to the *EcoRI* restriction site. The second and third introns were removed by yeast recombination using methods described in Chapter 3 and outlined in Figure A1.1A and B. A vector containing the *EcoRI-ClaI* fragment from *cr-1* lacking the second intron (pSM2) was constructed as follows. The PCR reaction mixtures contained 3 μ L 10X LA

Taq buffer, 1 μ L of a 1:10 dilution of pDIV6 (63 ng), 5 μ L dNTP, 2 μ L total of forward and reverse primer pairs (Cr-1EcoRIFw/Cr-1Exon2Rv, or Cr-1Exon3Fw/Cr-1ClaIRv, 100 pmol each, Table A1.1), 18.5 μ L water, and 0.5 μ L LA Taq polymerase.

Thermocycler temperatures used were: 94°C for 5 min., 35 cycles of: 98°C for 20 sec., 55°C for 30 sec., 68°C for 3.5 min.; and 72°C for 10 min. The sizes of the PCR products were confirmed by checking on a 1% agarose gel. The fragments (2 μ L PCR reaction each) and *XhoI/XbaI* digested pRS416 were transformed into yeast and construct pSM2 was recovered in *E. coli* as described in Chapter 2 (Figure A1.1A). The *EcoRI-ClaI* fragment from pSM2 was isolated using a step-wise restriction enzyme digest and agarose gel purification, and ligated into *EcoRI-ClaI* digested pDIV13 as described in Chapter 3 to create pSM4. This vector contains the *NdeI/ATG* to *ClaI cr-1* gene fragment lacking the first and second introns. After sequencing, this vector contained five point mutations in Exon 3. This was probably due to the low fidelity polymerase used. The mutations were corrected by replacing the *BamHI-ClaI* fragment of pSM4 with the *BamHI-ClaI* fragment of pDIV6, using methods described above. For simplicity, this vector is referred to as pSM4.

A vector (pSM11) containing the *ClaI*-end fragment of *cr-1*, lacking the third intron and replacing the stop codon with a *NotI* restriction site, was constructed using methods similar to pSM2, and the procedure is outlined in Figure A1.1B. The PCR reaction to amplify the third exon from *ClaI* and the fourth exon was similar to that described above, except that a 1 min. elongation time was used and different annealing temperatures were implemented (55°C for primer pair Cr-1ClaIFwYR/Cr-1Ex3RvHom,

and 65°C for primer pair Cr-1Ex4FwHom/Cr-1NotIRvYR; Table A1.1). These fragments were used for homologous recombination in yeast, and recovered in *E. coli* as described above. After sequencing, this vector contained a point mutation in Exon 3, which was corrected by replacing the *ClaI-XhoI* fragment of pSM4 with the *ClaI-XhoI* fragment of pDIV6, using methods described above. Again for simplicity, this vector is referred to as pSM11. The *NdeI-ClaI* fragment from pSM4, the *ClaI-NotI* fragment from pSM11, and *NdeI-NotI* digested pET22b were isolated and ligated as described in Chapter 3 to create plasmid pSM10. Plasmids pSM10, pET22b (empty vector), and pDIV18 (expresses a 56kDa fragment of CR-1) were transformed into chemical competent *E. coli* strain HMS174 (DE3) pLysS. HMS174 contains the *recA* mutation, which prevents loss of plasmids.

An overnight culture of each strain was cultured in 3 mL LB+amp+cam at 37°C, and 2 mL of the overnight cultures were used to inoculate 50 mL LB+amp+cam supplemented with 0.2% glucose. This culture was incubated at 37°C for 2 hours at 225 RPM (O.D.=0.6), then 50 mL of a 1 M stock of IPTG (1 mM total) was added and the culture incubated for an additional 3.75 hours with 1 mL samples taken every 1.25 hours. The samples were processed as described in Chapter 4 and subjected to western blot using a 7.5% acrylamide gel and the anti-CR-1 antibody as described in Chapter 3. As expected, pET22b produced no product, while pDIV18 produced a 56kDa protein, as described previously (Ivey et al., 2002). The full-length CR-1 protein was not expressed from the strain containing pSM10. However, there was a significant band below the 93kDa marker, suggesting degradation of CR-1 (Figure A1.2).

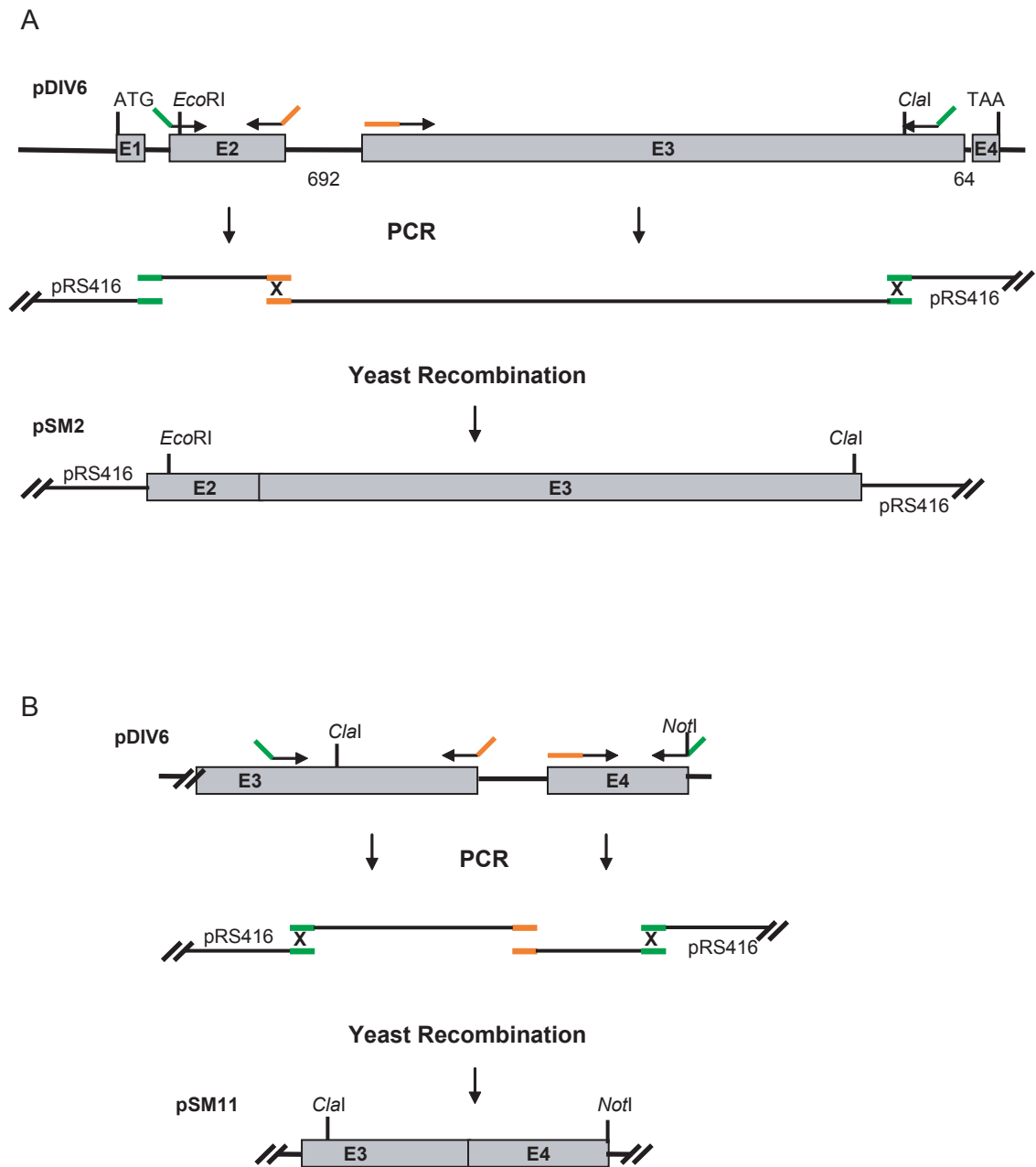


Figure A1.1: Schematic of the deletion of introns in the *cr-1* gene. The second (A, 692 bp) and third (B, 64 bp) introns of the *N. crassa cr-1* gene were removed using homologous recombination in yeast. Fragments to be recombined in pRS416 were amplified by PCR and transformed into yeast.

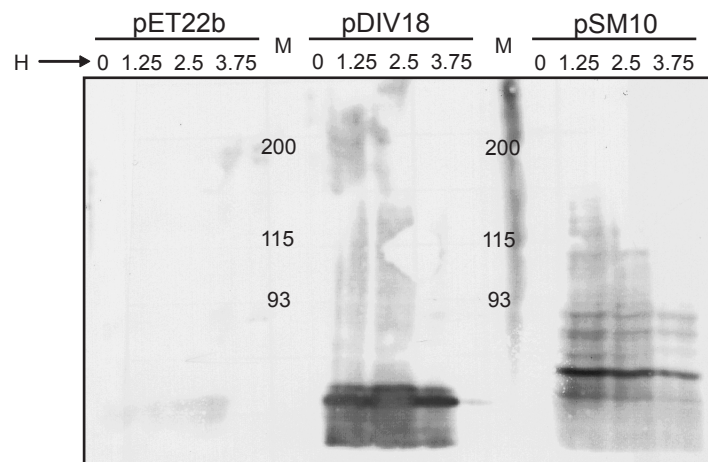


Figure A1.2: Expression of CR-1-6H in *E. coli*. Time course of CR-1-6H expression using HMS174 (DE3) pLysS. Hours shown indicate time after induction. Strains used were pSM10, which expresses full length CR-1, pDIV18, which expresses a 56kDa portion of CR-1, and pET22b, used as a control. H=Hours after induction. M=protein marker.

Table A1.1 Oligonucleotides used in this study

Name	Sequence (5'-3')
Cr-1EcoRIFw	GTAACGCCAGGGTTTTCCCAGTCACGACCATACGCAGACGCGGTTCGCAC
Cr-1Exon2Rv	CTTGTTCTGAACGGGTGCTTCGCCATAGCGAGCGATGTCGTGGCTTCTTG GTACAGAAAC
Cr-1Exon3Fw	GACATCGCTCGCTATGGCGAAGCACCCGTTTGAACAAGTCTCACTGGCC CCGATCGCG
Cr-1ClaIRv	GCGGATAACAATTTACACAGGAAACAGCCTCAGCTCGGATGGCCTTTG
Cr-1ClaIFwYR	GTAACGCCAGGGTTTTCCCAGTCACGACCAGTCGTATCTCCGCTGTCGC
Cr-1Ex3RvHom	ATTGCTATGTGGCGAACAGCGAGCGAAGTGATGCATGTCTCGATCCGGC TGATTTGAT
Cr-1Ex4FwHom	TTCTAAACTTCATGGAACATCAAATCAGCCGGATCGAGACATGCATCAC TTCGCTCGC
Cr-1NotIRvYR	GCGGATAACAATTTACACAGGAAACAGCAAGGAAAAAAGCGGCCGCT TCTTGCTCTGTATCACTTCC

Appendix 2: Construction of RGS gene deletion mutants in *N. crassa*

and *rgs* northern probe design

Overview

Neurospora crassa contains five *rgs* genes, named 1-5, which are homologous to the *A. nidulans* *rgs* genes described in Chapter 1. The construction and preliminary characterization of *N. crassa* *rgs* gene deletion mutants ($\Delta rgs1-4$) is described below. The $\Delta rgs-5$ mutant was isolated and characterized separately by Liande Li. Phenotypes of $\Delta rgs-1$ and $\Delta rgs-2$ resemble those of strains containing GTPase-deficient alleles of *gna-1* and *gna-3*, although further characterized was not performed to indicate the role of these *rgs* genes in G protein signaling. A list of the strains created, the NCU# for the genes deleted, and homologs in *A. nidulans* and *S. cerevisiae* are shown in Table A2.1.

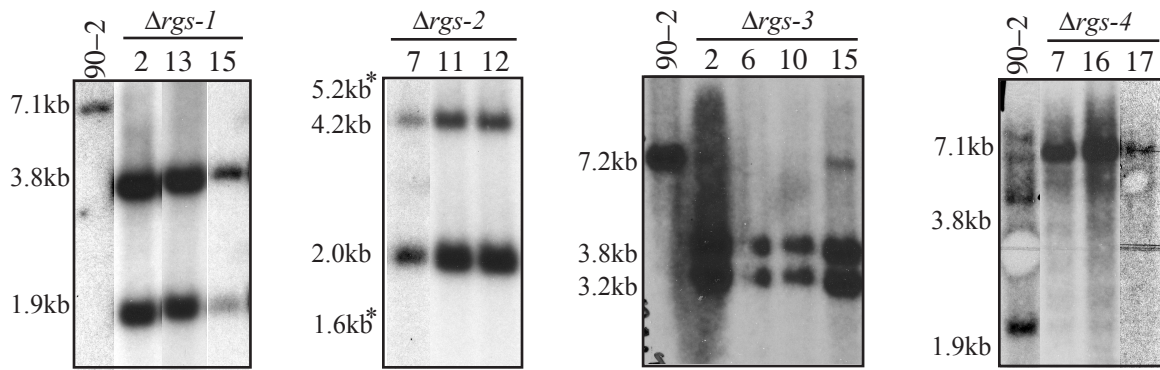
Methods and Results

All gene deletion mutants were constructed by the *Neurospora* genome project using homologous recombination at the gene locus, replacing the gene of interest with resistance to hygromycin as described in Chapter 3 (Colot et al., 2006). The $\Delta rgs-3$ mutant was obtained as a homokaryon, while the $\Delta rgs-1$, $\Delta rgs-2$, and $\Delta rgs-4$ mutants were obtained as heterokaryons, all in the *mat a* mating type. Homokaryons in both *mat a* and *mat A* mating types were obtained by crossing these strains as males to wild-type strain 74A (Table 3.1) as described in Chapter 3 for purifying the $\Delta ric8$ heterokaryon, except that ascospores were plated on FGS medium supplemented with hygromycin. Genomic DNA was isolated and all strains were verified by Southern analysis using the

knockout cassette as a probe, as described in Chapter 3. Southern results can be seen in Figure A2.1A, and the enzymes used and predicted fragments can be seen in Table A2.2.

The $\Delta rgs-1$ homokaryons were analyzed by culturing on VM plates for 2 days at 30°C or on VM slants for 3 days at 30°C and 4 days at 25°C as described in Chapter 3 (Figure A2.1B). All four Δrgs mutants produce fewer conidia as compared to wild-type. RGS-1 is predicted to act on GNA-1, and RGS-2 is predicted to act on GNA-3, based on the characterization of FlbA in *A. nidulans*. The $\Delta rgs-1$ mutant has very fluffy aerial hyphae, and the $\Delta rgs-2$ mutant also has fluffy aerial hyphae, but to a lesser extent than $\Delta rgs-1$. The $\Delta rgs-3$ and $\Delta rgs-4$ mutants have very sparse aerial hyphae as compared to wild-type. Phenotypes of these gene deletion mutants in *A. nidulans* have yet to be reported, though it has been shown that the *S. cerevisiae* homolog Rax1p (RGS-3) is necessary for bipolar budding and Mdm1p (RGS-4) is responsible for organelle inheritance during budding (Lafuente and Gancedo, 1999; McConnell et al., 1990). It will therefore be interesting to determine the relationships between these RGS proteins, G α subunits, and RIC8 in *N. crassa*.

A



B

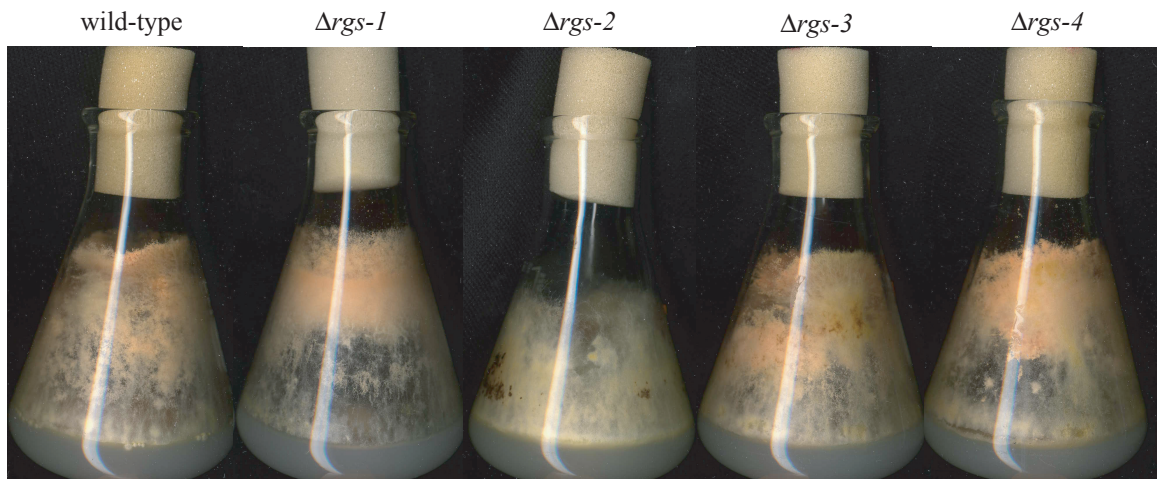


Figure A2.1: Δrgs mutants: southern verifications and basic phenotypes. A) Southern verification of the *rgs* gene replacement mutants. Southern analysis was used to verify the Δrgs mutation generated by the *Neurospora crassa* genome project using the knockout cassette as a probe. Note: for $\Delta rgs-3$, the control did not show up on the southern, and the predicted bands are indicated by (*). Strain 90-2 is the $\Delta mus-51$ deletion mutant used by the genome project to make the gene replacement mutant and is discussed in Chapter 3. B) Strains were inoculated on VM flasks and cultured for 3 days at 30°C, or on VM slants for 3 days at 30°C and 7 days at 25°C. Strains used were: wild-type (FGSC 2489), $\Delta rgs-1$ (rgs-1-2), $\Delta rgs-2$ (rgs-2-7), $\Delta rgs-3$ (rgs-3-15), and $\Delta rgs-4$ (rgs-4-17).

Table A2.1. *N. crassa* Δ rgs mutants, and RGS homologs in *N. crassa*, *A. nidulans*, and *S. cerevisiae*

Strain name	Genotypes	<i>N. crassa</i> ^a	<i>A. nidulans</i> ^b	<i>S. cerevisiae</i> ^c
rgs-1-2	Δ rgs-1::hph ⁺ mat a	RGS-1	FlbA	Sst2p
rgs-1-10	Δ rgs-1::hph ⁺ mat a	NCU08319.4	ANID_05893.1	NP_013557.1
rgs-1-13	Δ rgs-1::hph ⁺ mat A			
rgs-1-15	Δ rgs-1::hph ⁺ mat A			
rgs-2-7	Δ rgs-2::hph ⁺ mat a	RGS-2	RgsA	Rgs2p
rgs-2-12	Δ rgs-2::hph ⁺ mat a	NCU05435.4	ANID_05755.1	NP_014750.1
rgs-2-5	Δ rgs-2::hph ⁺ mat A			
rgs-2-11	Δ rgs-2::hph ⁺ mat A			
rgs-3-2	Δ rgs-3::hph ⁺ mat a	RGS-3	RgsB	Rax1p
rgs-3-10	Δ rgs-3::hph ⁺ mat a	08343.4	ANID_03622.1	NP_014945.1
rgs-3-15	Δ rgs-3::hph ⁺ mat a			
rgs-3-6	Δ rgs-3::hph ⁺ mat A			
rgs-4-7	Δ rgs-4::hph ⁺ mat A	RGS-4	RgsC	Mdm1p
rgs-4-16	Δ rgs-4::hph ⁺ mat A	03937.4	ANID_01377.1	NP_013603.1
rgs-4-17	Δ rgs-4::hph ⁺ mat A			

a. Protein name and ID#, *Neurospora* Database, www.broadinstitute.org/annotation/genome/neurospora

b. Protein name and ID#, *Aspergillus* Comparative Database, www.broadinstitute.org/annotation/genome/aspergillus_group

c. Protein name, *Saccharomyces* Genome Database, <http://www.yeastgenome.org>; and NCBI accession #, <http://www.ncbi.nlm.nih.gov/>

References for Appendices

Colot, H.V., Park, G., Turner, G.E., Ringelberg, C., Crew, C.M., Litvinkova, L., Weiss, R.L., Borkovich, K.A., and Dunlap, J.C. (2006). A high-throughput gene knockout procedure for *Neurospora* reveals functions for multiple transcription factors. *Proc Natl Acad Sci U S A* *103*, 10352-10357.

Ivey, F.D., Kays, A.M., and Borkovich, K.A. (2002). Shared and independent roles for a G α_i protein and adenylyl cyclase in regulating development and stress responses in *Neurospora crassa*. *Eukaryot Cell* *1*, 634-642.

Lafuente, M.J., and Gancedo, C. (1999). Disruption and basic functional analysis of six novel ORFs of chromosome XV from *Saccharomyces cerevisiae*. *Yeast* *15*, 935-943.

McConnell, S.J., Stewart, L.C., Talin, A., and Yaffe, M.P. (1990). Temperature-sensitive yeast mutants defective in mitochondrial inheritance. *The Journal of Cell Biology* *111*, 967-976.

VITA

Sara Josephine Martinez was born in Orange, CA on October 26th, 1980, the daughter of Pete and Alison Martinez. Sara's family has since grown to include parents Gary and Alison Augustine, Pete and Andrea Martinez, and siblings Lisa Gonzales (Augustine), Pete Martinez, and Ashlee Augustine. Sara married Richard Carl Wright on September 3rd 2005 and they welcomed their first child, a daughter named Lily Alison Wright, on January 21st, 2009.

Sara attended California State Polytechnic University, Pomona where she earned a Bachelor's degree in Chemistry in June 2003. She conducted undergraduate research in the lab of Dr. Lisa Alex through the Research Initiative for Scientific Enhancement (R.I.S.E.) program. Sara received the Chemistry Departmental Scholarship and the Science Educational Enhancement Services (S.E.E.S.) departmental scholarship and was a California State University Pre-doctoral Scholar.

Sara entered the Biochemistry and Molecular Biology program at the University of California, Riverside in September 2003. She received the Outstanding Teaching assistant award for Biochemistry courses in 2004-2005 from the Graduate Division. She will conduct her postdoctoral research at the University of California, San Diego, and plans on pursuing a faculty position.

Permanent Address: 10774 Mercer Ave.

Riverside, CA 92505